Title

Diatom-Inferred California Hydroclimatic Variations during the Late Quaternary

Author

Han, Jiwoo

Publication Date

2023

Peer reviewed|Thesis/dissertation

UNIVERSITY OF CALIFORNIA

Los Angeles

Diatom-Inferred California Hydroclimatic Variations during the Late Quaternary

A dissertation submitted in partial satisfaction of the requirements for the degree Doctor of Philosophy in Geography

by

Jiwoo Han

2023

ABSTRACT OF THE DISSERTATION

Diatom-Inferred California Hydroclimatic Variability

during the Late Quaternary

and Applicability of Transfer Functions from a Single Lake

by

Jiwoo Han

Doctor of Philosophy in Geography

University of California, Los Angeles, 2023

Professor Glen Michael MacDonald, Chair

In recent years, California has been suffering from severe hydroclimatic related challenges, such as droughts, fires, and deluges. Despite many ongoing efforts, uncertainties remain regarding the natural variability of hydroclimatic system and how anthropogenic impacts will affect future climate dynamics. To better understand the issues, it is essential to understand paleo-hydroclimatic variability over the long-term during the period that human beings had little impact on the climate. This dissertation aims to investigate long-term centennial to millennial hydroclimatic changes to understand natural variability to help differentiate this from anthropogenic impacts on the current climate and to plan for future climate change (e.g. formulating relevant policies, proposing contingency plans, etc.). Lake sediments preserve long hydroclimate records useful for resolving long-term variability.

Among the feasible proxy indicators used to reconstruct paleo-hydroclimate, I utilized diatom microfossils (microscopic algae) because they have been shown to record lake level and salinity changes within lakes that reflect changes in precipitation and evaporation. I analyzed the fossil and modern diatom flora from Kelly Lake in Northern California and from Baldwin Lake in Southern California. This dissertation focuses on the late Quaternary overall while focusing specifically on the Holocene changes in Northern California and Pleistocene changes in Southern California. From Kelly Lake, I established diatom-inferred water depth transfer functions to quantitatively infer the past lake level changes during the Holocene. The results show a meaningful correlation between modern diatom assemblages and water depths, allowing the construction of statistical transfer functions with high R^2 values (>0.95). This is the first such single-lake transfer function developed in California and one of only a handful worldwide. The transfer functions are then applied to the fossil diatom flora from a Holocene-length sediment core from Kelly Lake. The quantitatively reconstructed lake level changes in Kelly Lake indicate appreciable variations over the Holocene and suggest the influences from global drivers such as solar radiative and El Niño-Southern Oscillation forcings to the hydroclimatic variability in the Northern Coast Ranges. In Southern California, the qualitatively inferred salinity and water depth changes in Baldwin Lake showed abrupt change at about 70,000 cal yr BP when the orbitally controlled radiative forcing transitioned high seasonal variability to low seasonal variability. In both Northern and Southern California, the diatom records indicate a high degree of sensitivity by hydroclimate to external drivers related to external forcing factors such as ocean conditions and orbital variations.

This dissertation of Jiwoo Han is approved.

Thomas Welch Gillespie

Kyle C. Cavanaugh

Matthew E. Kirby

Glen Michael MacDonald, Committee Chair

University of California, Los Angeles

2023

TABLE OF CONTENTS

List of Figures

List of Tables

List of Equations

List of Appendix Figures

List of Appendix Tables

Acknowledgements

UCLA inspired me to dream of becoming a scientist/researcher. The lessons I learned at UCLA will always remain with me. Completing this dissertation would not have been possible without the advice, support, and love of many people. First and foremost, I am immensely grateful to my advisor, Glen MacDonald. I deeply respect his energy, passion, and knowledge, which have always been a source of inspiration for me. I am also thankful for his mentorship and academic support, which have played a crucial role in shaping me into an independent scholar.

I would also like to express my sincere gratitude to my committee members. I thank Thomas Gillespie for his academic advice and passion, smile, encouragement, and support. I thank Kyle Cavanaugh for his teachings, support, and academic guidance. I extend my appreciation to Matthew Kirby for his mentorship, academic advice, encouragement, positive inspiration, and humor. Lastly, I would like to thank my other mentor, Joe Carlin, for his invaluable academic advice, support, and positive energy.

Moreover, I would not have been able to complete this Ph.D. journey without the support of my colleagues and friends. I am grateful for their friendship: Lisa Martinez, Jessica Fayne, Jessie George, Elly Fard, Monica Dimson, Ben Nauman, Katie Glover, Scott Lydon, Lauren Brown, Chunyu Dong, Huilin Huang, Ye Liu, Jen Leidelmeijer, Judith Avila, Zhaoxin Ban, Flavia Lake, Anthony Laveault-Frigon, Michael Fischella, Dian Irawaty, and Lu Su.

I would also like to acknowledge the emotional support I received from my family and friends, without which I might not have been able to complete this Ph.D. program. Thank you to my dad and mom Tae Geun Han and Jung Ji Park, my husband Tae Hyung Kim, my brother Sungwoo Han, my uncles Jung Sam Park, Jung Gwan Park, Tae Hoon Han, as well as

my dongsaengdeul Hyemin Kim & Jihoon Sohn, Seul Lee, Kwon Heo, Jinsung Kim, Jane Chan, Mady Li, Sunah Shin, Suhyun Oh, Sooyoun Lee, Jihyun Yang, and Sihyun Park.

Additionally, I would like to express my heartfelt gratitude to Jungjae Park, who served as my advisor during my master's degree, for his invaluable advice and mentorship. His guidance enabled me to learn diatom analysis and understand paleoclimatology. I would also like to extend my thanks to Kota Katsuki, whose kind-hearted teaching helped me gain proficiency in diatom analysis. Lastly, I would like to thank Qiuhong Jin, Mark Constantine IV, Junbeom Bahk, and other lab members from SNU Quaternary Paleoclimatology, Paleoecology, and Biogeography Laboratory for their unwavering support.

I truly believe that "a blessing in disguise" was present throughout my entire experience. I am excited to embark on the next chapter of my journey as a scientist/researcher. I am grateful for the opportunities that UCLA has provided me, and I look forward to utilizing my knowledge and skills to make a positive difference in the world.

VITA

Education

Sept 2017 – Present	**University of California, Los Angeles (UCLA)** ***Ph.D. Candidate in Geography*** *(Advanced to candidacy in June 2019)**,*** Advisor: Dr. Glen Sproul dit MacDonald	**Los Angeles, CA, USA**
Aug 2015	**Seoul National University (SNU)** ***M.A. in Geography,*** Advisor: Dr. Jungjae Park	**Seoul, Korea**
Sept 2012	**University of California, Los Angeles (UCLA)** ***B.A. in Geography/Environmental Studies***	**Los Angeles, CA, USA**

Awards & Honors

- UCLA Doctoral Student Travel Grants for Conferences, Professional Development and Off-Campus Research (DTG), December 2021.
- Muir Fellowship August 2020.
- Laura Bassi Scholarship Foundation, 2nd set (publication support and partial fee waivers for editorial assistance), August 2020.
- UCLA Doctoral Student Travel Grants for Conferences, Professional Development and Off-Campus Research (DTG), December 2017.

Journal Publications (†: equal contribution)

1. M. Kirby, J. Barbosa, J. Carlin, G. MacDonald, J. Leidelmeijer, N. Bonuso, **J. Han**, B. Nauman, J. Avila, A. Woodward, S. Obarr, C. Poulsen, K. Nichols, R. Ramezan. Holocene hydroclimatic variability recorded in sediments from Maddox Lake (northern California Coast Range). *Quaternary Research*, 2023. https://doi.org/10.1017/qua.2023.18
2. **J. Han**, M. Kirby, J. Carlin, B. Nauman, G. MacDonald. A diatom-inferred water depth transfer function from a single lake in the northern California Coast Range. *Journal of Paleolimnology*, 2023. https://doi.org/10.1007/s10933-023-00281-0
3. K. Nichols, R. Ramezan, S. Arreola, M. Kirby, G. MacDonald, J. Carlin, J. Leidelmeijer, J. Avila, **J. Han**, B. Nauman, S. Loyd. Multiple Site Age-Depth Distribution Estimation using Paleoperspectives from Barley Lake, CA. *Environmetrics*, 2022. (in prep).
4. J. A. Leidelmeijer, M. E. C. Kirby, G. MacDonald, J. A. Carlin, J. Avila, **J. Han**, B. Nauman, S. Loyd, K. Nichols, R. Ramezan. Younger Dryas to early Holocene (12.9 and 8.1 ka cal yr BP) limnological and hydrologic change at Barley Lake, CA (northern California Coast Range). *Quaternary Research*, 103, 193-207. 2021. doi:10.1017/qua.2021.9
5. J. Park, **J. Han**, Q. Jin, J. Park, S. Yi. The Linke Between ENSO-like Forcing and Hydroclimate Variability of Coastal East Asia during the Last Millennium. *Scientific Reports*, 7(1), 8166, 2017. DOI:10.1038/s41598-017-08538-1

Conferences (*: presenter)

1. **J. Han***, M. E. Kirby, J. A. Carlin, B. Nauman, J. A. Leidelmeijer, G. S. dit MacDonald. Diatom-inferred Water Depth Transfer Function from a Single Lake in Northern California. *Annual Meeting of American Geophysical Union (AGU)*, Oral Presentation, New Orleans, December 2021.
2. **J. Han***. Diatom-inferred water depth transfer function from a single lake in Northern California. *Community Earth System Model (CESM)*, Oral Presentation, online, June 16, 2021.

3. J. A. Leidelmeijer*, M. E. Kirby, G. S. dit MacDonald, J. A. Carlin, N. Bonuso, S. J. Loyd, **J. Han**, B. Nauman, J. Avila, A. Woodward. Late Glacial to Early Holocene Paleolimnology inferred from Barley Lake sediments (Northern Coastal Ranges, California). *The Geological Society of America (GSA) Cordilleran Section – 116th Annual Meeting*, Conference paper, Pasadena, CA, May 2020.
4. M. E. Kirby*, G. S. dit MacDonald, J. Carlin, J. A. Leidelmeijer, J. Avila, A. Woodward, **J. Han**, B. Nauman, J. Barbosa, S. Hernandez, K. Campbell, L. Boggis, K. Nichols, R. Ramezan, C. Paulsen. The Holocene California Precipitation Dipole Tracked Using Lake Sediments. *The Geological Society of America (GSA) Cordilleran Section – 116th Annual Meeting*, Conference paper, Pasadena, CA, May 2020.
5. K. Campbell*, S. Hernandez, M. E. Kirby, G. S. dit MacDonald, J. Carlin, J. A. Leidelmeijer, A. Woodward, J. Avila, **J. Han**, B. Nauman, C. Poulsen. 12,500 years of Hydrologic Variability Recorded in Sediments from Tule Lake, CA. *The Geological Society of America (GSA) Cordilleran Section – 116th Annual Meeting*, Conference paper, Pasadena, CA, May 2020.
6. **J. Han***, G. S. dit MacDonald, M. E. Kirby, J. Carlin, B. Nauman. Analysis of Diatom Community Variation within Lake Depth in Surface Sediment Samples from Kelly Lake, California. *American Association of Geographers*, Poster Exhibition, Denver, Colorado, May 2020 (*canceled due to COVID-19*).
7. A. Woodward*, M. Kirby, J. Carlin, G. MacDonald, **J. Han**, B. Nauman, J. Avila, J. Leidelmeijer. A New Lake Sediment Record from North Yolla Bolly Lake (40° N) Reveals Multi-Scale Holocene Hydrologic Variability in Northwest California. *Annual Meeting of American Geophysical Union (AGU)*, Poster Exhibition, San Francisco, December 2019.
8. **J. Han*,** J. Park. Reconstructing Paleoenvironment of Hanon Paleo-Maar Lake in Jeju Island during the Last Deglaciation using Diatom Analysis. *Annual Meeting of American Geophysical Union (AGU)*, Poster Exhibition, Washington D.C., December 2018.
9. M. Kirby*, G. M. MacDonald, J. Carlin, J. Leidelmeijer, J. Avila, A. Rueckert, **J. Han**, B. Nauman, A. Woodward. The Late Holocene Dry Period identified in the Northern Coast Range of California (Barley Lake): Evidence for a mean state change in the average position of the California precipitation dipole?. *Annual Meeting of American Geophysical Union (AGU)*, Poster Exhibition, Washington D.C., December 2018.
10. J. Leidelmeijer*, M. Kirby, G. M. MacDonald, J. Carlin, S. J. Loyd, **J. Han**, B. Nauman, A. Woodward, J. Avila. Late Glacial to early Holocene paleolimnology inferred from Barley Lake sediments (Northern Coastal Ranges, California). *Annual Meeting of American Geophysical Union (AGU)*, Poster Exhibition, Washington D.C., December 2018.
11. J. Avila*, M. Kirby, G. M. MacDonald, J. Carlin, A. Woodward, **J. Han**, B. Nauman, J. Leidelmeijer. Using Holocene sediments from North Yolla Bolly Lake in the Northern Coast Range (CA) to investigate the California precipitation dipole. *Annual Meeting of American Geophysical Union (AGU)*, Poster Exhibition, Washington D.C., December 2018.

Teaching Experiences

Teaching Fellow at UCLA: **GEOG M110 & EEB M131 Ecosystem Ecology** (Fall 2022), **GEOG 106 World Vegetation** (Winter 2023)
Teaching Associate at UCLA: **GEOG 1 Earth's Physical Environment** (Winter 2020), **GEOG 5 People and Earth's Ecosystems** (Spring 2020; Spring 2021; Winter 2022; Spring 2022), **GEOG M102 Soil Environment** (Winter 2021), **GEOG M126 Environmental Change** (Fall 2020; Fall 2021)
Teaching Assistant at UCLA: **GEOG 111 Forest Ecosystems** (Spring 2019)
Teaching Assistant at SNU: **Biogeography** (Spring 2013), **Introduction of Geography** (Spring 2015)

Research Project and Work Experiences

California Precipitation Dipole: Spatiotemporal Variability and Forcings over the Past 3000 Years. National Science Foundation (NSF) Grant #1702825. 2017 – 2023.

Chapter 1 Introduction

As California has a large population and often limited water availability, and increasing drought impacts (Mann and Gleick 2015). It is becoming more and more important to understand prolonged hydroclimate anomalies such as droughts in the context of natural variability and what drives such fluctuations naturally over the long time-period of the late Quaternary (MacDonald et al. 2008; Woodhouse et al. 2010; Feakins et al. 2014; Kirby et al. 2014, 2019; Glover et al. 2017). Hydroclimate is a subdiscipline that investigates moisture fluxes in the atmosphere and surface (Legates 2000), so it examines the linkage between hydrologic cycles and the climate system. Due to the importance of understanding long-term base levels and variability in hydroclimate systems, especially in water-stressed regions, there are numerous paleoclimate studies in California because paleoclimate records are vital to understanding hydroclimate variability in the long-term. Long-term records provide important perspectives to future climate change in regards to potential human impacts on natural climatic variability (Smol and Cumming 2000; Colombaroli and Gavin 2010; MacDonald et al. 2016). In California, it is also important to provide a long-term perspective on the relationship between hydroclimatic variability and orbital and oceanic external forcings. This can be accomplished by reconstructing paleoclimate changes and comparing such records (Kirby et al. 2014; MacDonald et al. 2016).

Both Northern and Southern California have experienced varying degrees of prolonged aridity and associated vegetation impacts over the 21st century (Dong et al. 2019). There are many studies of terrestrial conditions in Northern California using fossil pollen and charcoal from lake sediments that have detected long-term climatic changes and their impacts in Northwestern California (Mohr et al. 2000; Whitlock et al. 2004, 2008; Bradbury et al. 2004; Briles et al. 2008, 2011; Colombaroli and Gavin 2010; Crawford et al. 2015; Briles 2017;

Knight et al. 2021, 2022; Leidelmeijer et al. 2021; Glover et al. 2021). However, research on hydroclimate variability within lakes is still needed. The earlier mid- to late Holocene and the glacial-interglacial transitions are optimal time periods to apply paleolimnological studies to decipher prolonged hydroclimatic anomalies (Smith et al., 2002) for better understanding near future climate change. Consequently, reconstructing paleohydroclimatic changes in Northern California Coast Ranges over the late Quaternary period using paleolimnological records would be of great value.

Southern California has also experienced periods of prolonged hydroclimate change over the late Quaternary (MacDonald 2007; Glover et al. 2017, 2021; Kirby et al. 2018). Sites such as Baldwin Lake and Lake Elsinore provide sedimentary records that extend into Pleistocene, providing paleohydroclimatic perspectives extending tens of thousands of years (Kirby et al. 2006, 2007, 2018; Glover et al. 2017, 2020; Martinez 2020). These long-term records from interior Southern California can be very helpful to comprehend the relationship between regional hydroclimate major climatic forcing factors such as the Earth's orbital variations.

There are various paleoclimatic archives (tree-rings, speleothems, oceanic sediments, etc), but lake sediment is one of the most valuable archives to provide long and continuous records of hydroclimate change in the past (Kirby et al. 2015; Saulnier-Talbot 2016; Melles et al. 2022) despite some difficulties in lake record interpretation (Mills et al. 2017). Lake sediment contains various sources of environmental information such as hydrology related biological and geochemical changes in the lake and inputs of materials outside lakes – sediment, pollen, charcoal, etc (Woodhouse 2004).

Salinity and lake level changes are perhaps the most robust paleolimnological indices to explore hydroclimate variability. Changes in salinity and lake water depth are sensitive

indicators of the variations in the precipitation to evaporation ratio (P/E), especially for closed lakes in arid and semi-arid regions (Fritz et al. 2010; Ramón Mercau and Laprida 2016). First, salinity reflects the amount of evaporation of lake waters. The evaporation of a closed lake exceeds water input during dry seasons, and it causes an increase in ion concentration of the lake, which leads to a rise of salinity (Fritz et al. 2010; Ramón Mercau and Laprida 2016). Salinity will increase based on the evaporative concentration, which usually is increased by climate drying, human-induced pollution, and seawater intrusion (Holmes 2001). Furthermore, salinity fluctuations can be interpreted as indicators of the frequency of droughts; high salinity indicates more prolonged and frequent drought (Fritz et al. 2000). Lake level change is another important indicator to comprehend hydroclimate variability from lake sediments. Water depth changes, especially from a closed lake, are influenced by the hydrological status of the lake, and it is triggered by the changes in temperature and/or the circulation of atmosphere and precipitation (Guo et al. 2016). Even if such changes are relatively small, the lake's biological, chemical, and physical environment fluctuate sensitively (Laird et al. 2011). Moreover, it has been shown that lake level change can be related to long-term radiative factors such as orbital forcing (Park and Cohen 2011). Lastly, lake level affects salinity for water bodies (Battarbee 2000), and lake levels and salinity changes are correlated with respect to effective moistures (Fritz et al. 2010), which indicate water balance (Davies et al. 2002). Therefore, fluctuations in salinity and lake level are significantly essential factors for rigorous hydroclimatic variability reconstruction.

Diatoms in lake sediments are a good indicator to estimate the variation of salinity and lake level. There are other bioindicators in lakes, such as ostracods and chironomids, but they are not as good as diatoms for salinity and lake level reconstructions (Battarbee 2000; Zhang et al. 2007). There are several reasons why diatoms are a good proxy indicator for both

factors: 1. Salinity and lake level are critical factors that shift diatom assemblages (Fritz et al. 2010). Salinity can be closely tied to the equilibrium of diatom assemblages in closed-basin lakes in arid and semi-arid regions, and it is related to the balance of evaporation and precipitation, such as drought frequency (Smol and Cumming 2000), 2. There are different dominant diatom species depending on salinity levels within a lake basin (Gasse et al. 1997; Fritz et al. 2010), 3. Additionally, there are benthic and planktonic diatom species, and the planktonic to the benthic ratio (P:B ratio) is one of the most reliable lines of evidence to detect lake level changes (Wolin and Stone 2010). There are several practical reasons why diatoms are an ideal indicator for paleolimnological studies; they are the prominent algal community in lake systems, well-preserved in sediments, well-studied in paleo- and neo-limnology (Gushulak et al. 2017). Therefore, investigating the variations of diatom fossil assemblages from lake sediments will provide a robust reconstruction of hydroclimate variability in the past. Although such reconstructions can be qualitative in nature, quantitative reconstructions of lake-level variations can also be derived from diatom-based statistical transfer function. Most importantly for regions of relatively scarce natural lakes, new research has shown that such quantitative transfer functions have recently been shown to be developable using transects of sediment samples from single lakes (Laird et al. 2010, 2011; Gushulak et al. 2017).

With the above research drivers and methodological considerations in mind, my dissertation consists of four research questions:

1) Is a single lake, with small size and relatively shallow water depth, sufficient to establish a diatom-inferred transfer function for lake depth from coastal Northern California where there are not many natural lakes?

2) Can the diatom-based transfer models be applied to fossil diatom flora and reconstruct lake level well, and if so, how has the hydroclimate of coastal Northern California changed over the Holocene?
3) How has the hydroclimate changed over the late Quaternary (MIS 5 – MIS 2) in Baldwin Lake, subalpine Southern California? How did the lake water depth and salinity change?
4) How do the past hydroclimatic variations revealed in the Northern California and Southern California paleohydroclimatic records relate to past changes in ocean conditions or radiative forcing such as produced by the Earth's orbital variations?

This dissertation consists of three linked studies in Chapter 2, 3, and 4 that are prepared in the context of producing peer-reviewed publications. Chapter 2, **A Diatom-Inferred Water-Depth Transfer Function from a Single Lake in Northern California Coast Ranges**, demonstrates developing diatom-based transfer functions is applicable to a small single lake in the Klamath Mountains, Northern California where there are not many natural lakes available for traditional development of a transfer function from multiple lakes. Chapter 3, **Holocene Hydroclimate Variations Reconstructed from Past Lake Level Fluctuations (10,100 cal yr BP to Present) in the Northern Coast Ranges of California**, validates the application and usefulness of the developed transfer functions from Chapter 2 and to reconstruct Kelly Lake water depth changes during the Holocene quantitatively and compare these to likely forcing factors. Chapter 4, **A 110 ka Late Quaternary Diatom Record of Salinity and Water Depth from Baldwin Lake, Subalpine Southern California**, demonstrates the late Quaternary hydroclimatic variations in San Bernardino Mountains focusing on salinity and water depth changes in Baldwin Lake and scrutinizes which drivers, how likely external drivers influenced on the hydroclimate.

Chapter 2 A Diatom-Inferred Water-Depth Transfer Function from a Single Lake in the Northern California Coast Ranges

(in Press as Han, J., Kirby, M., Carlin, J., Nauman, B., MacDonald, G. A diatom-inferred water-depth transfer function from a single lake in northern California Coast Range. *J paleolimnol* (2023). https://doi.org/10.1007/s10933-023-00281-0)

2.1 Abstract

This study examines the relationship between water depth and diatom assemblages from lake sediment surface samples at Kelly Lake, California. A total of 40 surface sediment samples (integrated upper 5 cm) were taken at various depths within the small (~3.74 ha) 5.7-meter-deep lake. Secchi depths, water temperature, pH, salinity, conductivity, and total dissolved solids were also measured. Some diatom species showed distinct association with depth (e.g., *Fragilaria crotonensis, Nitzschia semirobusta*). The relationship between the complete diatom assemblages and water depth was analyzed and assessed by depth cluster analysis, a one-way analysis of similarity, principal components analysis and canonical correspondence analysis. Statistically significant differences were found between the assemblages associated with shallow depth (0 m – 1.25 m), mid-depth (1.25 m – 3.75 m), and deep-water (3.75 m – 5.2 m) locations. The relationship between diatom assemblages and lake depth allowed two transfer models to be developed using the Modern Analogue Technique (MAT) and Weighted Averaging Partial Least Squares (WA-PLS). These models were compared and assessed by residual scatter plots. The results indicate that diatom-inferred transfer models based on surface sediment samples from a single, relatively small and shallow lake can be a useful tool for studying past hydroclimatic variability (e.g., lake

depth) from similar lakes in California and other regions where the large numbers of lakes required for traditional transfer function development may not exist.

2.2 Introduction

Paleolimnological transfer functions are often developed from multi-lake training sets and can be a useful paleolimnological tool for reconstructing many variables including lake depth (Gregory-Eaves et al. 1999; Gomes et al. 2014; MacDonald et al. 2016). However, in many hydrologically sensitive regions, including much of California (CA), natural lakes are relatively rare, making the use of multi-lake training sets unfeasible. CA has experienced prolonged hydroclimatic anomalies over the 21st century (e.g., severe droughts) that appear to be, at least in part, related to anthropogenic climate change (MacDonald et al. 2016; Swain et al. 2018; Dong et al. 2019; Glover et al. 2020; Zamora-Reyes et al. 2021). Understanding how recent CA hydroclimate variability relates to longer timescales (e.g., Holocene), natural variability has been an important topic of research over the past decade (Briles et al. 2011; MacDonald et al. 2016; Kirby et al. 2019). Unfortunately, instrumental climate records only extend back a little more than a century and do not capture the full range of potential natural hydroclimatic variability. Paleoclimatic approaches can provide proxy hydroclimatic records that extend back millennia. The proxy-climate archives provided by lake sediments are one useful source of such information, and although not as plentiful as in some regions, such lake archives are available in areas of CA.

Diatoms (Class: Bacillariophyceae), single-celled algae and phytoplankton, have been shown to be an important proxy indicator useful to investigate hydroclimatic variability as manifest in lake-level changes or changes in lake salinity (Fritz et al. 1991; Gasse et al. 1995; Smol and Cumming 2000; Battarbee 2000; Zhang et al. 2007; Kingsbury et al. 2012; Ramón

Mercau and Laprida 2016; Gushulak et al. 2017; Gushulak and Cumming 2020). There are several reasons why diatoms are good paleoenvironmental indicators – they are common in lake environments, they are sensitive to hydrological and limnological changes (e.g., lake depth, water chemistry), and their distinctive silica frustules are well-preserved and readily identified in lake sediments. Many studies have shown that diatoms can be used to reconstruct past variations in lake depths, including providing quantitative estimates using statistical transfer functions based on modern diatom-water depth relationships (Yang and Duthie 1995; Gregory-Eaves et al. 1999; Wolin and Stone 2010; Laird et al. 2010, 2011; Gomes et al. 2014; MacDonald et al. 2016).

This research will focus on diatom flora and water depth. Lacustrine hydrologic budgets, which are related to lake water depth, are closely associated with regional hydrologic budgets and the interplay between precipitation and evaporation. This association is especially robust in regions with strong seasonal precipitation/evaporation contrasts, such as CA and the American West, where winter precipitation and summer evaporation dominate the annual hydrologic budget of lakes (Shuman and Donnelly 2006; Wigdahl-Perry et al. 2016). Changes in lake level are closely related to paleohydroclimatic changes (Fritz 1990; Smol and Cumming 2000; Kirby et al. 2007; Blazevic et al. 2009; Laird et al. 2010; Kingsbury et al. 2012; MacDonald et al. 2016).

There are very few diatom-inferred paleoecological transfer functions from Californian lakes. Bloom et al. (2003) published a paper that established a diatom-inferred salinity and water temperature transfer function from a network of lakes (n = 57) in the Sierra Nevada. While the initial study was about salinity and water temperature, not water depth, this was expanded to include a water-depth transfer function in a subsequent publication (MacDonald et al. 2016). Unfortunately, few areas of CA outside formerly glaciated Sierra

Nevada contain an adequate lake density to make a traditional multi-lake-based diatom transfer function model.

In recent years, studies have shown that diatom-depth transfer functions can be successfully developed using multiple sediment surface samples taken from different depths in a single lake (Laird and Cumming 2009; Laird et al. 2010, 2011; Gushulak et al. 2017). The resulting transfer function can then be applied to sediment cores from the same lake (Laird and Cumming 2009; Laird et al. 2010; Faith and Lyman 2019). This approach is ideal for CA where lake basins in many regions are rare and the development of a multi-lake transfer function, which requires 30 lakes or more, is not possible. In this study, we address the question of whether or not there is a statistically significant difference in the diatom floral assemblages found in the sediments taken at different depths from a single lake. Moreover, we explore whether or not these relationships are statistically strong enough to develop diatom-depth transfer functions that could be applied to sediment cores from that same lake. The study site is Kelly Lake, a small lake in the mountains of northwestern CA. The results of this study support the potential wider usefulness of single-lake transfer-function development in other regions where there are insufficient lakes for traditional training-set development. Kelly Lake is also smaller and deeper than previously published sites from which such transfer function has been derived, increasing the range of lakes this approach might be applied to.

2.3 Study Site

Kelly Lake (41.91°N, 123.52°W; 1346 m asl) is located in the Klamath Mountains (Northern California Coast Range), approximately 10 km from the Oregon border (Figure 2-1). The study site is in the Confederated Tribes of Grand Ronde, Karuk, Cow Creek Umpqua, and Cayuse, Umatilla and Walla Walla Tribes' territory (Native Nation Digital 2021). The

lake is landslide formed, small (~3.74 ha), with a maximum water depth of 5.7 m. The surface drainage basin is small (~47 ha) and sits in sedimentary rocks and meta-volcaniclastic sedimentary rocks (Irwin 1994). Although presently a closed basin (as of 2019) with a small inlet, there is a spill point at the east shoreline, approximately 3 – 4 m above modern lake level, indicating that overflow is possible during wet years. Dead and felled trees are concentrated at the outlet area and suggest a dynamic lake level with flow over the spill. Some active springs characterize the surrounding drainage basin with modern inflow observed occurring at the lake's northwest shoreline. The vegetation surrounding the lake's fringe is mostly reeds and sedges, with submergent macrophytes and mosses near the shoreline. Above the shoreline, there is forested vegetation with an overstory of Jeffrey pine (*Pinus jeffreyi* Grev. & Balf.), Douglas fir (*Pseudotsuga menziesii* (Mirb.) Franco), sugar pine (*Pinus lambertiana* Douglas), incense cedar (*Calocedrus decurrens* (Torr.) Florin) and white fir (*Abies concolor* (Gord. & Glend.) Lindl. ex Hildebr.).

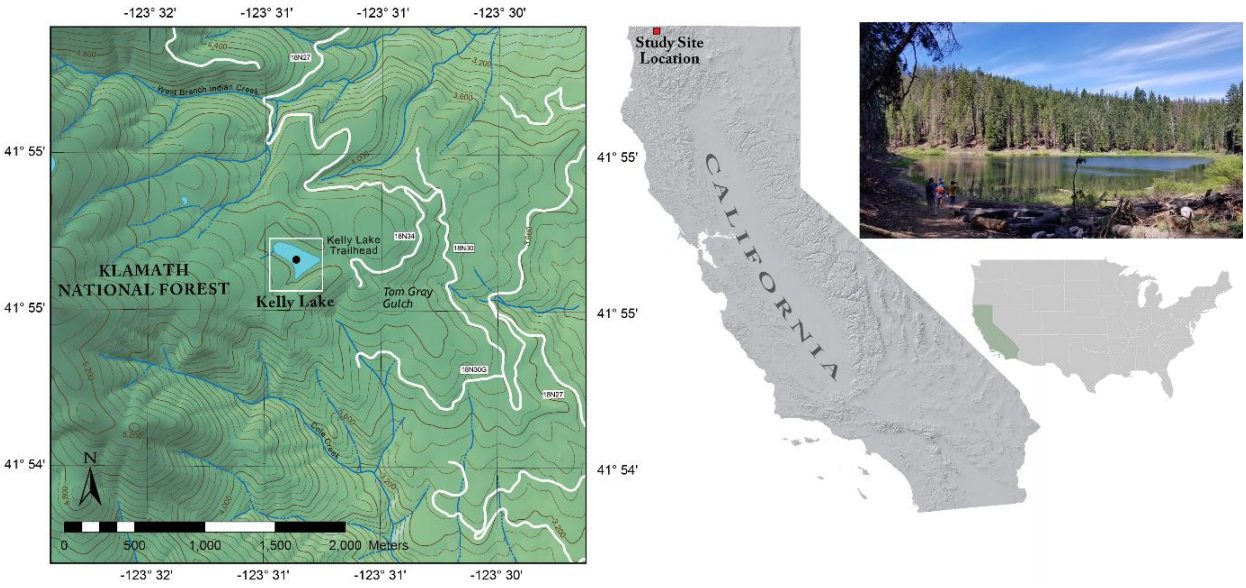

Figure 2-1 *Map and field picture of Kelly Lake in Klamath Mountains, California, USA. The view is from the outlet location approximately 3 – 4 m above modern lake level.*

The mean January and July temperatures of the region are approximately 3°C and 19°C, and the mean annual precipitation is 176 mm (Western Regional Climate Center 2016a; Figure 2-2). This data was collected from the Elk Valley Station (42.00°N, 123.43°W), which is the nearest station to the study site (~12km linear distance) at 521 m asl. The average winter precipitation (December, January, February) is approximately 353 mm, while the average summer precipitation (June, July, August) is roughly 17 mm. Kelly Lake experiences some snow during fall and winter, with ~ 1148 mm of total snowfall. Therefore, Kelly Lake's annual hydrologic budget is typical of the Mediterranean climate type and driven by variations in winter precipitation and summer evaporation.

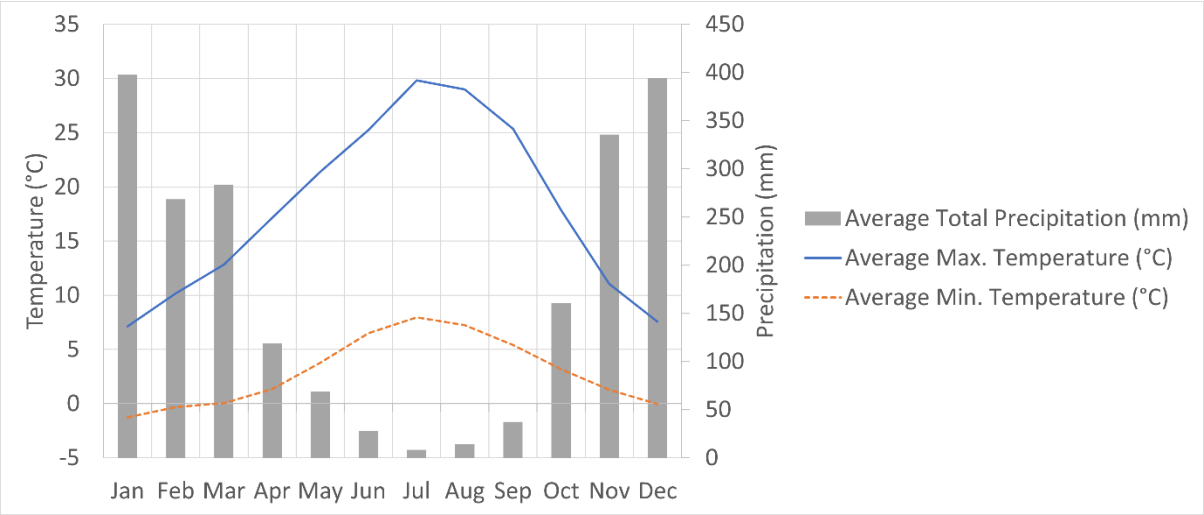

Figure 2-2 *Monthly mean precipitation and temperatures from Elk Valley in California, USA (site: 042749), which is the nearest climate station to Kelly Lake (Source: Western Regional Climate Center 2016).*

2.4 Methods

2.4.1 Fieldwork

In July 2019, 40 surface sediment samples were obtained at various lake-water depths from the upper 5 cm of the sediment-water interface using a mini-Glew gravity corer (Figure 2-3). Our sampling technique captured the sediment-water interface, visible in the clear plastic tube, ensuring that we did not over-penetrate into older sediments. The topmost sediments were extremely water-saturated with a diffuse sediment-water interface. We wished to obtain sufficient sediment for diatom analysis and other analyses from each surface site. We also were not aiming at the annual or near-annual resolution, but rather the integration of diatoms from the past decade or so to have an averaged observation of the diatom flora. We have obtained ^{137}Cs data from the central portion of the lake that indicate that the 1963 peak is deeper than 5 cm (5 – 10 cm) and ^{210}Pb data suggests sedimentation rates of ~3 yr/cm (Table 6-S2), therefore the upper 5 cm generally represents perhaps 15 years or so of time. Although there may have been some slight variations in lake conditions over this time period, we believe that our sampling regime captures a reasonable representation of the overall recent conditions of Kelly Lake. The samples were designated as KLSS2019 #. KLSS2019 1 to 26 and KLSS2019 33 to 40 were taken along three transects: nine samples from Transect 1, seventeen samples from Transect 2, and eight samples from Transect 3 (Figure 2-3, Figure 6-S1). Each sediment sample was collected at approximately 2 m distance from adjacent samples. KLSS2019 27 to 32 were collected at the very margin of the lake and from the lake's inlet emergent vegetation (Figure 2-3). Lake-water depths were measured at each sampling point. Secchi-disc depths were also measured at each sampling point to delineate the average depth of the modern photic and aphotic zones and the light

conditions at the sediment surface for each sampling point. Each sampling point with coordinates, the observed water depths, and Secchi-disc water depths were provided in Table 6-S3.

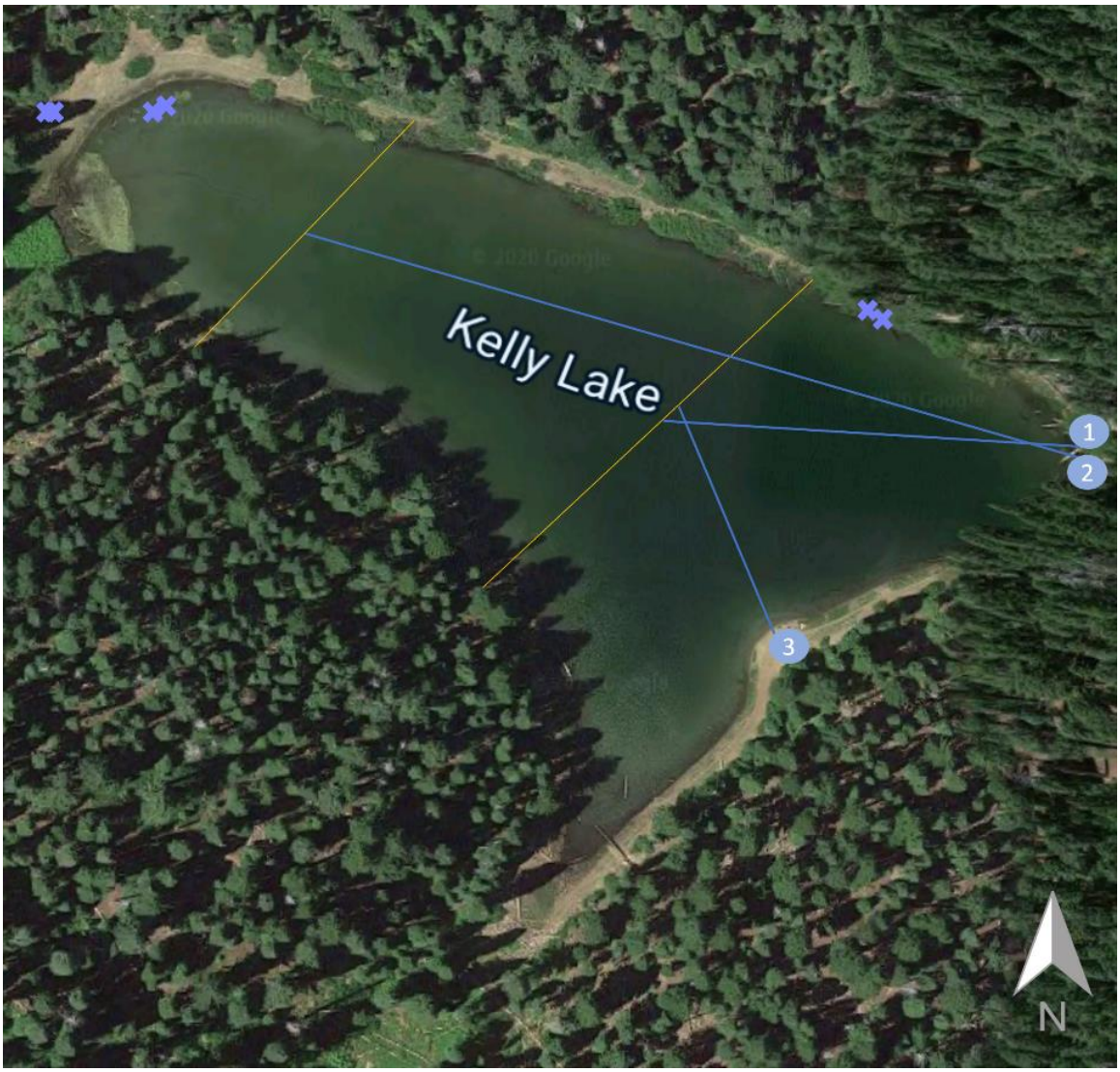

Figure 2-3 *Surface sediment samples from Kelly Lake (KLSS2019) were obtained along three transect lines (three blue lines with numbers 1, 2, 3) mostly (two yellow lines are ropes tied for the transects). Most samples were taken within the lake except for a few points near the margin and exposed shoreline outside of the lake (x marks). The samples along the transects were taken ~2 m apart at a constant interval.*

The lake's water chemistry was also measured near the surface at the center of the lake three times and averaged. Table 2-1 shows the average values of all the measurements. Five variables, such as pH, conductivity, water temperature, total dissolved solids, and salinity, were measured with a digital water testing meter (Apera Instruments PC60 Premium Multiparameter Tester Meter).

Table 2-1 *Average (n = 3) water chemistry and depth of photic zone in deep waters for Kelly Lake in July 2019.*

pH	Conductivity	Water temperature	Total dissolved solids	Salinity	Avg. photic zone depth
8.21	66.27µs/cm	23.4 ℃	42.57 ppm	0.03 ppt	4.12 m

2.4.2 Diatom sample preparation and identification

Approximately 0.2 g of wet surface sample was treated with 5 ml of 30% H_2O_2 in a 100-ml beaker with 10 ml of distilled water to remove organic materials in the sediments. After the sample was heated on a hot plate at 120℃ for an hour, the top solution was decanted. A micro spatula of sodium hexametaphosphate was put in the beaker for deflocculation. After 15 – 30 minutes of reaction, the beaker was filled with distilled water, and let the diatoms be deposited. The prepared diatoms were mounted using Pleurax (mountmedia) on microscope slides. At least 400 diatom valves were counted per sample at 1000x magnification under a light microscope (Nikon Labophot-2) with oil immersion. For diatom species identifications we followed the taxonomy of Krammer and Lange-Bertalot (1986, 1988, 1991a, 1991b) with supplementary printed and online sources (Kulikovskiy et al. 2016; Spaulding et al. 2019; Potapova et al. 2020; Jüttner et al. 2022).

2.4.3 Data selection and analysis

The taxa used for statistical analysis and calibration-set development were selected

after screening the diatom data. Taxa that appear at more than 5% abundance were selected for constructing the stratigraphic diatom diagram and constrained clustering, and taxa occurring at more than 1% abundance in at least one sample were chosen for statistical analyses and transfer function development. A diatom stratigraphy diagram was drawn in R version 4.1.3 (RStudio Team 2020) using the rioja package (Juggins 2020). A depth-constrained cluster analysis (CONISS) was also performed in R with the vegan package (Oksanen et al. 2020) to determine if lake-depth zones could be discerned in the diatom assemblages from Kelly Lake. The cluster analysis-based zones were calculated with the Bray-Curtis distance method to measure the dissimilarity between communities (Grimm 1987). A one-way analysis of similarity (ANOSIM) was also conducted using PAST (PAleontological STatistics, version 4.01) software package to test statistically the differences in the distribution of diatom assemblages among the identified depth zones (Hammer et al. 2001). Principal component analysis (PCA) was conducted in R on the covariance matrix to further explore differences in the diatom assemblages from different lake depths and the important diatom taxa contributing to those differences. Canonical correspondence analysis (CCA) with Monte Carlo permutation tests (999 permutations) was also performed in R with the vegan and CCP packages to examine if water depth is a significant variable on the diatom distribution for developing a transfer function (Oksanen et al. 2020; Menzel 2022). The CCA incorporated 22 diatom taxa from 40 surface samples and two environmental variables – water depth of the surface sample location and its depth below the photic zone as measured using the Secchi disc. Lastly, two diatom-inferred water-depth transfer functions were developed with the modern analogue technique (MAT), and with weighted average partial-least squares (WA-PLS) using the PAST software. The dissimilarity for MAT was measured using squared chord distance. The root mean square error of prediction (RMSEP) was estimated for both models, and the RMSEP values are based on the

degree of error between the observed and the expected value. Thus, the lower the value, the more significant it is.

2.5 Results

2.5.1 Diatom diagram

I identified over 150 diatom taxa in Kelly Lake. Among them, 21 taxa (14 genera and 17 species) were selected for statistical analysis. These all appeared at >5% abundances in at least one sample (Figure 2-4). There were thirteen benthic taxa (*Navicula* spp., *Achnanthidium* spp., *Achnanthicium rosenstockii* (Lange-Bertalot) Lange-Bertalot, *Gogorevia exilis* (Kützing) Kulikovskiy & Kociolek, *Gomphonema acuminatum* Ehrenberg, *Grunowia tabellaria* Rabenhorst, *Meridion constrictum* Ralfs, *Nitzschia semirobusta* Lange-Bertalot, *Pseudostaurosira parasitica* (W.Smith) E. Morales, *Staurosira construens* Ehrenberg, *S. venter* (Ehrenberg) Cleve & J.D.Möller, *Melosira* spp., *Fragilariforma nitzschioides* (Grunow) Lange-Bertalot), five planktonic taxa (*Aulacoseira* spp., *A. italica* (Ehrenberg) Simonsen, *A. pusilla* (F.Meister) A.Tuji & A.Houki, *Fragilaria crotonensis* Kitton, *Fragilaria* spp.), and three tychoplanktonic taxa (*Achnanthidium minutissimum* (Kützing) Czarnecki, *Staurosirella pinnata* (Ehrenberg) D.M.Williams & Round, *Pseudostaurosira brevistriata* (Grunow) D.M.Williams & Round). Due to the difficulties in identification under 100x light microscopy, some *Staurosira* spp., *Staurosirella* spp., *and Pseudostaurosira* spp. are counted together as *S & S & P* spp. Figure 2-4 shows the diatom diagram and the CONISS dendrogram where the Kelly Lake surface sediment samples are divided into three diatom-water depth zones: shallow (0 – 1.25 m), mid-depth (1.25 – 3.75 m), and deep-water zones (3.75 – 5.2 m).

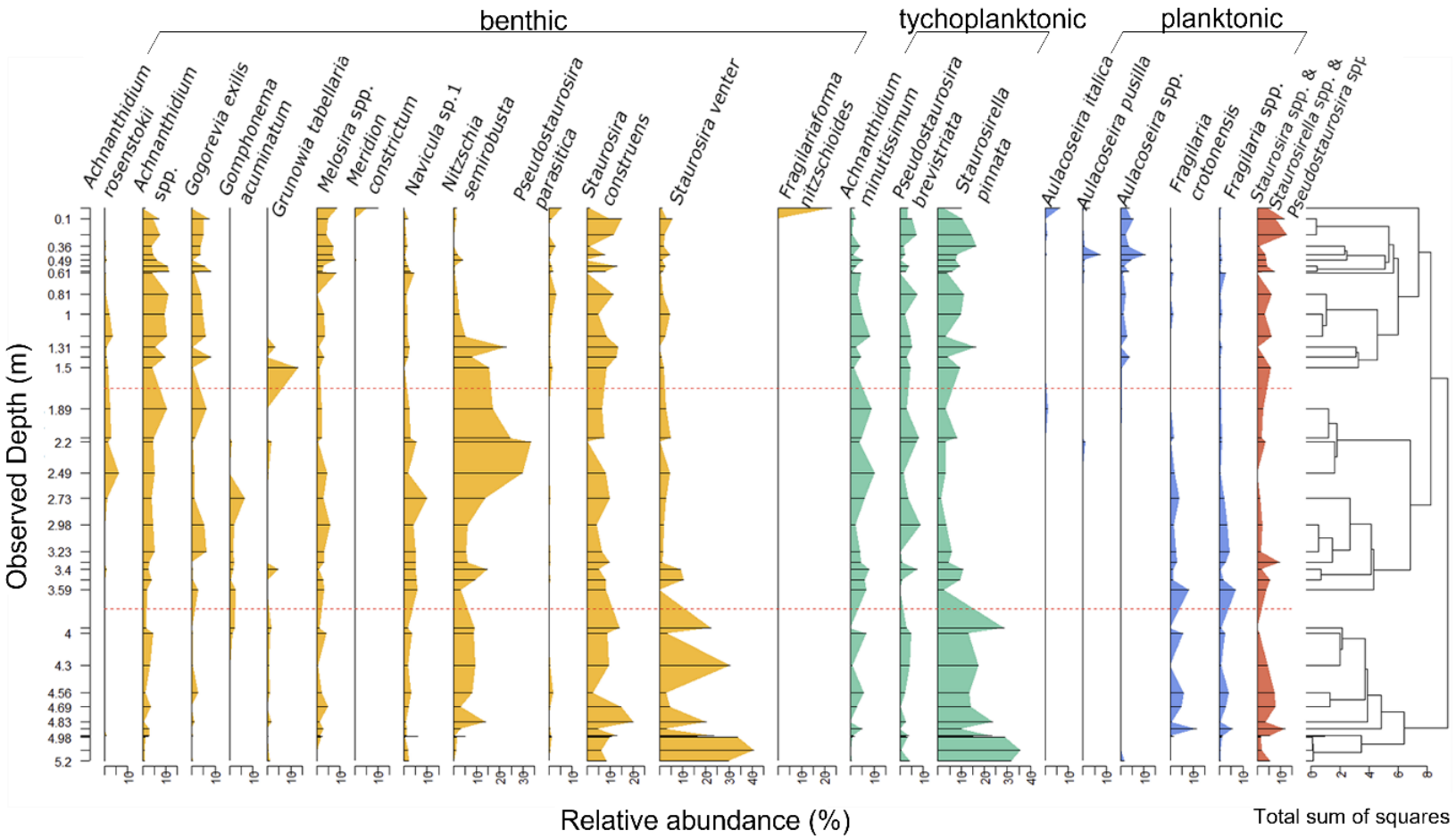

Figure 2-4 *Diagram of diatom taxa which appear in more than 5% in at least one sample in surface sediment samples from Kelly Lake (KLSS2019). The y-axis indicates lake-water depth. The x-axes indicate the relative abundances in % for the diagram part and the total sum of squares for the CONISS part. Yellow color-coded indicates benthic, green color-coded means tychoplanktonic, blue color-coded indicates planktonic, and red-color coded means sum of broken or unidentifiable girdle-view species from Staurosira spp., Staurosirella spp., and Pseudostaurosira spp.*

2.5.2 A one-way analysis of similarity (ANOSIM)

According to the CONISS analysis, Kelly Lake was divided descriptively into three depth zones, which are shallow (0 – 1.25 m), mid-depth (1.25 – 3.75 m), and deep (3.75 – 5.2 m). The deep-water zone generally represents samples where the sediment-water interface is in the aphotic zone of the lake. A cluster analysis that was unconstrained by depth and thus allowed samples to be freely grouped was also performed (Figure 6-S2). It displays prominent clusters of samples from the constrained cluster zones, particularly samples from the shallow and deep-water zones. However, there are also some clustering of mixed samples and some samples which do not cluster closely with any others. ANOSIM was subsequently conducted to determine whether there was a statistically significant difference between the three depth zones by examining the similarity of the diatom communities (Elmslie et al. 2020).

There are statistically significant differences between the three depth zones based on the result of ANOSIM. The P values in Table 2-2(a) indicate significant differences between the groups. The values are close to 0, which allowed us to reject the null hypothesis ("there is no difference") and indicated that there were statistically significant differences between the diatom assemblages from the three different water depth zones (i.e., shallow, mid-depth, and deep zones).

R values were also calculated in ANOSIM, which showed the strength of the depth factors on the samples. Generally, if an R value is lower than 0.2, it means that the factors had a small effect on the variables. However, the R values in Table 2-2(b) were larger than 0.2. Accordingly, it further indicates that the lake depth was influential on the composition of diatom communities observed in the lake sediments and the differences between the depth zones.

Table 2-2 *Results of ANOSIM significance parameters between depth zones of surface sediment samples from Kelly Lake. (a) indicates P values showing significance levels, (b) indicates R values showing the strength of the factors on the samples.*

(a) P values

	Shallow	Mid-depth	Deep
Shallow		0.0027	0.0001
Mid-depth	0.0027		0.0001
Deep	0.0001	0.0001	

(b) R values

	Shallow	Mid-depth	Deep
Shallow		0.2983	0.5265
Mid-depth	0.2983		0.4732
Deep	0.5265	0.4732	

Therefore, the ANOSIM results indicate that there were differences in the diatom communities by specific depth zones, and lake depth was an influential factor in the diatom assemblage composition in the sediments of Kelly Lake.

2.5.3 Principal component analysis (PCA)

The cumulative variation of PCA Axis 1 and Axis 2 was 70.5%, the first two axes were considered in this study (Figure 2-5). The diatom assemblages were clustered on the PCA biplot by depth, reinforcing the conclusion that lake depth has a strong control on the diatom assemblages preserved in the sediments. PCA Axis 1 appears to represent water depths between middle to deep, while PCA Axis 2 reflects shallow to middle water depths. The three most important diatom taxa in determining these PCA axes were *Staurosirella pinnata*, *Staurosira venter* and *Nizschia semirobusta*.

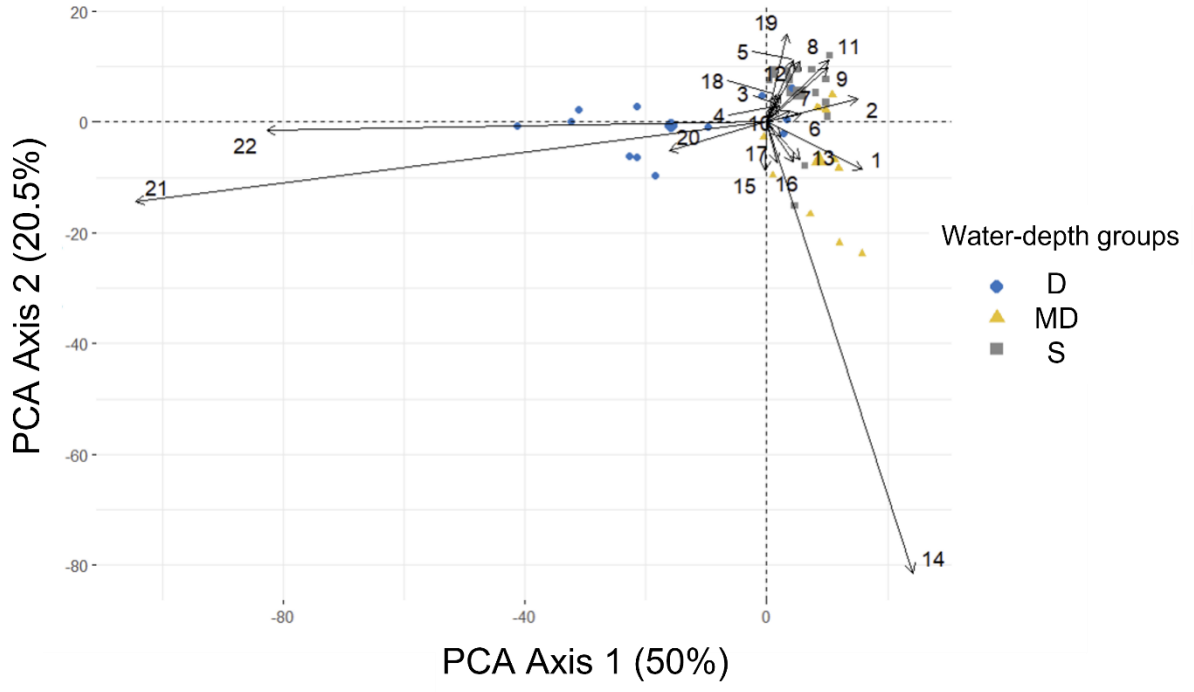

Figure 2-5 *Principal component analysis biplot showing main diatom taxa and the surface sediment samples by water-depth groups from Kelly Lake. Water-depth groups are: D: deep (3.75 – 5.2 m), MD: mid-depth (1.25 – 3.75 m), S: shallow (< 1.25 m). The diatom taxa codes are as follows: 1=Achnanthidium minutissimum, 2=Achnanthidium spp., 3=Aulacoseira italica, 4=Aulacoseira pusilla, 5=Aulacoseira spp., 6=Fragilaria crotonensis, 7=Fragilaria spp., 8=Fragilariforma nitzschioides, 9=Gogorevia exilis, 10=Gomphonema acuminatum, 11=Melosira spp., 12=Meridion constrictum, 13=Navicula sp. 1, 14=Nitzschia semirobusta, 15=Grunowia tabellaria, 16=Achnanthidium rosenstockii, 17=Pseudostaurosira brevistriata, 18=Pseudostaurosira parasitica, 19=Staurosira & Staurosirella & Pseudostaurosira spp., 20=Staurosira construens, 21=Staurosira venter, 22=Staurosirella pinnata*

2.5.4 Canonical correspondence analysis (CCA) with Monte Carlo permutation tests

Analysis of diatom-lake environment variables using CCA analysis, including data sets used for transfer function development, typically yield a percentage of diatom variance explained of between 4% to 23% (Weckström and Korhola 2001; Finkelstein et al. 2014). The CCA analysis indicates that the depth of the sampling site is important in determining the taxonomic composition of the diatom flora recovered. CCA Axis 1, which is strongly associated with lake depth at the surface sample location, accounted for 15.5% of the variance (Figure 2-6). CCA Axis 2 is more associated with the depth below the photic zone

and accounted for 1.3%. CCA Axis 1 was indicated as significant by Monte Carlo permutation texts ($p \leq 0.01$; Fig. S3). Species 8 = *Fragilariforma nitzschioides* and 12 = *Meridion constrictum* are associated with shallow and ephemeral sites and were found at the shallowest sampling sites at the edge of the lake and ordinate at the extreme negative end of CCA Axis 1, while 6 = *Fragilaria crotonensis*, 20 = *Staurosira construens*, 21 = *Staurosira venter*, 22 = *Staurosirella pinnata* are considered as planktonic and tychoplanktonic species, more likely to be relatively abundant in deeper waters, and ordinate at the positive end of CCA Axis 1.

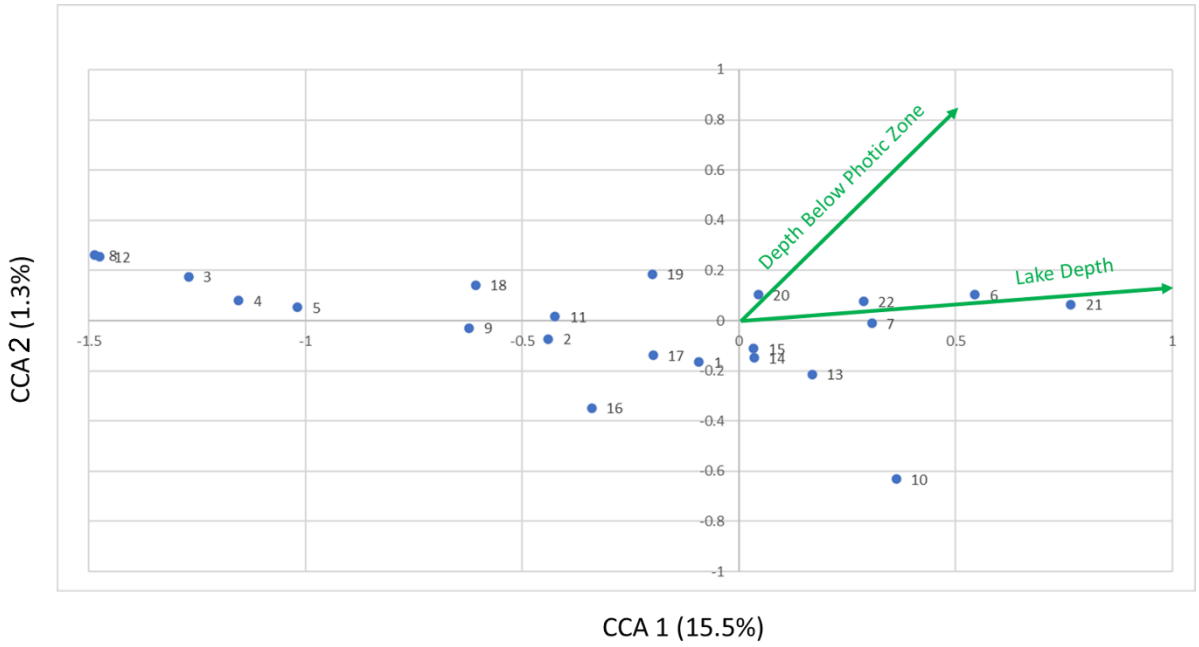

Figure 2-6 *CCA axis 1 vs. axis 2 biplot showing ordination of the main diatom taxa indicated by taxon species code (see Figure 2-5 for diatom taxa and codes) and with the axes loadings for the variables Lake Depth and Depth Below the Photic Zone.*

2.5.5 Diatom-lake depth transfer function models

Two diatom-lake depth transfer functions were developed using MAT and WA-PLS. Model construction incorporated diatom taxa that occur >1% in at least one sample.

The first diatom-inferred water depth inference model was developed using WA-PLS (Figure 2-7a). The R^2 value is 0.96 and indicates a high degree of correlation between the observed depths and diatom-inferred depths. In this study, the third component for WA-PLS has the lowest RMSEP value (0.66). Therefore, the third component was selected for the WA-PLS transfer function. As seen in the graphs (Figure 2-7a), the WA-PLS model performed better in mid-depths between 2 and 3 m than in shallow and deep depths.

The second transfer function was developed using the MAT method (Figure 2-7b). The R^2 value of the MAT transfer function is 0.98, and the RMSEP value is 0.39. In general, the MAT model displays good performance; it performs well in shallow and deep zones and shows a slight over-representation in the mid-depths.

a. WA-PLS transfer function

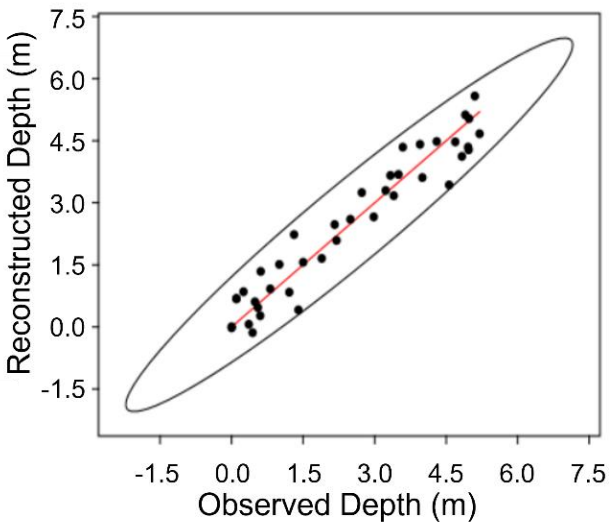

b. MAT transfer function

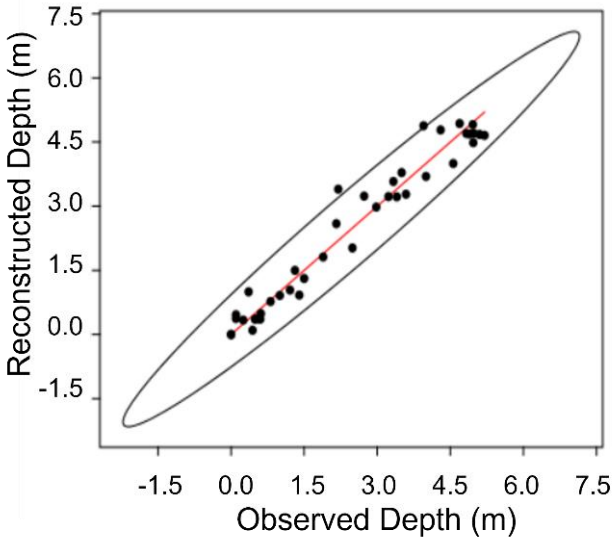

Figure 2-7 ***a.*** *Diatom-inferred water-depth transfer function using WA-PLS,* ***b.*** *Diatom-inferred water-depth transfer function using MAT. The 95% confidence ellipses are indicated.*

2.5.6 Residual scatter plots

Residual scatter plots (Figure 2-8) determined whether there is a trend, and thus a bias, in the models. This was done to determine whether there is a trend in residuals, and thus a bias, in the models. The residuals in the MAT model show a lower trend than the residuals in the WA-PLS model according to the R^2 values. The residuals in MAT are more scattered in the mid-depths, while the ones in WA-PLS are more scattered at the edges of the depths. Even though MAT shows a lower trend than WA-PLS, both have small R^2 values and small slopes. Thus, the residuals in both MAT and WA-PLS do not suggest a strong bias.

a. MAT residuals

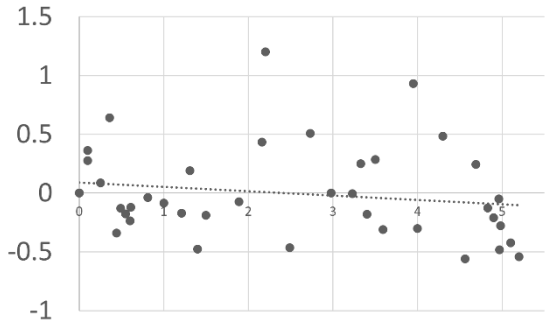

b. WA-PLS residuals

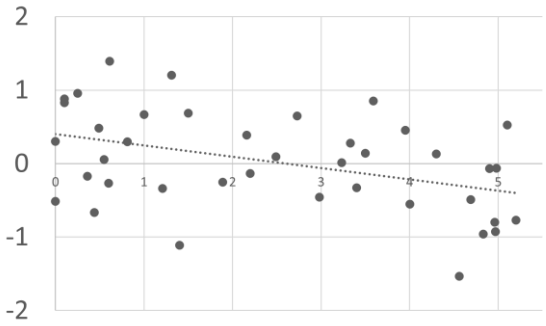

Figure 2-8 *Residual scatter plots for the two diatom-inferred water-depth transfer functions developed for Kelly Lake. a. Residuals of the MAT transfer function, b. residuals of the WA-PLS transfer function.*

2.6 Discussion

The statistical analysis indicates that the diatom assemblages found in the surface sediments at Kelly Lake can be statistically grouped into three different depth zones. There are at present a few studies that have examined the relationship between the composition of the diatom community and water depth from a single small lake (Laird and Cumming 2009; Laird et al. 2010, 2011; Gushulak et al. 2017). It is notable that the studies cited above are from boreal

Canada and represent lakes that are both much larger (19 ha – 1,808 ha) and deeper (18 m – 32 m) than Kelly Lake. Not only do our results extend the potential usefulness of single lake transfer functions to the Mediterranean climate region of CA, but they also demonstrate its applicability to relatively small and shallow lakes. Our study adds to growing evidence that differences in diatom assemblages related to lake depth are preserved in the sediments of small lakes and have the potential for developing lake-specific diatom-depth transfer functions. Some aspects of diatom ecology pertinent to the results, and the water depth inference models developed here are discussed below.

2.6.1 Diatom ecology

Although there are a variety of factors that affect diatom assemblages in the lacustrine environment, this study indicates that the diatom assemblage compositions in Kelly Lake have a clear correlation with lake-water depths. There are three depth zones identified in Kelly Lake: shallow (0 – 1.25 m), mid-depth (1.25 – 3.75 m), and deep zones (3.75 – 5.2 m). These three distinct depth zones are similar to those discerned for a previous single lake conducted in Canada; although there are many co-occurring diatom species in the Canadian lakes and this study, there were few equivalent major diatom assemblages (Laird and Cumming 2009; Laird et al. 2010). Recent work by Gushulak and Cumming (2020) indicates that light availability may be the most important factor controlling such depth-dependent diatom assemblage distributions within individual lakes. It is notable that at Kelly Lake the deep zone identified by the constrained cluster analysis is largely within the aphotic zone that ranges in depth from 3.32 – 4.90 m.

Although details of the ecology of many diatom species remain uncertain, the statistical results from Kelly Lake regarding depth and diatom assemblages can be assessed in light of the known ecology for some individual diatom taxa that show strong depth preferences. Some individual diatom taxa show strong depth preferences. For example, *Fragilaria crotonensis* rarely appears at shallow depths, but it begins to appear at middle depths and becomes dominant in deep zones (Figure 2-4). *F. crotonensis* is known as planktonic and non-motile (Morales et al. 2013). The species forms ribbon-like floating colonies and are associated with the pelagic zone. They prefer strong turbulence to stay afloat (Rioual 2000). *Staurosirella pinnata* is also one of the predominant species in the deep zone. Although some studies demonstrated *S. pinnata* as benthic or planktonic (Fluin et al. 2010; Laird et al. 2011; Park et al. 2017; Hofmann et al. 2020), it can be considered as tychoplankton because of its lifestyle (Hobbs et al. 2017). The species is also known as well adapting to low light penetration conditions (Laird et al. 2010). These characteristics of *S. pinnata* explain why it appears dominantly at larger depths in Kelly Lake, even under some low photic or aphotic conditions (Figure 6-S1) because it could inhabit greater depths as tychoplankton, or as a benthic form tolerant to low light conditions.

There are also many distinguishing species for mid-depth zones in Kelly Lake. *Nitzschia semirobusta* is the predominant species for the mid-depth zone. This species is known as a motile benthic species and has a wide tolerance for trophic status even though it favors oligotrophic conditions (Bartozek et al. 2018). As the water chemistry results from Kelly Lake indicate oligotrophic to mesotrophic conditions, it seems the water chemistry of the lake is favorable to *N. semirobusta*. Also, the environment with enough light penetration and the species' motility helped this species to be dominant in mid-depth areas.

Pseudostaurosira parasitica is mainly found in shallow depth zones, and this is readily explainable because the species is benthic and must remain in the photic zone to survive (Morales 2010b). Abundant *Aulacoseira* spp. are indicative of the shallow zone. The genus is well-known for including a variety of planktonic species, especially meroplankton (having both benthic and planktonic characteristics depending on their life cycle stages). There are possible reasons why *Aulacoseira* spp. appear more predominantly in the shallow than the deep in Kelly Lake. Some *Aulacoseira* spp. (e.g., *A. pusilla*) prefer shallow depths to take in more nutrients and light (Rioual 2000) or low lake level and enhanced convective mixing (Dean et al. 1984; Rioual 2000). These reasons might suggest why *Aulacoseira* spp. appears in shallow depth sediments in Kelly Lake.

In addition to the relationships between taxa and three depth zones, there are also a few species typically found in environments at the very margin/edge of the lake or near the shore (e.g., *Meridion constrictum* and *Odontidium mesodon*). These species inhabit very shallow or flowing water or live on emergent plants (Potapova 2009a; Hoidal 2013; Leira et al. 2017).

Conversely, some species are abundant at a wide range of depths, such as *Achnanthidium minutissimum* and *Pseudostaurosira brevistriata*. For example, *A. minutissimum* is ubiquitous in diatom-based, paleolimnological studies. Although they are normally classified as benthic, their habitat preferences are variable. Some studies have found that *A. minutissimum* occurs at ~2 m or shallower depths (Yang and Duthie 1995; Moos et al. 2005), while another study found it occurs at a broad range of depths (Laird et al. 2010). One study concluded that the species is largely found on submerged *Isoetes* (Haberyan 2018). While *A. minutissimum* may not be a useful species for representing distinct depth zones, it may signify zones of overall ecotone changes within a lake (Moos et al. 2005). Similarly, *P. brevistriata* has a complex ecology, classified as

tychoplanktonic and non-motile (Morales 2010a). As a result, it is not surprising that *P. brevistriata* is found at various depths at Kelly Lake.

By interpreting diatom assemblages according to each species' habitat preferences and the subsequent statistical results, we conclude that there are clear divisions based upon water depth zones, and water depth is a crucial factor in the composition of diatom assemblages preserved in the Kelly Lake surface sediments.

2.6.2 Water depth inference models

A good transfer-function model should meet two conditions: 1) observations and estimates must be strongly positively correlated, 2) there should be no trends in the residuals (Yoon et al. 2017). There are many ways to develop a transfer function, and WA-PLS and MAT are the two of the most common techniques (Bloom et al. 2003; Cunningham et al. 2005; Laird et al. 2011; Park 2011; Faith and Lyman 2019). In this study, both MAT and WA-PLS perform well in terms of the requisite conditions. However, overall, the MAT transfer model showed better performance than the WA-PLS model with higher R^2 and lower RMSEP values. However, for both transfer functions, the R^2 values were higher than 0.95, and both models showed good representations of diatom-inferred water depths.

In this study, the dissimilarity measure for MAT was determined using a squared chord, which is a metric to assess the signal-to-noise relationship. This distance metric is considered the best for evaluating modern analogs (Jackson and Williams 2004; Kemp and Telford 2015). It is said that chord-squared distance is more acceptable for closed compositional assemblage data, such as relative abundances, because it highlights the major patterns, while it down-weights rare species (Kemp and Telford 2015). Both MAT and WA-PLS are vulnerable to uneven sampling

of the elevation gradient (Kemp and Telford 2015), but most of the samples in this study have been collected evenly, so the weakness should not be influential here.

There are over- and under-estimations at deep and shallow depths in the WA-PLS model within the 95% confidence ellipse, and this could reflect the "edge effect" problem common for weighted average-based models, such as WA and WA-PLS (Birks 2010). This problem causes over- or under-estimations at the edges of the sample depths. However, Kemp and Telford (2015) argued that the influence of "edge effects" is lessened in WA-PLS. The results of our study show that WA-PLS does seem to present some "edge effect" as there are more variable residuals at deep and shallow depths (the edges; Figure 2-8b). The WA-PLS in this study performs better for the middle depths. Conversely, there are over-estimations in the MAT model for the mid-depth ranges, especially in the range of 2 and 3 m. Both models have over- or under-estimations at different depth zones; therefore, inferences of past depths might best be made by using both models.

2.7 Conclusion

There are clear, statistically significant differences between diatom assemblages and lake-depth in the surface sediments of Kelly Lake. The correlations are strong enough to develop single-lake diatom-inferred lake depth transfer models. Our findings indicate that a quantitative reconstruction of past lake depth using diatom assemblages is reasonable for Kelly Lake. As in many parts of the world, CA has few natural lakes outside of the formerly glaciated Sierra Nevada Mountains, yet regional information on long-term hydroclimatic variability throughout the state is very important in providing a context for 21st century climate change. Kelly Lake is in a different climatic zone and is also smaller in area and shallower in depth than the Canadian

lakes previously examined to develop single lake transfer functions for depth. This suggests a potentially wider applicability of this approach in terms of region being studied and lake characteristics. The ability to use surface samples from a single lake, coupled with a core from that lake to reconstruct past lake depths, is an important and still developing methodological advance for reconstructing past hydroclimatic variations.

Chapter 3 Holocene Hydroclimate Variations Reconstructed from Past Lake Level Fluctuations (~ 10,100 cal yr BP to Present) in the Northern Pacific Coast Ranges of California

3.1 Abstract

The diatom-inferred water depth transfer functions that were previously developed in Chapter 2 are applied to the Kelly Lake long core to reconstruct Holocene paleohydroclimatic variability in the Northern Pacific Coast Ranges of California. Both Modern Analogue Technique (MAT) and Weighted Averaging Partial Least Squares (WA-PLS) models successfully reconstructed the lake level changes at Kelly Lake, but the WA-PLS component 3 reconstruction performed better than the MAT reconstruction. Kelly Lake's water depth variations during the Holocene can be divided into three distinctive phases – early, mid, and late Holocene (i.e., Zone 1, 2, 3). The lake sediments captured the 8.2 ka event (shallowest, ~ 0.98 m) at ca. 8,100 cal yr BP, the Medieval Climate Anomaly (shallow, ~1.5 m) at ca. 950 cal yr BP, and the Little Ice Age (deepest, ~7.6 m) at ca. 800 cal yr BP. These records are consistent with some of the previous hydroclimatic studies in Northern California. The reconstructed paleohydrologic variability in the Northern California Coast Ranges suggested that the region was influenced by oceanic and atmospheric dynamics, based on the record of the sea surface temperatures off the coast of California (ODP 1019) and solar forcing records from the temperatures in the Northern Hemisphere ($\delta^{18}O$ NGRIP). This study contributed to supporting the use of the single lake transfer function methodology to a wider scope of geographic and environmental research sites.

3.2 Introduction

California has experienced enhanced hydroclimatic variability over the last decades. Hydroclimatic-related disasters such as severe droughts, wildfires, and deluges (e.g., Dixie Fire in 2019, 2022-2023 winter deluge) have become major problems in the state (Kirby et al. 2010; Swain 2015; MacDonald et al. 2016; Wang et al. 2017; Loisel et al. 2017; Dong et al. 2019; Zamora-Reyes et al. 2021; Williams et al. 2022). The California state government invested approximately $53.9 billion budget in 2022 to tackle extreme weather problems and the climate crisis (California 2022). It is important to place the hydroclimatic conditions of the present and anticipated future within a longer-term context. The goal of the research presented in this chapter is to reveal Holocene variations in hydroclimate in the Northern California Coast Ranges by quantitatively reconstructing paleo-lake level changes. The transfer functions developed in Chapter 2 are applied in this chapter to reconstruct quantitatively the past lake level changes at Kelly Lake over the Holocene.

Such regional studies are required as distinct patterns in Northern and Southern California in terms of hydroclimatic variations seem to be related to a hydroclimatic dipole between the north and the south (Dong et al. 2019). The hydroclimate/precipitation dipole defines the boundary, which is around 40°N, where precipitation see-saw signals occur (Dettinger et al. 1998; Wise 2010). This precipitation anomaly is influential to the hydroclimatic variability in California (Dettinger et al. 1998; Wise 2010; Dong et al. 2019).

The Northern Pacific Coast Ranges are a good place to capture natural hydroclimatic variations of the past and potential precipitation dipole effects. The latitude where Kelly Lake is located is approximately 42°N, which is close to the proposed 40°N boundary of the dipole. As

lake sediment preserves a good archive of long-time natural climatic records, the Kelly Lake downcore sediments will be studied in this chapter to research the past hydroclimatic variations of the region.

With this background in mind, the research questions from this chapter are as below:

1) Are the diatom-based MAT and WA-PLS transfer functions applicable to a small size and mid-water depth reconstruction at Kelly Lake? How close are the fossil diatom assemblages to the modern diatom assemblages?
2) What is the hydroclimatic variability over the Holocene in the Northern Pacific Coast Ranges apparent in the Kelly Lake fossil diatom record? Are these diatom-reconstructed variations supported by other sediment-based proxies from the lake?
3) How do major hydroclimatic variations in the North Pacific Coast Ranges as deduced from Kelly Lake compare to global drivers of climate change over the Holocene?

3.3 Background

3.3.1 Previous postglacial paleoenvironmental works in the Northern Pacific Coast Ranges

There are several postglacial paleoenvironmental and paleolimnological studies that have been conducted around the Northern California and Southern Oregon border region. These studies can be somewhat inconsistent in paleoclimatic interpretations.

Mohr et al. (2000) reconstructed fire history using charcoal and pollen records from Bluff Lake (41.33°N, 122.55°W, 1,921 m elevation) and Crater Lake (41.40°N, 122.58°W, 2,288 m elevation) in the eastern Klamath Mountains for the past 15,500 years. According to the study, the inferred climate was warm and dry during the early Holocene and wetter and cooler during

the late Holocene. The two lakes' records showed consistent fire event frequencies: high at ~ 8,400, 4,000, and 1,000 cal yr BP, and low at ~ 4,800 cal yr BP.

Bradbury et al. (2004) analyzed fossil diatom records from Upper Klamath Lake (42.40°N, 121.88°W, 1,263 m elevation) in south-central Oregon and inferred increased diatom productivity occurred after 15,000 cal yr BP. Dry conditions with lowering lake levels and extended marsh environments occurred during the mid-Holocene, returning shallow but open water environments after the mid-Holocene.

Briles et al. (2008) reconstructed vegetation and fire history from Bolan (41.90°N, 123.65°W, 1,550 m elevation) and Sanger (42.02°N, 123.46°W, 1,638 m elevation) Lakes in the Siskiyou Mountains and suggested low fire frequencies with increased Pacific Ocean upwelling and fog production during the early Holocene and cooling climate during the Late Holocene.

Starratt (2012) reconstructed Holocene lake level changes in Medicine Lake (41.61°N, 121.55°W, 2,036 m elevation) to the northeast of Mount Shasta in Northern California mainly using *Cyclotella*/*Navicula* diatom ratio and *Abies*/*Artemisia* pollen ratio. He concluded that the climate was relatively dry during the early Holocene followed by increased lake level with organic-rich fine-grained sediment deposited in the lake basin during the early to mid-Holocene. The Medicine Lake water level fluctuated with variations in effective moisture availability during the mid- to late Holocene after the lake was divided into two small shelf areas at around 5,500 years ago.

Crawford et al. (2015) researched the human land-use impacts on vegetation from sediment cores of Fish Lake (41.23°N, 123.46°W, 541 m elevation) and Lake Ogaromtoc (41.53°N, 123.57°W, 596 m elevation) in the western Klamath Mountains. They distinguished

human impacts from climate-driven vegetation changes by analyzing pollen and charcoal. They reconstructed that the mid-Holocene experienced a cooling pattern with increase in shade-tolerant vegetation, the Medieval Climate Anomaly (MCA) was warmer and drier with increased charcoal input and favored by shade-intolerant vegetation, the Little Ice Age (LIA) was a cool period with less fires and favored by shade-tolerant taxa. At the end of the LIA, the climate warmed with increased fires and open-forest and shade-intolerant vegetation developed.

Leidelmeijer et al. (2021) reconstructed the hydrological history of Barley Lake (39.58°N, 122.98°W, 1,658 m elevation) in the Mendocino National Forest during the Younger Dryas to the early Holocene. They revealed that during the Younger Dryas, biological productivity was low, and the lake was shallow and subsequently higher productivity developed during the early Holocene.

Kirby et al. (2023, accepted) studied relative lake level changes of Maddox Lake (40.55°N, 123.42°W, 857 m elevation) in Trinity County, California, by analyzing geochemical proxies. They observed high lake level during the 8.2 ka cooling event, lower lake level during the mid- to late Holocene including the MCA, and increased lake level during the LIA.

3.3.2 Study site

Kelly Lake (41.91°N, 123.52°W) is a small lake with a 4 ha lake area and 47 ha surface drainage basin. It is located at 1,346 m asl near Happy Camp, California (Figure 3-1). The lake sits in sedimentary and volcanic clastic rocks (Irwin 1994). The Klamath Mountains where the lake is located are in the northern California Coast Range. The site is in the traditional territory of the Confederated Tribes of Grand Ronde, Karuk, Cow Creek Umpqua, and Cayuse, Umatilla and Walla Walla Tribes (Native Nation Digital 2021).

The climate of the Klamath Mountains is a Mediterranean climate (dry warmer summer and wet cool winter) and under the influence of Pacific Tropical High (summer) and Aleutian Low (winter) (Bradbury et al. 2004; Crawford et al. 2015; Briles 2017). The Klamath Mountains stretch from the coast to over 200 km inland, so the temperature and precipitation varies latitudinally within the range. According to Briles (2017), the coastal regions in the mountains have more than 250 cm mean annual precipitation, while inland (near and east of Highway I-5) regions have mean annual precipitation between 30 to 80 cm. Kelly Lake near Happy Camp is located mid-way between the Pacific Ocean and I-5. The annual mean precipitation around the Kelly Lake region is ~125.7 cm (Western Regional Climate Center 2016a), which was measured at the closest station (Elk Valley, 42.00°N, 123.43°W) from the Happy Camp (Figure 3-2). The nearest station is at 521 m asl. and about 12 km far from Kelly Lake. The average winter precipitation (DJF) is ~ 35.3 cm with ~ 114.8 cm of total snowfall. The average summer precipitation (JJA) is ~ 1.7 cm. The surrounding vegetation around Kelly Lake in July 2019 mainly consisted of forest dominated by sugar pine (*Pinus lambertiana* Douglas), Jeffrey pine (*Pinus jeffreyi* Grev. & Balf.), incense cedar (*Calocedrus decurrens* (Torr.) Florin), Douglas fir (*Pseudotsuga menziesii* (Mirb.) Franco), and white fir (*Abies concolor* (Gord. & Glend.) Lindl. ex Hildebr.). Sedges, reeds, and mosses surrounded the lake margin, and there were a lot of submergent macrophytes in the water. More details of vegetation and field site of Kelly Lake can be found in 2.3 Study Site in Chapter 2.

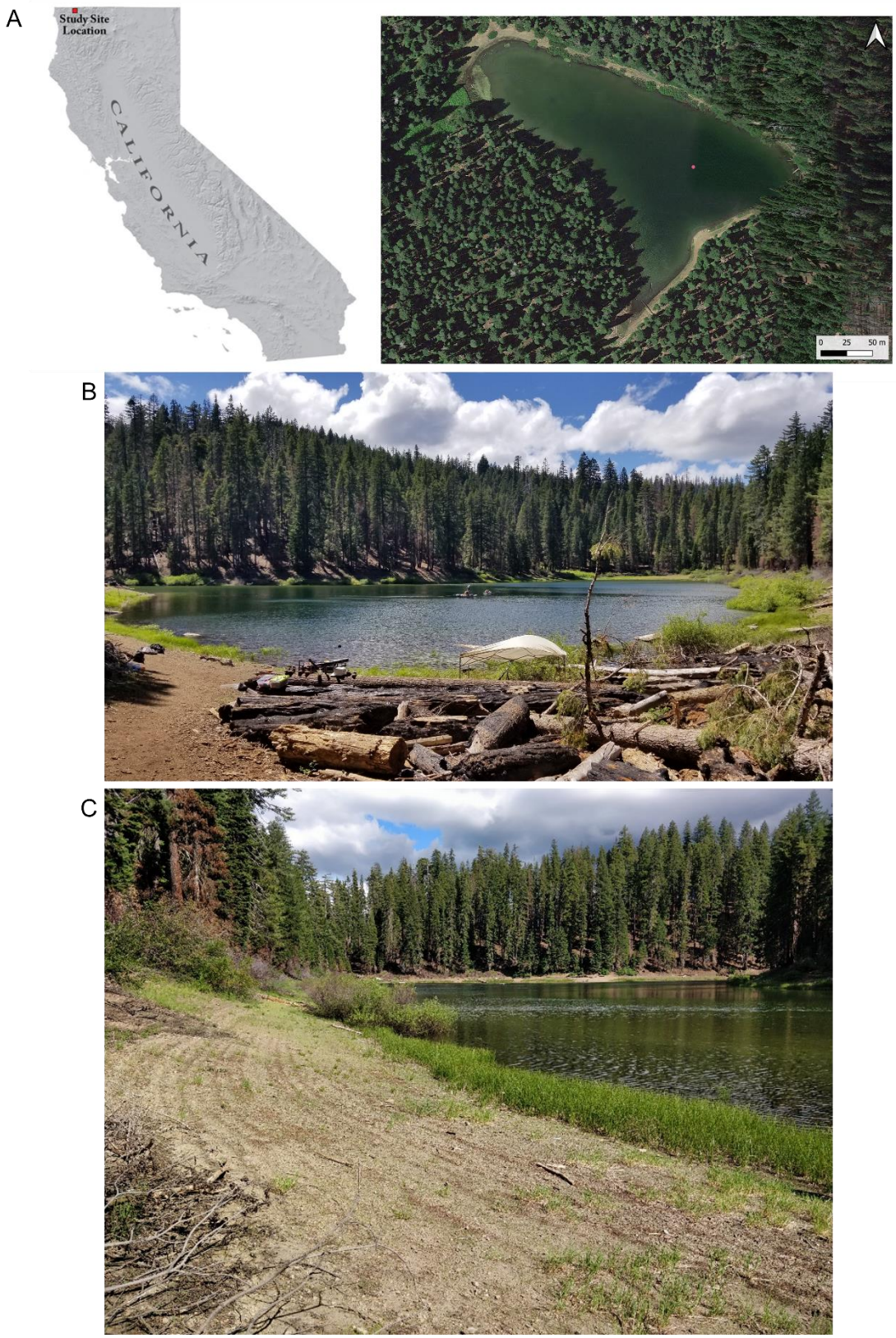

Figure 3-1 *A & B) A map and picture of Kelly Lake with KL19 coring point (pink dot) and C) shoreline changes at Kelly Lake (photo taken in July 2019).*

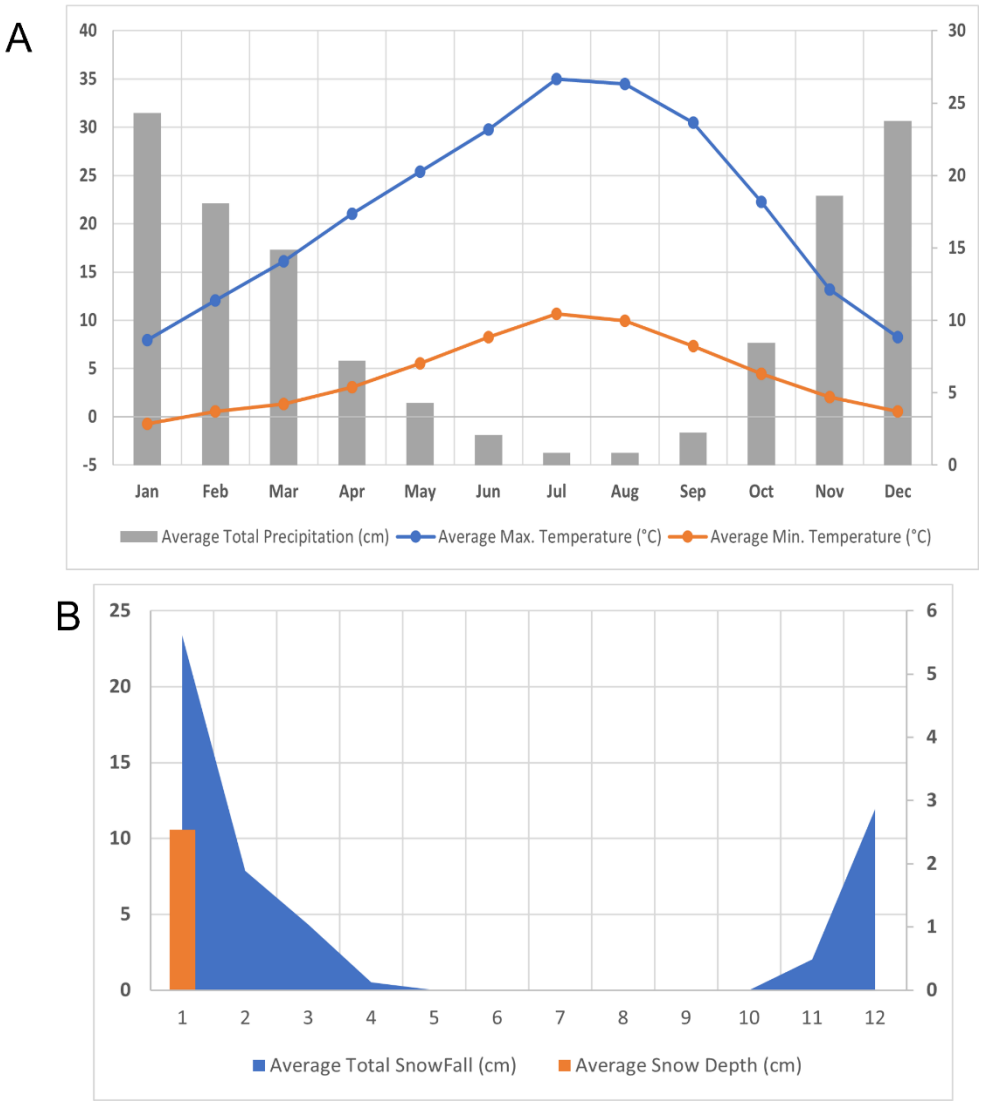

Figure 3-2 *A) Average total precipitation and average maximum and minimum temperatures, B) Average total snowfall and snow depth. The climate data was measured in the Happy Camp RS in the Klamath Mountains, which is the closest weather station from Kelly Lake (Western Regional Climate Center 2016a).*

3.4 Methods

3.4.1 Collecting sediment samples and data in the field

The sediment samples collected from the coring of Kelly Lake were designated cores KLGC19-1 and KLRC19-2 respectively. I refer to both cores as KL19 for simplicity. We recovered the two cores from the same spot because we could not recover the first 87.5 cm of KLRC 19-2 core. Therefore, KLGC19-1 (Gravity core) provides samples from the top of the sediments to a depth of 87.5 cm and KLRC19-2 (Russian core) provides samples for the rest of the core, which went down to 462 cm, and were used in this study.

The sediment coring was conducted July 16th, 2019. Immediately after the cores were extracted from the lakebed, they were moved to the lake shore and treated separately. After the Gravity core (KLGC 19-1) was collected, it was moved to a flat ground and subsampled. After letting the sediment core stabilize, it was subsampled at 1 cm intervals and bagged in whirl-paks. The Russian core, KLRC 19-2, was carefully opened in the field site over a clean tarp and the core stratigraphy described in notes and pictures. The core segments were wrapped in plastic and foil and placed in PVC pipes for protection during transport. We stored the cores at the University of California Los Angeles MacDonald Paleoclimate Laboratory (KLRC 19-2) and at California State University Fullerton Paleoclimatology Laboratory (KLGC 19-1) separately.

The water chemistry from the lake was also measured. The average water chemistry values (n = 3) indicated that Kelly Lake during the summer contained freshwater with low salinity, is oligo- to mesotrophic, and is warm (salinity = 0.03 ppt, pH = 8.21, conductivity = 66.27 μS/cm, water temperature = 23.4 ℃, total dissolved solids = 47.57 ppm) (Han et al. 2023).

3.4.2 Geochemical analyses: magnetic susceptibility (MS), % total organic matter (% TOM), % total carbonate (% TC), grain size

Geochemical analyses, such as MS, % TOM, % TC, and grain size, were performed at CSU Fullerton Paleoclimatology Laboratory. All the analyses were conducted at 1 cm intervals. MS was also measured by a Bartington MS2 magnetic susceptibility meter. The same samples were combusted to measure the sequential loss on ignition (LOI), such as % TOM and % TC, at 550°C and 950°C for 2 hours. To measure grain size, the samples were treated with 30% H_2O_2, 1N HCl, and 1N NaOH using a Malvern Mastersizer 2000 grain size analyzer with a Hydro 2000G dispersion unit. The same method was used following CSU Fullerton Paleoclimatology Laboratory protocols as referred to Kirby et al. (2007), Leidelmeijer et al. (2021), and Kirby et al. (2023, accepted) with references to Dean (1974) and Heiri et al. (2001). MS and % TOM were measured for both KLGC19-1 and KLRC19-2 cores, while %TC and grain size measurements were conducted only at KLRC19-2.

3.4.3 Radiocarbon dating: Bacon in R

Materials, such as woody material, pine needles, pieces of bark or pinecone, seeds, leaves, etc. from KLGC 19-1 and KLRC 19-2 were dated at W. M. Keck Carbon Cycle Accelerator Mass Spectrometer (KCCAMS) Facility at UC Irvine. The samples for radiocarbon dating were prepared with a three-day lab treatment including Acid-Base-Acid treatment (1N HCl, 1N NaOH, 1N HCl), combustion lab, and graphitization. Cs-137 and Pb-210 dating were also performed for the very upper part of the Gravity core in the Coastal and Marine Geology Laboratory at CSU Fullerton. A total of 23 dates were obtained. With the 23 dates, an age-depth model was established using rbacon age-depth modeling package using Bayesian statistics in RStudio to produce the KL 19 chronology (Blaauw and Christen 2011).

3.4.4 Diatom sampling and analysis

The sediment cores were subsampled at 8 cm intervals with ~ 137 years resolution, and a total of 59 samples were prepared for diatom analysis. To remove organic matter from the sediments, 0.1 g of wet samples were treated with 30% hydrogen peroxide (5 mL) and distilled water (10 mL). The samples were boiled at 120℃ for an hour and the top solution was decanted. To disaggregate diatoms from the sediment, one micro spatula of sodium hexametaphosphate was added for reaction (15 to 30- min). After doing 8-hr precipitation twice, the final solution was syringed on microscope scope slides using a micropipette, and diatoms are fixed on the slides using Pleurax (mountmedia). Hydrogen chloride was not applied because there were no carbonates at the study site.

Approximately 400 diatom valves were counted for each sample using a Nikon Labophot-2 light microscope at 1000x oil magnification. Diatom identification used the following references: Krammer and Lange-Bertalot (1986, 1988, 1991a, 1991b), Identification Book of Diatoms from Russia (Kulikoyskiy et al. 2016), and online sources (Kulikovskiy et al. 2016; Spaulding et al. 2019; Potapova et al. 2020; Jüttner et al. 2022).

3.4.5 Diatom stratigraphic data analyses

The diatom data from KL19 was cleaned and selected for stratigraphic and statistical analyses. First, the data was cleaned by identifying unknown species and/or merging down some unknown species that turned out to be similar/same taxa. After that, the raw data was transformed into a relative abundance (%) to select diatom taxa that appear at more than 5% abundance in at least one sample as dominant taxa. Depending on the characteristics of analyses, all data or 5% dominant taxa data were chosen for each analysis.

The stratigraphic diagram of diatom data was drawn in RStudio version 2022.12.0+353 (RStudio Team 2020). The rioja package was used for a stratigraphic diagram (Juggins 2020) to illustrate the changes in diatom assemblages over time. The variations in the diagram were zoned by a depth-constrained cluster analysis (CONISS) using the vegan package (Oksanen et al. 2020).

Diatom concentration (in valves/g of dry sediment) was also calculated using the modified equation (Equation 2) from Katsuki et al. (2003) with Dr. Katuski's advice.

$Diatom\ vavles\ per\ 1g\ of\ dry\ sediment$ [$valves$/1g of dry sediment]=$counted\ diatom\ valves$ [$valves$]×$cover\ slide\ glass\ area$ [$mm2$]$counted\ area$ [$mm2$]×$beaker\ water\ volume$ [mL]$pipet\ water\ volume$ [μL]×1000 [$mL \rightarrow \mu L$]×1$dry\ sediment\ volume$ [g]

($Dry\ sediment\ volume\ [g] = wet\ sediment\ volume\ [g]\ \times\ (1 - water\ content\ rate)$*) … Equation 3-1*

Diatom concentration shows the absolute number of diatom valves per 1 g of dry sediment in a unit of [valves/1g of dry sediment]. The absolute number of diatom valves can be impacted by water temperature, lake productivity, runoff, and so on (Han 2015), so it can be an indicator of lake productivity and other related environmental variables.

3.4.6 Principal Component Analysis (PCA)

PCA was performed with the 5% dominant taxa data to explore if there are distinctive groups of diatoms in the samples that may have ecological explanations related to lake depth. The analysis was conducted in CANOCO 5.15 (ter Braak and Šmilauer 2012).

3.4.7 Shannon-Wiener species diversity (H'), Hill's N2, Pielou's evenness (J'), and richness indices (S)

Community ecology analyses were applied to measure the ecological diversity of the diatom flora. Species diversity was measured by the Shannon-Wiener diversity index (*H'*) and Hill's N2. Hill's N2 provides more sensitive values in common species changes because *H'* examines the number of species that appear in a sample (relative abundance), while Hill's N2 shows the species' effective existence in a sample (Shannon 1948; Hill 1973; Weckström and Korhola 2001). Pielou's evenness index (*J'*) was also performed to examine how even the species in the samples were (Pielou 1966). If all the diatom species occur in equal numbers in a sample, then *J'*=1. If one species dominates then *J'* will be close to zero (Pielou 1966). Species richness (*S*) is a simple way of measuring biodiversity, which counts the number of different species in a sample. As the *S* from a sample is higher, it means the sample has richer taxa with more ecological complexity.

Each index was calculated with the following equations.

Shannon-Wiener species diversity index (H') = $-\sum P_i(\ln P_i)$ ... Equation 3-2

Pielou species evenness index (J') = $H'/\ln(S) = H'/H'_{max}$ ... Equation 3-3

Hill's N2 = $1/\sum P_i^2$ ... Equation 3-4

3.4.8 Planktonic to benthic (P:B) ratios

The dominant species which appear more than 5% in at least one sample was included to calculate P:B ratio with the following Equation 1 in Excel. A P:B ratio is an indicator of water depth. The higher P:B ratio, the more planktonic species, and it normally means that the water depth is deeper. In this study, plankton includes both planktonic and tychoplanktonic taxa.

$$P{:}B\ ratio = \Sigma planktonic\ taxa / \Sigma(planktonic + benthic\ taxa) \times 100 \quad \ldots \text{Equation 3-5}$$

3.4.9 Application of the transfer functions (MAT and WA-PLS) to downcore sediment samples

The diatom-lake depth transfer functions developed in Chapter 2 were applied to the downcore sediment samples from Kelly Lake (KL19) using C2 version 1.8.0 (Juggins 2007). After both surface sediment and downcore sediment data were input in C2, the software program applied to the transfer functions and calculated past lake levels. Both Modern Analogue Technique (MAT) and Weighted Averaging Partial Least Squares (WA-PLS) were applied with cross-validation such as leave-one-out and bootstrapping.

3.5 Results

3.5.1 Core stratigraphy

KLGC 19-1 was driven from 0 – 87.5 cm using a Gravity corer (Figure 3-3A). The core was homogenous medium to dark brown mud. KLRC 19-2 was driven from 87.5 – 462 cm using a Russian corer (Figure 3-3B, C, D, & E). The overall color of the cores was mostly brown, in variations from light brown to dark brown. The color gradually became grayish toward the bottom of the core. At the top of the core, it was medium-brown organic-rich sediment with gyttja until 275 cm (D1, D2 or Figure 3-3B & C). The D3 (Figure 3-3D) core from 275 to 375 cm was also organic-rich with color variations in light, red, and medium brown with faintly banded layers (~ 0.25 – 2 cm width). Also, there were many organic macrofossils. At the bottom of the cores (D4, Figure 3-3E) between 375 to 387.5 cm, there were faint laminated layers with clastic-rich sediment. At 413.5 – 414 cm, the layer was a pinkish tan layer with possibly a tephra layer. Based on the age-depth model, the thin tephra layer was at ~ 7,700 cal yr BP, so it is likely

to be related to Mazama Ash, but it was not sent and examined at the USGS for accuracy. At 406 to 412 cm, a large pinecone was found. Overall, the core was brown and organic-rich with a good number of macrofossils (e.g., seeds, woody fragments, pinecones, twigs, etc.).

Figure 3-3 *Core stratigraphy images of KLGC 19-1 and KLRC 19-2. A) KLGC19-1 (0 – 87.5 cm), B-E) KLRC19-2 Drive(D) 1 (87.5 – 175 cm), D2 (175 – 275 cm), D3 (275 – 375 cm), and D4 (375 – 462 cm).*

3.5.2 Chronology of KL19 using a Bacon Age-depth model

The result of 23 dates was provided in Table 3-1.

Table 3-1 *KL19 calibrated dating result (^{14}C, ^{210}Pb, and ^{137}Cs) measured at UCI Keck Lab and CSU Fullerton Coastal and Marine Geology Lab.*

UCIAMS ID	Sample name	Depth (cm)	fraction modern	±	D^{14}C (‰)	±	^{14}C age (BP)	±	cy BP for surface, Cs137, and Pb210	Material Dated ALL USED IN AGE MODEL (Bacon 07/12/22)
KLGC19-2	surface	0.5						0	-69	surface
KLGC19-3	Cs-137	7.5						2	-13	Cs-137
KLGC19-4	Pb-210	22.5						27	61.1	Pb-210 (PLUM)
KLGC19-1 264234	KLGC19-1 40-41 cm .15mgC	40.5	0.9565	0.0016	-43.5	1.6	355	15		woody material
KLGC19-1 264235	KLGC19-1 80-81 cm .015mgC	80.5	0.8581	0.0103	-141.9	10.3	1230	100		woody material
KLRC19-2 229282	KLRC19-2 129-130cm .13mgC	129.5	0.8701	0.0020	-129.9	2.0	1120	20		pine needle
229283	KLRC19-2 142-143cm	142.5	0.8557	0.0019	-144.3	1.9	1250	20		pine needle
264236	KLRC19-2 176-177 cm .10mgC	176.5	0.7496	0.0018	-250.4	1.8	2315	20		charred wood and insect parts?
229284	KLRC19-2 196-197cm	196.5	0.7700	0.0018	-230.0	1.8	2100	20		piece of pine cone or bark?
229285	KLRC19-2 204-205cm	204.5	0.7636	0.0019	-236.4	1.9	2165	25		pine needle
229286	KLRC19-2 240-241cm .21mgC	241.5	0.7145	0.0016	-285.5	1.6	2700	20		pine needle
229287	KLRC19-2 268-269cm	268.5	0.6869	0.0015	-313.1	1.5	3015	20		piece of pine cone?
264237	KLRC19-2 280-282 cm combo .054mgC	281	0.6433	0.0046	-356.7	4.6	3540	60		woody and charred material
229288	KLRC19-2 306-307cm	306.5	0.6239	0.0014	-376.1	1.4	3790	20		pieces of bark?
229289	KLRC19-2 327-328cm	327.5	0.5986	0.0013	-401.4	1.3	4120	20		wood - not charred
229290	KLRC19-2 350-351cm	350.5	0.5615	0.0013	-438.5	1.3	4635	20		pine needle
229291	KLRC19-2 365-366cm	365.5	0.5205	0.0014	-479.5	1.4	5245	25		piece of pine cone? and small pine needle
229292	KLRC19-2 397-398cm	397.5	0.4742	0.0013	-525.8	1.3	5995	25		pine needle
229293	KLRC19-2 404-405cm	404.5	0.4474	0.0011	-552.6	1.1	6460	20		pieces of wood - uncharred
229294	KLRC19-2 425-426cm	425.5	0.4038	0.0010	-596.2	1.0	7285	25		leaf
264238	KLRC19-2 435-437 cm combo	436	0.3864	0.0009	-613.6	0.9	7640	20		woody and charred material
264239	KLRC19-2 446-447 cm	446.5	0.3376	0.0008	-662.4	0.8	8725	20		seeds
264240	KLRC19-2 456-457 cm .11mgC	456.5	0.3261	0.0023	-673.9	2.3	9000	60		seeds

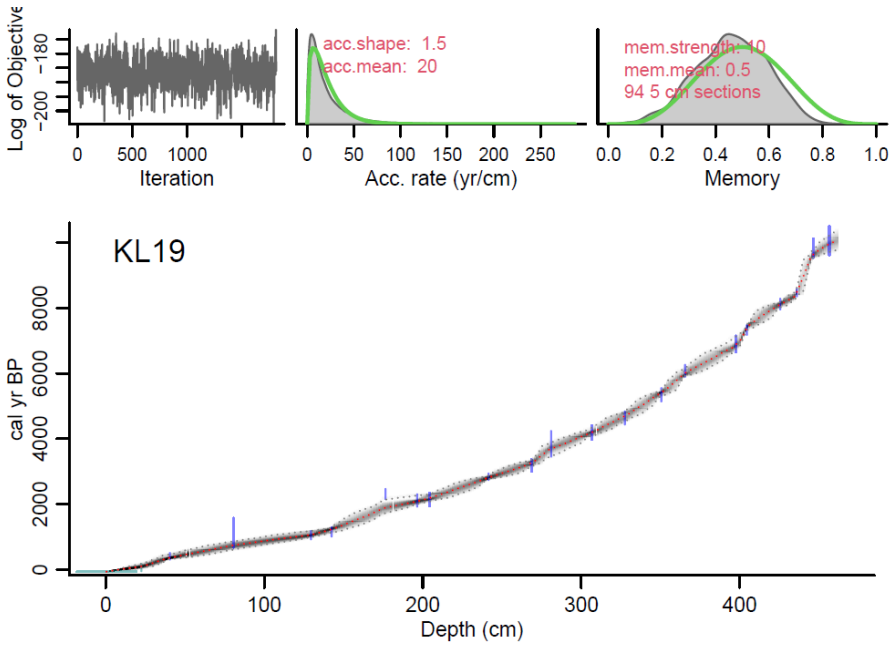

Figure 3-4 *Chronology of KL19*

The weighted mean average ages of KL19 sediments from rbacon age model in RStduio were turned out from -65 cal yr BP (0cm) to 10,062 cal yr BP (462 cm); – 65 cal yr BP is 2,015 CE (common era), and 10,062 cal yr BP is 12,012 BCE (before the common era).

3.5.3 Sediment analyses: MS, % TOM, % TC, grain size

The results of MS, % TOM, % TC, and grain size are provided in Figure 3-5 at 1cm intervals. In the paleolimnology field, MS is an indicator of soil erosion, runoff, and clastic input from lake watersheds (Blumentritt and Lascu 2014; Leidelmeijer et al. 2021). Normally, a high value indicates more runoff/high precipitation/deep water depth, while a low value means less runoff/low precipitation/shallow water depth (Kirby et al. 2023, accepted). According to the MS result, Kelly Lake had high runoff and clastic input during the early Holocene in general with peaks at 9,716 and 9,752 cal yr BP (MS = +0.6). During the mid-Holocene, there is another peak at 5,850 cal yr BP (MS = +0.7). Afterward, the MS kept decreasing and maintained a fairly flat except for the big trough at 1,910 cal yr BP (MS = -1.4).

The LOI results such as % TOM and % TC are also provided in Figure 3-5. It shows the organic matter and carbonate contents in Kelly Lake sediments. There was not enough material left after LOI 550°C above 88.5 cm, so there was no data for % TC above the depth. Allochthonous (terrestrial origin) and autochthonous (in situ origin) sources can be detected by % TOM (Kirby et al. 2007). A high % TOM indicates a shallow lake level (Kirby et al. 2007). Also, % TC indicates relative lake levels; a high % TC represents shallow lake depth (Kirby et al. 2007). In Kelly Lake, the low % TOM and % TC suggested consistency with what the MS results represented in deep water during the early Holocene. The changes in % TOM and % TC from Kelly Lake's downcore record have an increasing trend at a long-time scale with higher variability as it goes to the late Holocene. % TC increased a little bit during the early and mid-

Holocene, but it dropped abruptly at 4,408 cal yr BP, and it showed several troughs (856, 1,000, 1,349, 2,335, & 2,590 cal yr BP) and high ridges (1,861 & 2,106 cal yr BP) during the late Holocene. % TOM displayed more variability than % TC. It abruptly declined at 9,716 cal yr BP during the early Holocene and continued to increase before the mid-Holocene. During the mid-Holocene, it maintained steady in general except for the maximum peak at 7,623 cal yr BP. It reached the minimum at 1,519 cal yr BP and began to oscillate a lot at around 1,070 cal yr BP.

The grain size results are shown in Figure 3-5, such as % clay, % silt, and % sand. In general, high % clay values are often used for an indicator of deep-water depth, and higher % sand values are considered as higher precipitation with more runoff into a lake basin (Kirby et al. 2014; Leidelmeijer et al. 2021; Kirby et al. 2023, accepted).

Overall, % clay is negatively correlated with % silt. The % sand is partially negatively correlated with % silt. All the values had relatively low variability during the early Holocene, and as it entered mid-Holocene, the values began to fluctuate greatly until the early Holocene. During the Holocene, % clay had a decreasing trend line, while % sand showed a slightly increasing trend line. % clay maintained high during the early Holocene with an abrupt increase at around 9,000 cal yr BP. % clay slowly decreased and maintained slightly low until and started to rise at around 1,500 cal yr BP. % sand values maintained relatively low (~ 10%) until ~ 5,000 cal yr BP, and it rose to ~ 15% after then. It decreased ~ 0% at around 3,800 cal yr BP and increased again ~ 3,150 cal yr BP. % sand maintained fairly steady afterward with the highest peak (36%) at 1,150 cal yr BP. % silt showed a similar trend with % sand overall.

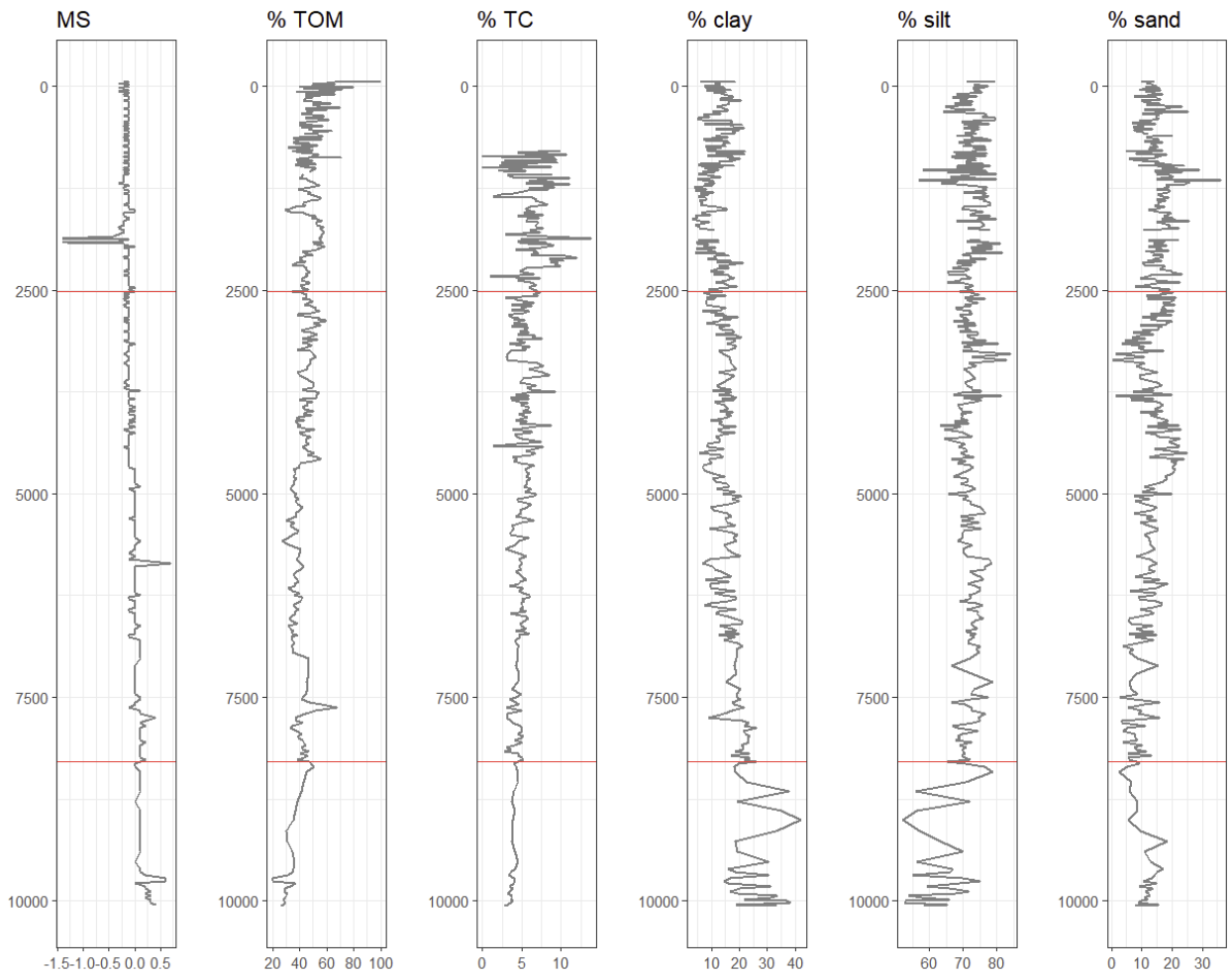

Figure 3-5 *Geochemical results such as magnetic susceptibility (MS), LOI (% TOM & % TC), and grain size (% clay, % silt, & % sand) at 1cm intervals.*

3.5.4 Diatom stratigraphy and diatom concentration

Approximately 160 taxa were identified from Kelly Lake downcore sediment samples. 25 taxa were chosen as major species which appeared at more than 5% in at least one sample. There were 25 taxa with 5 spp. level identification. The major diatom assemblages' stratigraphy is shown in Figure 3-6 with CONISS clustering results (Bray-Curtis distance method). The diatom taxa are colored yellow (benthic), green (tychoplanktonic), and blue (planktonic) based on habitat preferences. Several species are 3 times exaggerated by the grey shading to indicate very low values in certain ranges. Based on the diatom assemblages from KL19, three zones can be

recognized with boundaries at 8,293 and 2,520 cal yr BP with the similarity in diatom assemblage changes and the reconstructed lake level changes (Figure 3-6).

Three zones were determined based on CONISS. Zone 1 (0 – 2,520 cal yr BP, 0 – 225 cm) has dominant species of *Encyonema minutum* (Hilse) D.G.Mann, *Melosira* spp., *Navicula sovereignii* Bahls, *Navicula* spp., *Navicula* sp.1, *Nitzschia fonticola* (Grunow) Grunow, *Nitzschia semirobusta* Lange-Bertalot, *Punctastriata mimetica* E.A.Morales, *Achnanthidium pusillum* (Grunow) Czarnecki, *Sellaphora pupula* (Kützing) Mereschkovsky, *Achnanthidium minutissimum* (Kützing) Czarnecki, *Staurosira construens* Ehrenberg, *Staurosira venter* (Ehrenberg) Cleve & Möller, *Staurosira* sp.1, *Staurosirella pinnata* (Ehrenberg) D.M.Williams & Round, *Fragilaria crotonensis* Kitton, Zone 2 (2,520 – 8,293 cal yr BP, 225 – 433 cm) appear dominated by *Encyonema minutum, Encyonema perelginense* Krammer, *Encyonopsis subminuta* Krammer & E.Reichardt, *Melosira* spp., *Navicula radiosa* Kützing, *Navicula* spp., *Navicula* sp.1, *Nizschia fonticola, Sellaphora pupula, Achnanthidium minutissimum, Staurosira construens, Staurosira venter, Staurosirella pinnata, Fragilaria crotonensis, Fragilaria* spp. as the dominant species, and Zone 3 (8,293 – 10,062 cal yr BP, 433 – 462 cm) is typified by *Epithemia* spp., *Gomphonema gracile* Ehrenberg, *Gomphonema* spp., *Melosria* spp., *Navicula* sp.1, *Placoneis explanata* (Hustedt) S.Mamaya, *Sellaphora pupula, Staurosirella pinnata, Fragilariforma mesolepta* (Rabenhorst) Kharitonov dominantly.

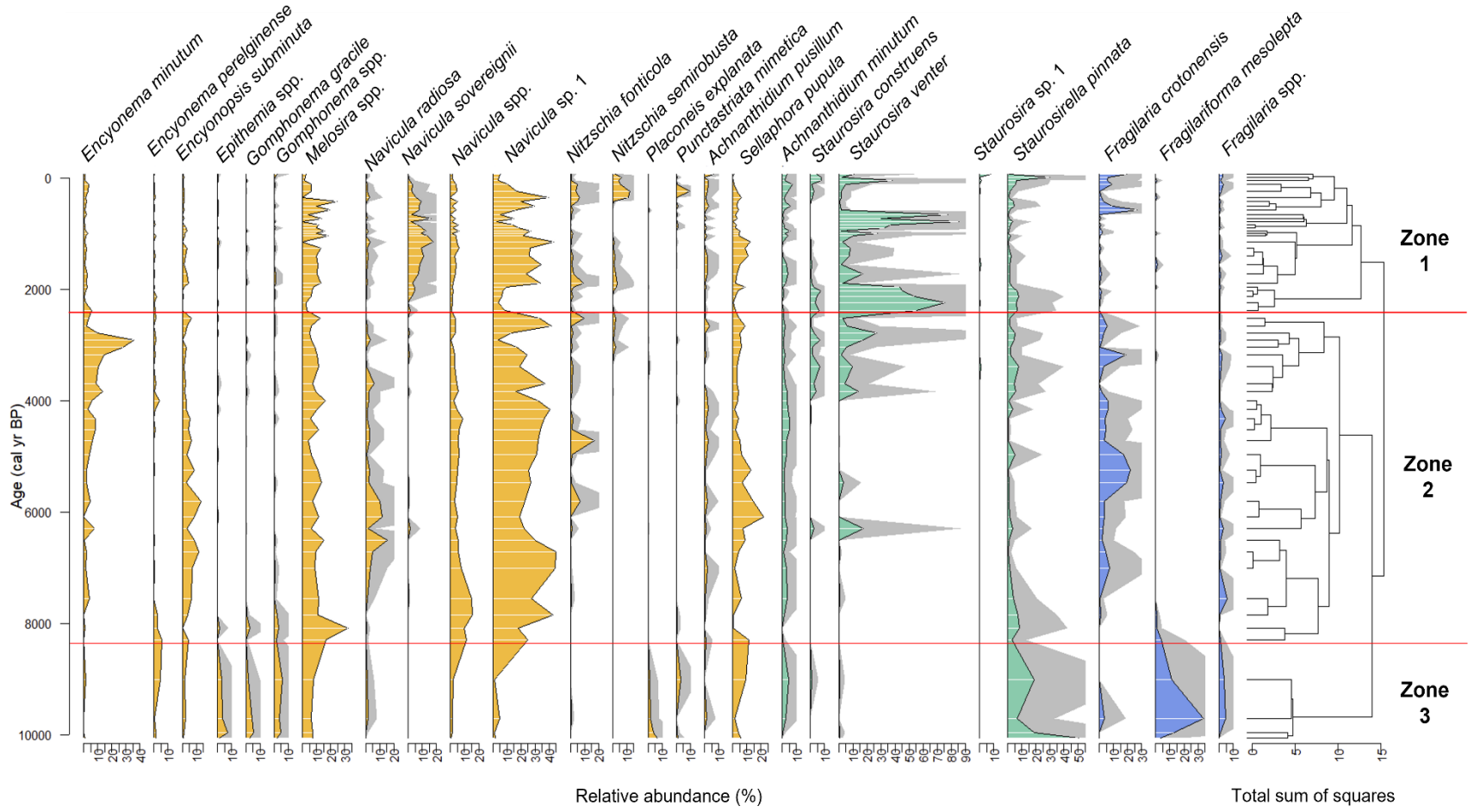

Figure 3-6 *Diatom stratigraphic diagram showing the 25 major diatom taxa (>5%) from Kelly Lake downcore (KL19) with zonation based on CONISS. The grey shades indicate 3 times exaggeration of the original data.*

There are several species that only appeared dominantly in one zone, such as *Nitzschia semirobusta, Punctastriata mimetica, Achnanthidium pusillum, Staurosira* sp.1 (Zone 1), *Encyonopsis subminuta, Navicula radiosa, Fragilaria* spp. (Zone 2), and *Epithemia* spp., *Gomphonema gracile, Gomphonema* spp., *Placoneis explanata, Fragilariforma mesolepta* (Zone 3).

Diatom concentration is shown in Figure 3-7. The absolute number of diatom valves in Kelly Lake maintained low values from the early to mid-Holocene. It reached a minimum number at 8,086 cal yr BP, while the maximum peak was at 2,246 cal yr BP. Afterward, it declined for the rest of the period. Overall, the diatom assemblages in Kelly Lake stayed quite steady with several abrupt changes in diatom concentration.

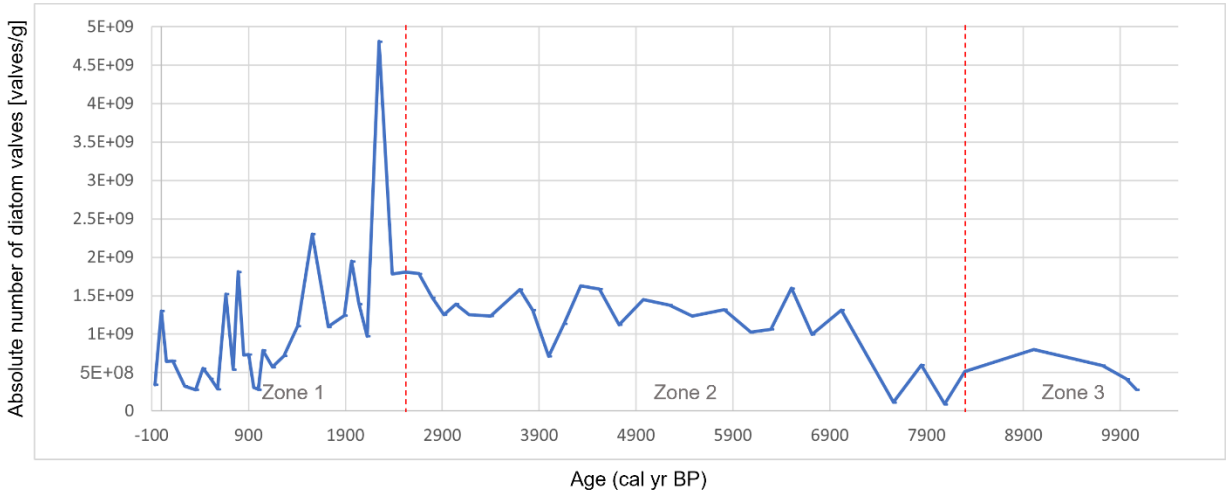

Figure 3-7 *Diatom concentration of KL19.*

3.5.5 PCA

Figure 3-8 shows the biplots of the PCA results of KL19. The cumulative explained variation of Axis 1, 2, and 3 is 45% (Table 3-2). Up to Axis 6, the cumulative explained variation was about 65%. The eigenvalue of Axis 1 was 20%, Axis 2 explained 14.2%, and Axis 3

explained 10.2%. Axis 1 was associated with the CONISS zonation. Positively high Axis 1 values were associated with Zone 3, while the lesser values seemed to be related to Zone 1 and 2. Based on diatom taxa loadings, Axis 2 was assumed as indicating water depth. High Axis 2 values represent deep water depth, Axis 2 negative values indicate shallow water depth.

Table 3-2 *PCA eigenvalues and explained variation of KL19 diatom taxa.*

	Axis 1	Axis 2	Axis 3	Axis 4
Eigenvalues	0.202	0.142	0.102	0.0753
Explained variation (cumulative)	20.20	34.40	44.56	52.09

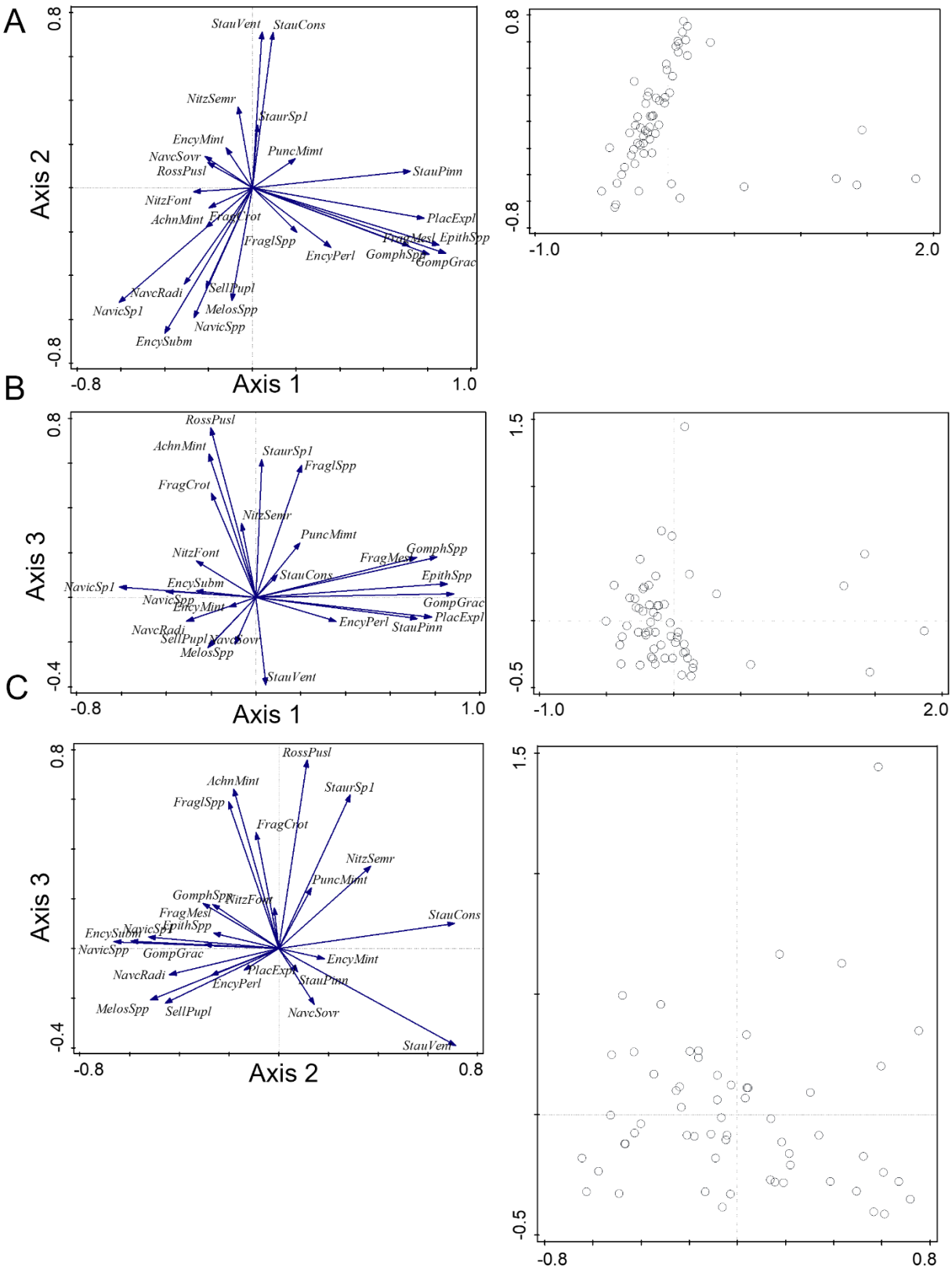
A
StauVent
StauCons
NitzSemr
StaurSp1
EncyMint
NavcSovr
PuncMimt
RossPusl
StauPinn
NitzFont
PlacExpl
AchnMint
FragCrot
FragMesl
EpithSpp
FraglSpp
EncyPerl
GomphSpp
GompGrac
NavcRadi
SellPupl
NavicSp1
MelosSpp
NavicSpp
EncySubm
Axis 2
Axis 1
0.8
-0.8
1.0
2.0
-1.0
B
RossPusl
AchnMint
StaurSp1
FraglSpp
FragCrot
NitzSemr
PuncMimt
NitzFont
GomphSpp
FragMesl
StauCons
EpithSpp
NavicSp1
EncySubm
NavicSpp
GompGrac
EncyMint
PlacExpl
EncyPerl
StauPinn
NavcRadi
SellPupl
NavcSovr
MelosSpp
StauVent
Axis 3
Axis 1
0.8
-0.4
1.5
-0.5
C
RossPusl
AchnMint
StaurSp1
FraglSpp
FragCrot
NitzSemr
PuncMimt
GomphSpp
NitzFont
FragMesl
StauCons
EncySubm
NavicSp1
EpithSpp
NavicSpp
GompGrac
EncyMint
NavcRadi
PlacExpl
EncyPerl
StauPinn
MelosSpp
SellPupl
NavcSovr
StauVent
Axis 3
Axis 2
0.8
-0.4
1.5
-0.5
-0.8

Figure 3-8 *PCA results of the diatom assemblages from KL19. A) Axis 1 and 2, B) Axis 1 and 3, C) Axis 2 and 3.*

3.5.6 Species diversity (H'), Hill's N2, Pielou's evenness (J'), richness indices (S)

The results of Shannon-Wiener diversity (*H'*), Hill's N2, Pielou's evenness (*J'*), and species richness (*S*) indices are provided in Figure 3-9. As shown in Figure 3-9, *H'*, Hill's N2, and *J'* appeared to have similar trends over time, while *S* showed variations for certain periods (e.g., the beginning of the Holocene, ~ 7,500 cal yr BP). The overall indices remained stable during the mid-Holocene after rising at the onset of the Holocene, but they have pronounced variations in the late Holocene. This result was similar to diatom assemblage changes, the P:B ratio, and the reconstructed lake level by transfer functions. These will be compared in the discussion.

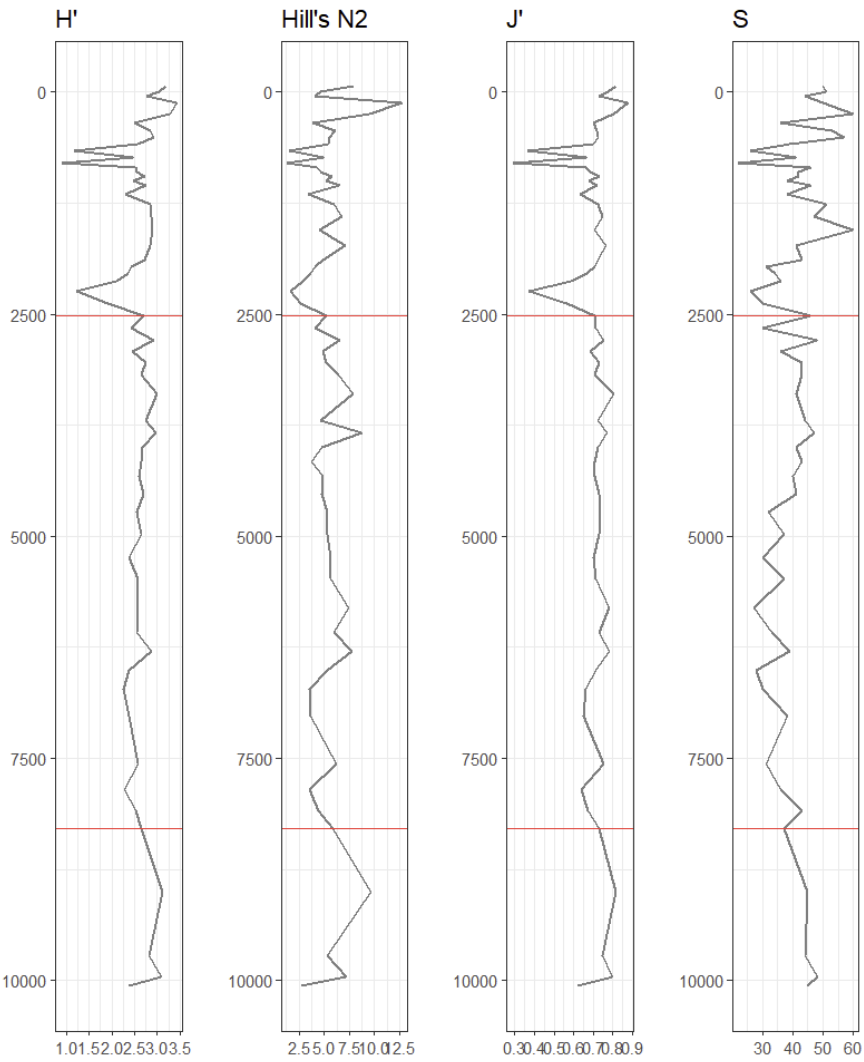

Figure 3-9 *KL19 Species indices. H' = Shannon-Wiener diversity index, J' = Pielou's evenness index, S = species richness.*

3.5.7 P:B ratio

The planktonic and benthic variation results are provided in Figures 3-10. In Figure 3-10A, the variations of planktonic and benthic species were drawn separately, and Figure 3-10B offers the P:B ratio. P included only planktonic taxa, while B included only benthic taxa. No tychoplanktonic taxa were included in the first graph. In the P:B ratio, P included planktonic taxa and tychoplanktonic taxa, and B included benthic taxa.

The benthic species changes showed that a number of benthic species gradually thrived at the onset of the Holocene. During the mid-Holocene, it oscillated but maintained flat values overall. Around 2,200 cal yr BP, the benthic ratio dropped abruptly and rose after that. It dropped again at ~ 800 cal yr BP, oscillated until ~ 600 cal yr BP, and gradually decreased after 120 cal yr BP (Figure 3-10A). The change in planktonic ratio is similar to the P:B ratio.

According to the P:B ratio, planktonic species rose abruptly during the early Holocene. Throughout the Holocene, planktonic diatoms gradually decreased after around 8,000 cal yr BP. There were fluctuations in the number of planktonic species in Kelly Lake during the mid-Holocene, but the main trend was downward with occasional peaks. In the late Holocene, planktonic diatoms fluctuated more and rose again but less than in the early Holocene.

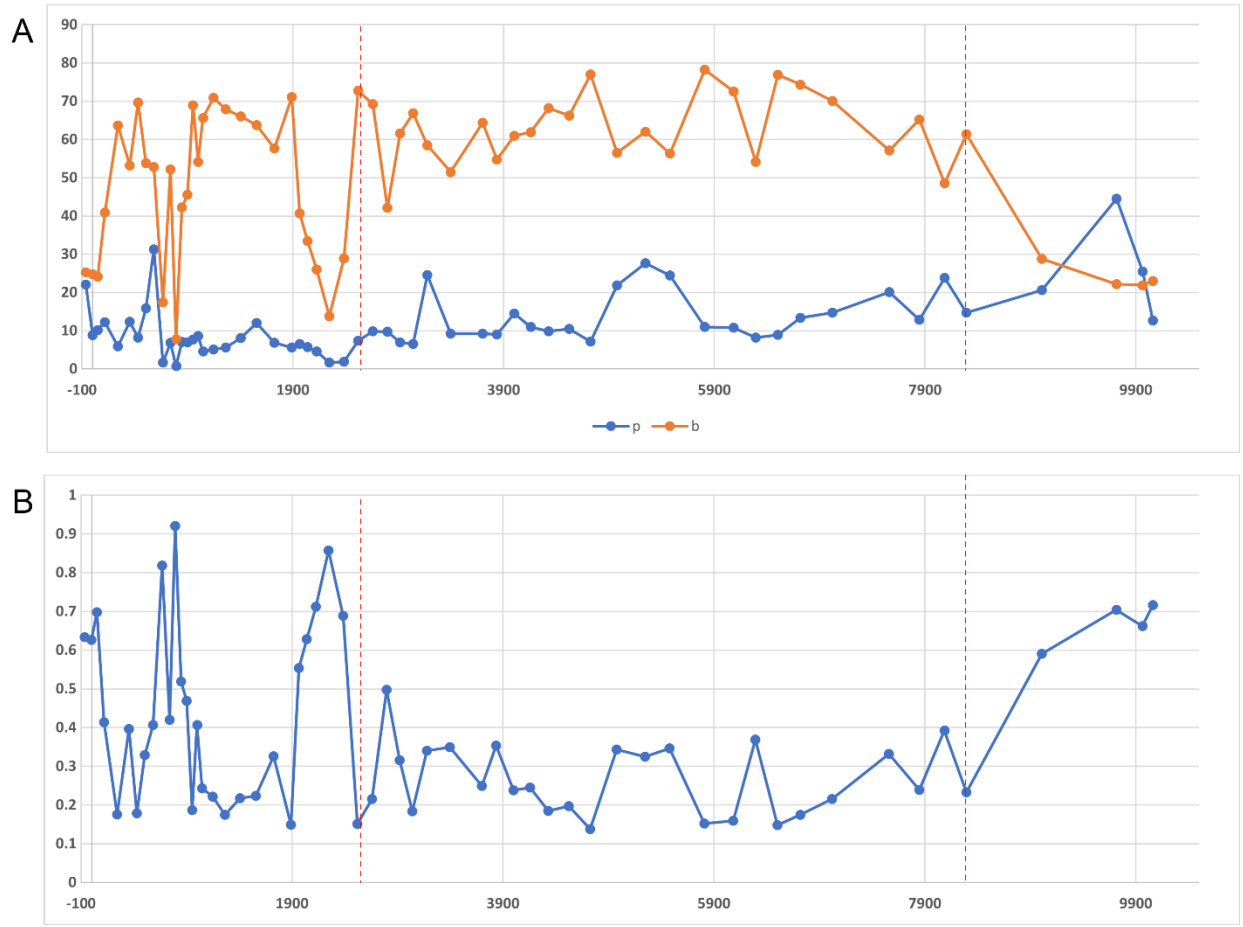

Figure 3-10 *A) respective planktonic and benthic variations over time, B) P:B ratio.*

The overall P:B ratio trend showed that the planktonic diatom ratio kept declining gradually until ~ 1,000 cal yr BP with several humps, and it turned into an abrupt increasing trend in recent ages.

3.5.8 Application of transfer functions to KL19

The past lake level reconstruction was conducted using the MAT and WA-PLS transfer functions described in Chapter 2 (Figures 3-11 A & B). As aforementioned, both leave-one-out cross-validation (LOOCV) and bootstrapping were performed for cross-validation, and the results turned out the same. LOOCV is a validation method by extracting one validation set and estimates the error rate of the set from the training set (the remaining dataset, n-1). This is

repeated for every validation set. The estimated error rates are going to be averaged to estimate the test error. Therefore, LOOCV is one of the best ways to estimate test error, which does not over-estimate (Fauvel et al. 2014; Rushing et al. 2015).

Bootstrapping is also one of the most widely used statistical techniques for validation, especially for estimating uncertainty that is difficult to calculate (Chen et al. 2012). Bootstrapping extracts new sets of samples from the original dataset and repeats the process numerous times (e.g., 1000 times), and this technique estimates standard error in this way (Bonnell and Vilette 2021). After both cross-validation methods ran, the results came out the same; therefore, the results with LOOCV were provided in this study.

The total number of samples for the transfer functions was 40, and a total of 68 taxa were included for the transfer models, which appeared at least 1 % in at one sample. The details were explained in *Section 2.4.3* in Chapter 2. Each model's detailed result is explained as follows.

Using the established diatom inferred transfer functions of the Modern Analogue Technique (MAT) and Weighted Averaging Partial Least Squares (WA-PLS), the lake level changes in Kelly Lake during the Holocene were reconstructed (Figures 3-11 A & B). For WA-PLS reconstruction, component 3 was chosen as described in Chapter 2. This component had the lowest RMSEP, largest Jack_R^2, second lowest Jack_Max_Bias, low % Change, and high R^2 values. For MAT reconstruction, weighted average MAT was selected as it provided higher R^2, lower Jack_Max_Bias, and lower RMSEP. The values of Estimated ObservedDepth by cross-validation by average of 10 closest analogues were selected for MAT, and the values of Jackknife estimated ObservedDepth by WA-PLS Component 3 were chosen for WA-PLS.

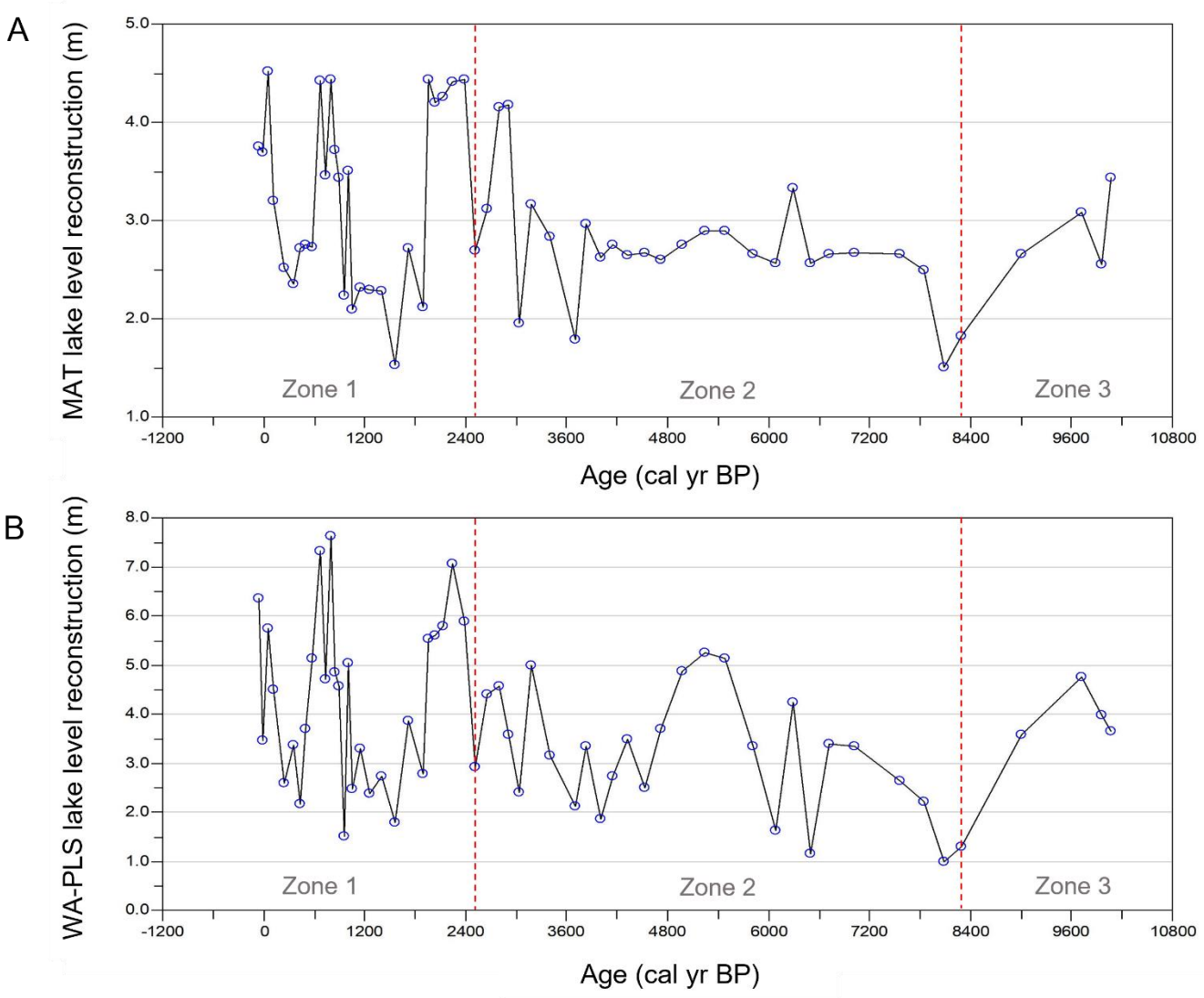

Figure 3-11 *A) MAT reconstruction of lake level changes of Kelly Lake during the Holocene, B) WA-PLS reconstruction of lake level changes of Kelly Lake over the Holocene.*

The reconstructed lake level changes by MAT and WA-PLS seemed similar overall but not identical. The MAT reconstruction provided the Kelly Lake level changed between 1.83 and 4.52 m, while the WA-PLS reconstruction suggested that it changed between 1.28 and 7.61 m. The water depth where the KLGC 19-1 and KLRC 19-2 were taken ranged from 5.3 – 5.7 m; therefore, the MAT reconstruction came out a little lower than its actual depths. There are reasons why the MAT reconstruction had this error and will be explained in *Section 3.6.1*.

The reconstructed lake level showed less fluctuations during the mid-Holocene and more variability as getting into the late Holocene. Both clearly showed the 8.2ka event, MCA (~ 952 cal yr BP), and LIA (~ 793 cal yr BP) with abrupt changes in reconstructed lake level. Late Holocene levels, although variable, were the deepest of the record.

3.6 Discussion

A number of water depth-related proxies were measured in the Kelly Lake sediment core. The application of MAT and WA-PLS transfer function was successfully conducted, and the lake level of Kelly Lake during the Holocene was reconstructed from this.

There are four sections in the Discussion. First, I will discuss the similarities and differences in the MAT and WA-PLS reconstructions of lake depth. Second, I will compare the transfer function lake depth reconstructions to the P:B ratio and to the other sedimentary and diatom-based indicators of lake level changes and their impacts found in the Kelly Lake core. I will then briefly compare the Kelly Lake results to other regional reconstructions. In the final section, the reconstructed hydroclimatic variations from this study will be compared to potential climatic forcing factors.

3.6.1 Differences between the MAT and WA-PLS reconstruction

The MAT and WA-PLS reconstruction displayed some differences in the reconstructed water depth although they had similar overall trends. The MAT reconstruction may underestimate lake depth and the WA-PLS reconstruction matches better in comparison to the recent lake depth. Therefore, in this section, I will explore why there were differences in the MAT and WA-PLS reconstruction.

Table 3-3 *Comparison between measured water depth and reconstructed water depths from MAT and WA-PLS (component 3) at Kelly Lake.*

	Measured in the field	MAT reconstruction	WAPLS3 reconstruction
Modern water depth	~ 5.7 m	~ 3.7 m	~ 6.2 m

The WA-PLS transfer function reconstruction was better than the MAT reconstruction with more reasonable estimated lake depth values. The reconstructed depths provided the lake water depth at the sample site. When the KLGC19-1 and KLRC19-2 were cored, the water depths were ~ 5.35 m and ~ 5.70 m respectively. The core site water depth where the KLRC19-2 was obtained was not recorded accurately, but it is assumed ~ 5.6 m due to the proximity to the coring point where the KLRC 19-1 was taken at 5.65 m of water depth. The deepest water depth from the MAT was ~ 4.50 m, and the reconstructed lake depth at the most recent period (present) was just ~ 3. 70 m. On the other hand, the deepest lake depth reconstructed by the WA-PLS was ~ 7.50 m, and the reconstructed recent water depth was 6.2 m (Table 3-3).

When MAT is used for reconstruction, it compares the modern and fossil samples and measures the mathematical dissimilarity of the assemblages. To calculate the dissimilarity coefficients, it uses squared chord distance (Overpeck et al. 1985). With the dissimilarity

coefficient formula ($d_{ij} = \sum_k (p_{ik}^{\frac{1}{2}} - p_{jk}^{\frac{1}{2}}))^2$, when d_{ij}: dissimilarity coefficient, i,j: multivariate samples, p_{ik}: proportion of species k in sample i), the dissimilarity between the modern and fossil samples are measured, and paleo-lake level can be reconstructed (Overpeck et al. 1985). That is, the MAT method to estimate the past lake level based on the modern data collected at Kelly Lake. By finding and matching the closest modern data with the fossil data, the average of 10 closest analogues are selected and used for the reconstruction. The fossil data (KLRC19-2) was obtained with the water depth of ~ 5.70 m, but the modern data (KLSS2019 from Chapter 2) only had samples that were taken from depths down to 5.20 m. Therefore, the MAT model from this dissertation could not show more than 5.20 m depth in the reconstruction. Also, thus, the dissimilarity (or mathematical distance between the modern and fossil samples) was large. Probably, the dissimilarity measure at other depths such as 3.00 or 4.00 m was good and reconstructed well. Due to these reasons, the MAT reconstruction provided at least 2.00 m shallower estimate than the WA-PLS reconstruction. Because there are no other quantitative estimates of the lake level changes at Kelly Lake during the Holocene, I cannot check whether the MAT and WA-PLS reconstruction is perfectly right or wrong. However, I can deduce that the reconstructed water depth that the MAT transfer function is lower than observed water depth at the coring point, which was ~ 5.60 m. Therefore, using the MAT transfer function, it is unlikely to reconstruct the past lake level changes in specific properly because of absence of modern data deeper than 5.20 m.

3.6.2 Comparison of WA-PLS reconstruction with other diatom and sedimentary data from Kelly Lake

The diatom-inferred lake level reconstruction by the WA-PLS component 3 transfer function will be compared here to other indices from Kelly Lake. According to the Kelly Lake

downcore diatom data, the Holocene can be divided into early (10,100 – 8,300 cal yr BP), mid (8,300 – 2,500 cal yr BP), and late Holocene (2,500 cal yr BP – present). These will cover Preboreal (10,000 – 9,000 cal yr BP) and Boreal (9,000 – 8,000 cal yr BP) for the early Holocene, Atlantic (8,000 – 5,000 cal yr BP), Subboreal (5,000 – 2,500 cal yr BP) for the mid-Holocene, and Subatlantic (2,500 cal yr BP – present), which are recognized chronozones (Mangerud et al. 1974). The division of the Holocene used here is fairly close to that used in the previous studies from the region (Mohr et al. 2000; Bradbury et al. 2004; Briles et al. 2008; Starratt 2012; Crawford et al. 2015; Leidelmeijer et al. 2021; Knight et al. 2022). In this subsection, I am going to infer Kelly Lake's water level changes during the early Holocene by focusing on diatom-related and geochemical proxies.

3.6.2.1 Early Holocene (~ 10,100 – 8,300 cal yr BP)

At around 10,000 cal yr BP, the climate around the Klamath Mountains was becoming warmer than prior to the onset of the Holocene. According to the reconstructed Kelly Lake water depth, the deepest water depth was close to 5 m during the early Holocene. It started to fall sharply around 9,700 cal yr BP (Figure 3-12). The sharp fall in water depth continued until 8,100 cal yr BP during the beginning of the mid-Holocene (Zone 2).

In Figure 3-12, the WA-PLS component 3 reconstruction (WAPLS3), P:B ratio, diatom concentration, and the diatoms that only appeared dominantly during the early Holocene are presented. At the end of the early Holocene there was a sharp decrease in the reconstructed lake level by WAPLS3, P:B ratio decreased sharply, and diatom concentrations decreased. The Zone 3 diatoms, *Fragilaria mesolepta, Gomphonema gracile, Gomphonema spp., Placoneis explanata, Surirella spp., and Epithemia spp.,* also fell sharply at the end of the early Holocene. Normally *Gomphonema gracile* occurs in (mild) eutrophic and alkaline water (pH above 7.0)

with high conductivity (Karthick et al. 2011; Zorzal-Almeida and Fernandes 2013) and favors a moderate P concentration levels (Slate and Stevenson 2007). *Fragilaria crotonensis* has a low optimum for nitrogen (Bahls et al. 1985), and *F. crotonensis* shows the abrupt decline as well. Another Zone 3 diatom, *Epithemia* spp. prefers alkaline hard water as well but with low N/P microhabitats (poor in NO_3, NH_4, and high phosphorus availability from the submerged aquatic plants) (Wehr et al. 2015). Considering these, Kelly Lake's hydrologic environment during the early Holocene was nitrogen-limited, alkaline, high nutrient content, and high conductivity water. I included *Surirella* spp. even though it is not a dominant species in KL19 samples because of the distinctive characteristics of the taxa. The taxa appeared at very low abundance during the Holocene except for the early Holocene. *Surirella* spp. is motile, and they inhabit a wide water chemistry range (Spaulding et al. 2021). Also, the species is epipelic, which means that *Surirella* spp. lives on organic and inorganic sediments which is the interface of water and sediment (Round et al. 1990; Spaulding et al. 2021). With the characteristics, it can be deduced that the photic zones of Kelly Lake would reach the bottom or close to the bottom of the lakebed, which makes sense that the reconstructed water depth was less than 5.00 m in comparison to the average photic zone depth in deep waters was 4.12 m (Chapter 2, Table 2-1).

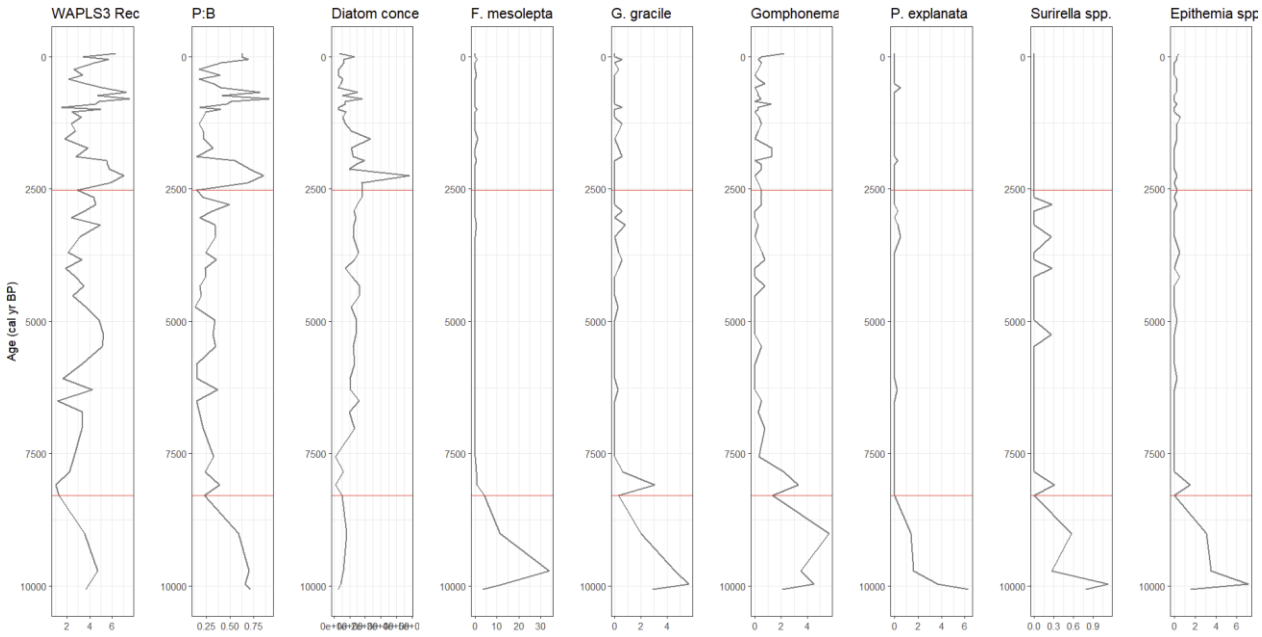

Figure 3-12 *Kelly Lake level changes reconstruction, the P:B ratio, diatom concentration, and Zone 3 diatoms with zonation. distinctive variability around 8,086 cal yr BP.*

Based on the information from Zone 3 diatoms, the diatom-related indicators and geochemical proxies were also compared (Figure 3-13). Newly in this figure, PCA Axis 2 (PC2), species richness (*S*), Shannon-Wiener species diversity index (*H'*), species evenness (*J'*) (diatom-related indicators), LOI (total organic matter in % at 550°C and total carbonate in % at 950°C), magnetic susceptibility grain size (% clay, % silt, % sand) (geochemical indicators) are provided. The three α-diversity indicators, *S, H',* and *J',* are useful to assess environmental impacts and biodiversity (Stevenson 1984). During the early Holocene, *S*, *H',* and *J'* maintained high values, and they suggest that the aquatic environment of Kelly Lake was favorable to a diversity of diatom species. The high MS, low % TOM, and high % clay suggest that Kelly Lake experienced wet climate and moderately high-water levels during the early Holocene, which is consistent with the high lake levels reconstructed by WA-PLS transfer function. The diatom-related diversity indicators (*H', J', S*) did not show a prompt response to the sediment dynamics,

but there could be some delays in ecological response of the diatom assemblages in Kelly Lake as the Holocene developed.

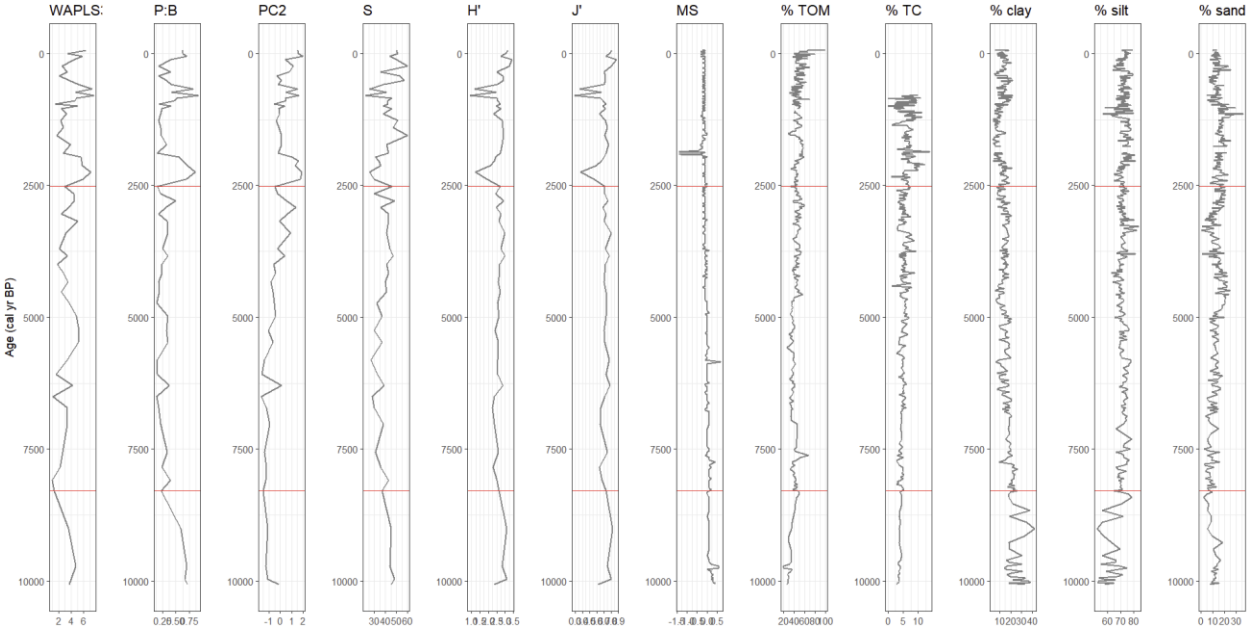

Figure 3-13 *Diatom-related and geochemical proxies over the Holocene: PCA Axis 2 (PC2), species richness (S), Shannon-Wiener species diversity (H'), Pielou's evenness (J') (8cm-interval), % total organic matter (TOM), % total carbonate (TC), Magnetic susceptibility (MagS), and grain size results such as % clay, % silt, and % sand (1cm-interval).*

3.6.2.2 Mid-Holocene (8,2300 – 2,500 cal yr BP)

Mid-Holocene is a long period that appears to have had somewhat a steadier hydroclimate than the early and late Holocene. Previous studies have mainly concluded that the area of the Klamath Mountains was dry during the mid-Holocene (Bradbury et al. 2004; Hudson et al. 2021), while Kelly Lake level and downcore diatoms showed that there were some variations at the lake level, it was generally lower than the subsequent late Holocene. Figure 3-14 provides the reconstructed lake level, the P:B ratio, diatom concentration, and diatoms that only appeared in Zone 2 (Zone 2 diatoms). *Encyonopsis subminuta,* which was a dominant species from KL19 and a Zone 2 diatom, mainly thrived during the mid-Holocene. The species is

epilithic inhabiting the surface of rocks (Hofmann et al. 2020). *Navicula radiosa* inhabits high conductance and high nutrient status and is known as a species with high tolerance to humans (Yang and Duthie 1995; Potapova 2011). Based on the characteristics of the two taxa, Kelly Lake during the period was likely to be in high nutrient condition with high conductivity and low to intermediate water depths.

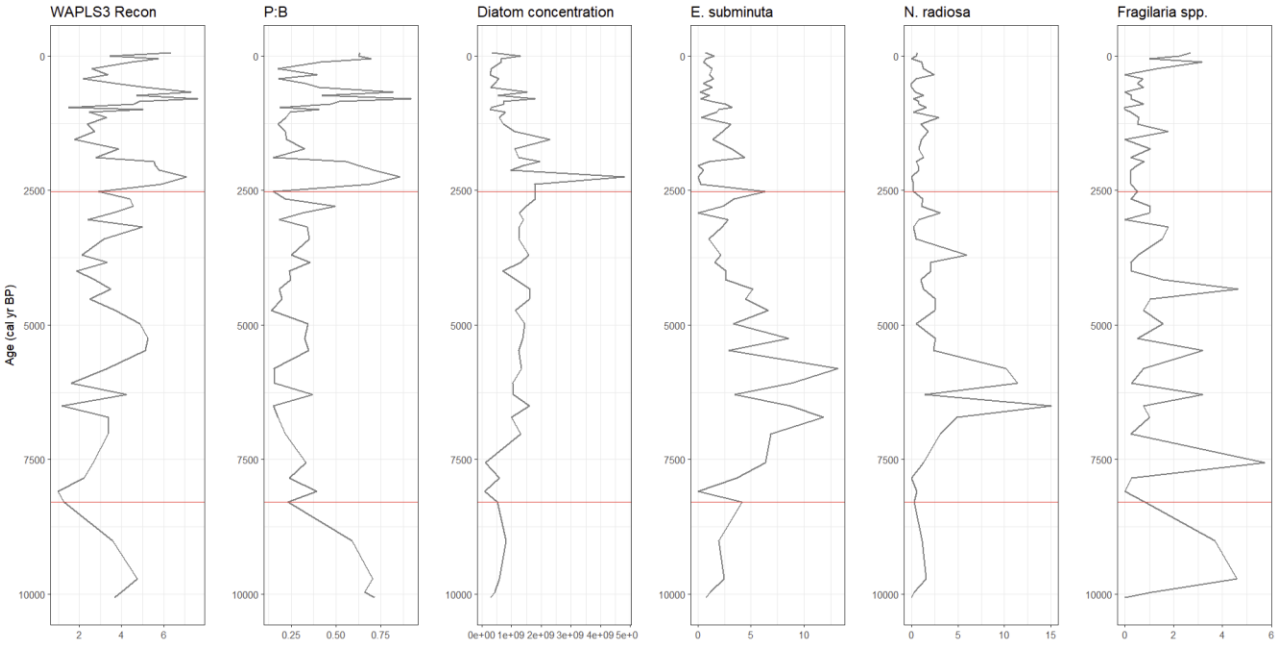

Figure 3-14 *Reconstructed Kelly Lake level, the P:B ratio, and mid-Holocene diatoms from Kelly Lake. The red lines indicate zone divisions.*

Also, the appreciable increase of *Fragilaria crotonensis* (Figure 3-6) during the transition to the late Holocene suggests that the lake changed into mesotrophic or eutrophic from oligotrophic and may have begun to experience more windy climates because *F. crotonensis* is an indicative species with increased nitrogen (Bailey-Watts 1986; Morales et al. 2013) as well as high summer turbulence and strong windy conditions (Rioual 2000). There is not much change in geochemical indicators but increasing % TOM and decreasing % suggest increasing productivity and some shallowing. Overall, Kelly Lake during the mid-Holocene was evolving

into a meso- to a eutrophic lake with intermediate water depth, increasing nitrogen and nutrient concentrations, windy climates, and stratification.

3.6.2.3 Late Holocene (2,500 cal yr BP – present)

The late Holocene is assumed to extend from ~ 2,500 cal yr BP to present in this study according to the diatom-inferred zonation by CONISS (Figure 3-6). As shown in Figure 3-15, Kelly Lake began to display higher variability during the late Holocene than before. During this period, the MCA and LIA are distinctively observed from the Kelly Lake record: the MCA appeared around at 950 cal yr BP and LIA around at 790 cal yr BP. The lake level reconstruction and the P:B ratio showed similar timed fluctuations to the events with peaks approximately at 670, 790, and 2,250 cal yr BP and sharp troughs around at 950 cal yr BP. There was a little time gap that might be caused by ecological inertia, but diatom concentration showed a similar sharp increase with the times. The diatom taxa (Zone 1 diatoms) in Figure 3-15 that appeared only during the late Holocene (Zone 1), such as *Nitzschia semirobusta*, *Punctastriata mimetica*, *Achnanthidium pusillum*, *Staurosira* sp.1, represented differently from the changes in lake level changes, the P:B ratio, and diatom concentration, but in general, the Zone 1 diatoms appear similarly in a trend for a long-time scale.

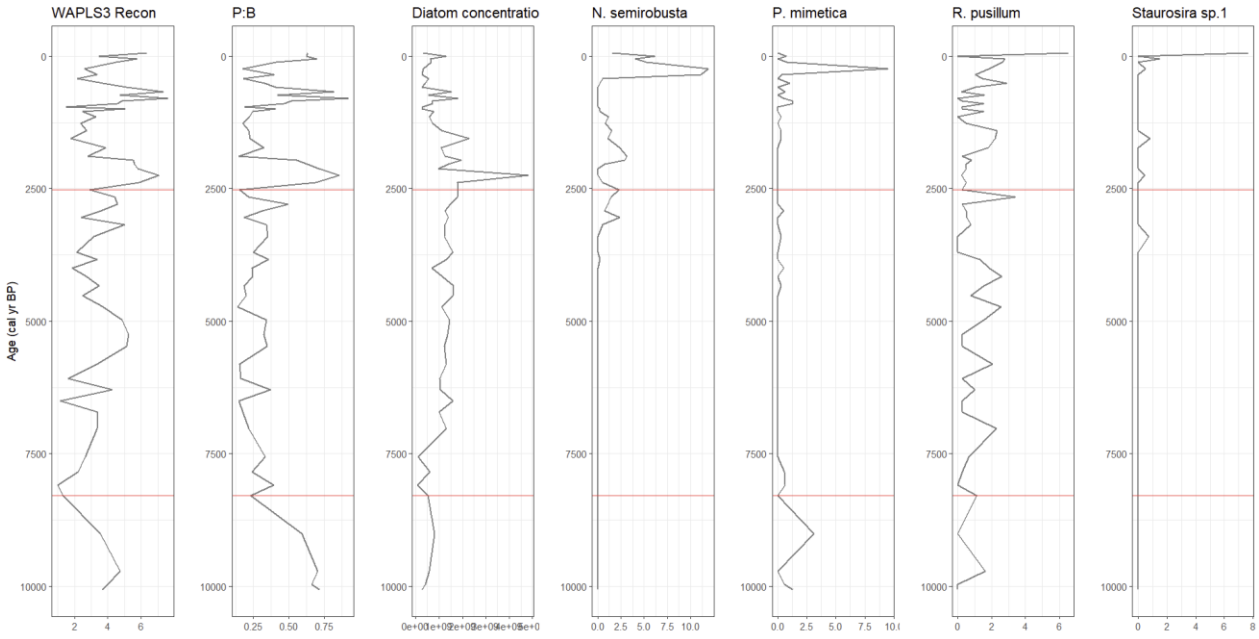

Figure 3-15 *Late Holocene diatoms.*

Kelly Lake during the late Holocene was likely mesotrophic with abundant nitrogen and a deeper depth than before according to the favorable ecology conditions of Zone 1 diatoms. *P. mimetica* prefers mesotrophic environments (Cremer and Koolmees 2010), low conductivity, and alkaline water with moderate P concentrations and abundant N (Morales 2005). The *S, H'*, and *J'* values maintained high values and fluctuations during the late Holocene, and this can be supported by abundant nutrient status with moderate P and rich N. *A. pusillum* prefers oligotrophic and cold water (Potapova 2009b). They are benthic with slight motility and attach to a surface flat (Potapova 2009b). The low (high) in *A. pusillum* is consistent with high (low) lake levels from WAPLS3 Recon (Figure 3-15). *N. semirobusta* inhabits a wide range of nutrient status and is benthic but with moderate motility (Underwood 2013; Bartozek et al. 2018). *Staurosira* sp. 1 was not identified at a species level, but *S. venter* also very flourished during the late Holocene. *S. venter* is epipsammic, which grows on sand grains (Hofmann et al. 2020). The species sticks to a sand grain firmly even though the sand grain rolls over lakebeds and tolerates

dark anaerobic environments even if the sand grain rolls down to a deeper depth (Hofmann et al. 2020). The deepened but fluctuated water depth at Kelly Lake can be supported by the prosperity of *S. venter* during the late Holocene.

The diatom-related and geochemical proxies also showed that Kelly Lake underwent high variability in water depth as well as ecological and geochemical conditions during the late Holocene (Figure 3-13). *S, H', J'*, % TOM, %TC, MS, % clay, % silt, and % sand have more variability than previous periods except for magnetic susceptibility. This infers the climate during the late Holocene fluctuated appreciably. As Kelly Lake's water depth deepened, planktonic species compared to benthic species became abundant, but this led to a decrease in species richness, diversity, and evenness. The increase in % TOM suggests an increasing trend in productivity. Although the % clay declines, and this could be interpreted as shallowing, the % sand increased starting about 5,000 cal yr BP with some variations, but is generally high in the late Holocene, consistent with greater runoff. The variations of MS, % TOM, % TC, % clay, % silt, and % clay show long term trends through the mid- to late Holocene appear indicative of an increasing productivity/preservation of organic matter and may not be tied to variations in lake depth.

3.6.3 Comparison with other regional reconstruction of hydroclimatic variability in the Northern Pacific Coast Ranges

The Kelly Lake reconstruction added to a range of differing Holocene hydroclimatic inferences for the region (Figure 3-16 & Table 3-4). According to the WA-PLS component 3 reconstruction, Kelly Lake water depth reached up to 4.74 m during the early Holocene, but it declined abruptly to 0.98 m at around 8,100 cal yr BP. Bradbury et al. (2004) similarly inferred

initially moist conditions, followed by dry conditions with lowering lake levels and extended marsh environments during the mid-Holocene. In contrast, Briles et al. (2008) also stated that it was warm and dry from 10,000 to 9,000 cal yr BP in the Siskiyou Mountains, Northern California, as summer insolation declined, with evidence of the lowest abundance in *Abies* and *Pseudotsuga* that favor wetter environment. Mohr et al. (2000) also suggested a dry and warm climate in the eastern Klamath Mountains in the early Holocene. Starratt (2012) also concluded that the climate was dry during the early Holocene followed by increased lake level in the mid-Holocene.

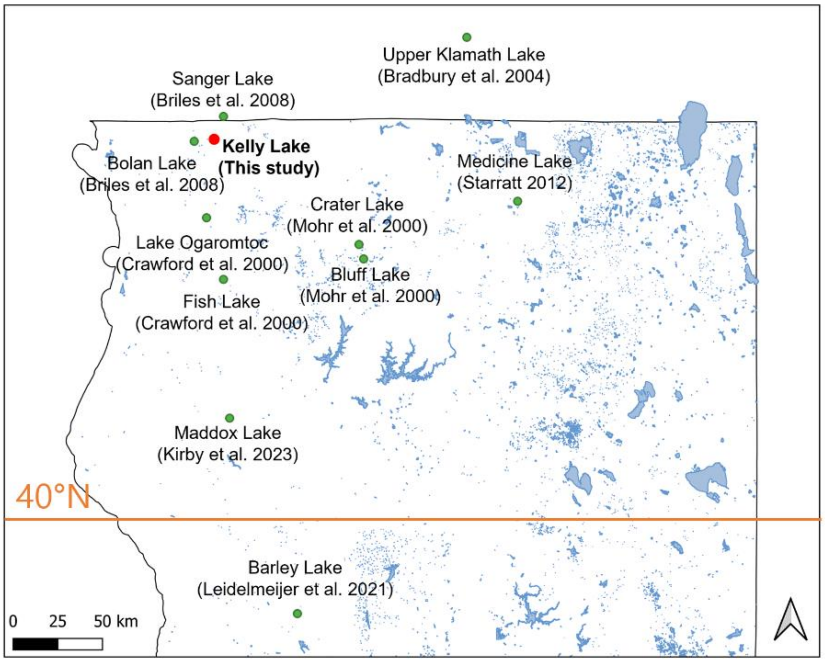

Figure 3-16 *The locations of previous studies and this study in Northern California.*

Table 3-4 *Hydroclimatic reconstruction in Northern California from previous studies and this study.*

Time periods according this study (cal yr BP)	**Mohr et al. (2000)** *Eastern Klamath Mountains, N. CA*	**Bradbury et al. (2004)** *South-central Oregon State*	**Briles et al. (2008)** *Siskiyou Mountains, N. CA*	**Starratt (2012)** *Northeast of Mount Shasta, N. CA*	**Crawford et al. (2015)** *Western Klamath Mountains, N. CA*	**Leidelmeijer et al. (2021)** *Mendocino National Forest, N. CA*	**Kirby et al. (2023, in press)** *Trinity County, N. CA*	**This study** *Klamath Mountains, N. CA*
Late Holocene (~ 2,500 – Present)	Dry, High fire frequency	Wetter than previous	Max. fire frequency after 2,400 → Wetter, Low fire frequency over the last 1,000 years	Wet	Cool, Dry →Wet	——	Dry → Wet	Dry → Wet, Deepest water depth with increased variability
Mid Holocene (~ 8,300 – 2,500)	Dry	Dry	Cooler, Wetter than before → Warmer and drier	Dry → Wet	Cooler than present, Well established modern forest structure	——	Wetter than before → Dry	Maintained dry
Early Holocene (~ 10,100 – 8,300)	Warm, Dry	Wet → Dry	Warm, Dry	Dry	——	Dry → Wetter	Dry	Wet → Dry
Methodology	Pollen, Charcoal	Diatom, LOI, XRF	Pollen, Charcoal	Diatom	Pollen, Charcoal	Grain size, LOI, MS	Grain size, LOI, MS	Diatom, Grain size, LOI, MS

There were fluctuations in Kelly Lake water depths during the early to mid-Holocene transition (Figure 3-13, WAPLS3 Recon), and in particular, the lowest water depth is highly likely to be associated with the 8.2 ka event (Thomas et al. 2007). The lake reached the lowest lake level at around 8,100 cal yr BP, which was ~ 0.98 m at the start of the mid-Holocene. The 8.2 ka event was a global cooling event that lasted approximately 150 years (Thomas et al. 2007) that was triggered by meltwater from Lake Agassiz flowing into the Labrador Sea. This caused a collapse of the Atlantic Meridional Overturning Circulation (Aguiar et al. 2021). Evidence of the 8.2 ka event has been found by other regional studies from Northern California (Barron et al. 2003; Kirby et al. 2023, accepted) and coastal and/or Southern California (Kirby et al. 2006; Oster et al. 2017; Starratt et al. 2021; Homann et al. 2022).

After the lake experienced the 8.2 ka event, the lake water depth abruptly decreased, but it maintained ~ 2.73 m of water depth on average during the mid-Holocene. Noticeably, Kelly Lake experienced the swift hydrologic changes, decrease in water depth, during the transition period from early to mid- Holocene, and the lake also underwent the 8.2 ka event in the Klamath Mountains, which were consistent with other lake sediment records in Northern California. As noted above, the dry mid-Holocene conditions of Kelly Lake relative to the early Holocene are consistent with some other studies from the region (Bradbury et al. 2004b) and at odds with others (Mohr et al. 2000; Briles et al. 2008; Starratt 2012).

The Kelly Lake record suggests increased water depth and increased variability in the late Holocene relative to the early Holocene. Not all studies find similar evidence. Crawford et al. (2015) found out that shade-intolerant (e.g., *Quercus*) decreased and shade-tolerant (e.g., *Pseudotsuga, Abies*) increased between ~ 2,800 and 1,000 cal yr BP in the western Klamath Mountains. This indicates a cool and wet climate. Similarly, Bradbury et al. (2004) concluded

that the late Holocene was moister than the mid-Holocene based on lake level inferences. According to Briles et al. (2008), however, the region experienced the maximum magnitudes in fire frequency after 2,400 cal yr BP inferred by increase in *Pseudotsuga*. A late Holocene Dry Period (LHDP) was proposed by Leidelmeijer et al. (2021) at Barley Lake (~ 2,300 – 300 cal yr BP) and Kirby et al. (2023, accepted) at Maddox Lake (~ 2,800 – 1,850 cal yr BP).

The reconstructed lake level at Kelly Lake during the MCA at around 950 cal yr BP, was shallow (the reconstructed water depth = 1.49 m). This is accordant with Knight et al. (2022)'s suggested warm and dry climate conditions in the Klamath Mountains during the MCA, between 1,200 and 850 cal yr BP. Mohr et al. (2000) also stated that it was dry with high fire frequency in the eastern Klamath Mountains around 1,000 cal yr BP. Not long after the MCA, the LIA developed. Kelly Lake reached the maximum lake depth (the reconstructed water depth = 7.61 m) during the LIA at around 800 cal yr BP. This is consistent with Knight et al. (2022), who inferred wet climatic conditions in the Klamath Mountains at ~ 750 cal yr BP to 50 cal yr BP. This is also in accordance with Crawford et al. (2015) who concluded that the region experienced a cool and wet climate at this time. Although the lake level at Kelly Lake dropped abruptly to 2.00 – 3.00 m at around 500 cal yr BP, it rose again afterward and maintained quite a deep-water depth (~ 4.00 – 5.00 m). This might be consistent with low fire-episode frequency and increase in *Sequoia* at Sanger Lake over the last 1,000 years (Briles et al. 2008).

The range of discrepancies between Kelly Lake and some other studies from the region, and indeed between the previous studies may reflect that sites such as Kelly Lake and Upper Klamath Lake are located at a higher latitude than the other sites mentioned and the differences might be related to the precipitation dipole boundary (Dettinger et al. 1998; Wise 2010). In addition, the distance of the sites inland and orographic factors might influence the local

climates. Finally, the range of hydroclimatic proxies used and the many sources of variability in ecosystems being studied may be making reconstructions and comparisons challenging.

3.6.4 External drivers of hydroclimatic variations at Kelly Lake and coastal Northern California

The Kelly Lake downcore diatom records and global-scale proxy data are compared and discussed here in order to consider the regional signals in the context of global drivers of climate change. Summer solar insolation at 42°N has decreased, while winter solar radiation at 42°N has increased over the Holocene. These insolation forcings could result in increased winter precipitation and less evaporation during summer (Leidelmeijer et al. 2021). The long-term Holocene cooling is apparent in the $\delta^{18}O$ NGRIP ice-core record that follows the changes in insolation (Figure 3-17 A, B). This is consistent with the overall changes in lake level at Kelly Lake, which increased in the late Holocene with increased winter solar insolation and decreased summer solar insolation. Eastern tropical Pacific sea surface temperatures (SSTs) increased over the Holocene (Figure 3-17G), which is consistent with increasing precipitation in California (Allen and Luptowitz 2017). However, there is much additional hydroclimatic variation apparent in the Kelly Lake record.

Once source of hydroclimatic variation at Kelly Lake may be the Pacific Ocean and features such as El Niño-Southern Oscillation (ENSO) system. Mark et al. (2022) reconstructed paleo-flood frequency (El Niño event) from Laguna Pallcacocha in Ecuador (Figure 3-17F). The results suggested moderate, reduced, and enhanced ENSO activities from the early to mid- to late Holocene, and they inferred this El Niño activity was associated with the long-term variations in

tropical solar insolation. The flood frequency pattern displays some correspondence with Kelly Lake's water depth variations (Figure 3-17K).

The El Junco grain size (sand %) record from Galapagos Islands, eastern equatorial Pacific also displays an ENSO-related signal during the Holocene (Conroy et al. 2008). More sand is interpreted as representing wetter and more variable climate conditions in the late Holocene. This may be reflected in the higher lake levels, but greater lake level variability observed in the Kelly Lake record in the late Holocene. However, we also need to be aware that California's climate is strongly affected by upwelling (Huyer 1983), so it is not only influenced by insolation. Upwelling brings a cooler climate, and ENSO activity interrupts this upwelling. This might explain why Ocean Drilling Program Site (ODP) 1019 SSTs, discussed below, do not fully follow the trend of eastern equatorial Pacific SSTs.

The alkenone-based reconstructed SST from ODP 1019 at 41.68°N by Barron et al. (2003), which is almost the same latitude where Kelly Lake samples were collected. The ODP 1019 SST records were likely to be related to Pacific Decadal Oscillation (PDO) and ENSO. The ODP 1019 SSTs suggested that the SSTs increased abruptly after the onset of the Holocene even higher than the modern SST, stayed steadily lower than the modern SST during the mid-Holocene, and increased to the modern SSTs. The increased SSTs can be linked to the higher possibility of heavier precipitation and higher flood frequency (Hatsuzuka and Sato 2022) in this Coast Ranges, which would influence the early, mid- and late Holocene lake level differences at Kelly Lake (Figure 3-17I, J, K). In particular, the latitudes between 38°N and 43°N are the regions that respond to ENSO or other climatic cycles sensitively with the maximum magnitudes seasonally (Strub et al. 1987; Barron et al. 2003). Therefore, the changes in lake level at Kelly

Lake can be closely related to the past ODP 1019 SSTs regarding the characteristics as well as the proximity of the two sites.

According to the eastern equatorial Pacific alkenone-based SST records (Figure 3-17G), the SSTs kept increasing around the equator from the beginning of the Holocene (Dubois et al. 2011). The eastern equatorial Pacific SST change is an important driver of ENSO activity and the climate mechanisms between the tropical Pacific and the high latitude areas (Dubois et al. 2011; Glover et al. 2020). The increasing trend in the eastern equatorial Pacific SSTs can be linked to increasing heat energy around the equator over the Holocene, and it would influence regional hydroclimate changes around the Pacific Coast Ranges in North America. That is, warmer eastern equatorial Pacific SSTs mean more precipitation in California. Therefore, the high variability during the late Holocene can be explained by the higher eastern equatorial Pacific SSTs. Also, the moist conditions during the early Holocene in the Klamath Mountains can be explained by the influence of the eastern equatorial Pacific SST.

Lastly, the high lake levels at Kelly Lake approximately from 10,000 to 9,000 cal yr BP seems to be consistent with more precipitations from lower temperatures indicated by NGRIP, fairly higher floods by Mark et al. (2022), and higher % sand by El Junco record. Therefore, the Kelly Lake record suggests that the Klamath Mountains responded sensitively to orbital and oceanic forcing over the Holocene.

California's precipitation patterns are highly impacted by SSTs in the Pacific and Northern Hemisphere temperature changes. Orbital changes and solar radiation are the main drivers of such factors. Orbital changes (i.e., eccentricity, obliquity, precession) can affect the distribution and amount of solar radiation received on Earth, and the insolation variability influences temperature gradients. Northern Hemisphere (NH) temperatures inferred from ice

cores also indicate the distribution of heat energy that received from the Sun, and it can provide insights into past climate variations over centuries to millennia. NH temperature changes can indirectly impact California's precipitation by influencing atmospheric circulation patterns and large-scale climate phenomena (e.g., Pacific Decadal Oscillation (PDO)). In particular, SSTs in the equatorial and eastern Pacific Ocean play an important role in shaping California's precipitation patterns such as the development of atmospheric circulation patterns and the position and intensity of the Intertropical Convergence Zone. The PDO reflects the impacts by SSTs in the Pacific in a long-term perspective, and the occurrence of ENSO events that show SST anomalies in the equatorial Pacific for short-term can also provide the variability of the Pacific Ocean in a longer timescale. However, there are other factors that can modulate California's precipitation patterns, such as human impacts, and it makes the complexity of precipitation patterns in California.

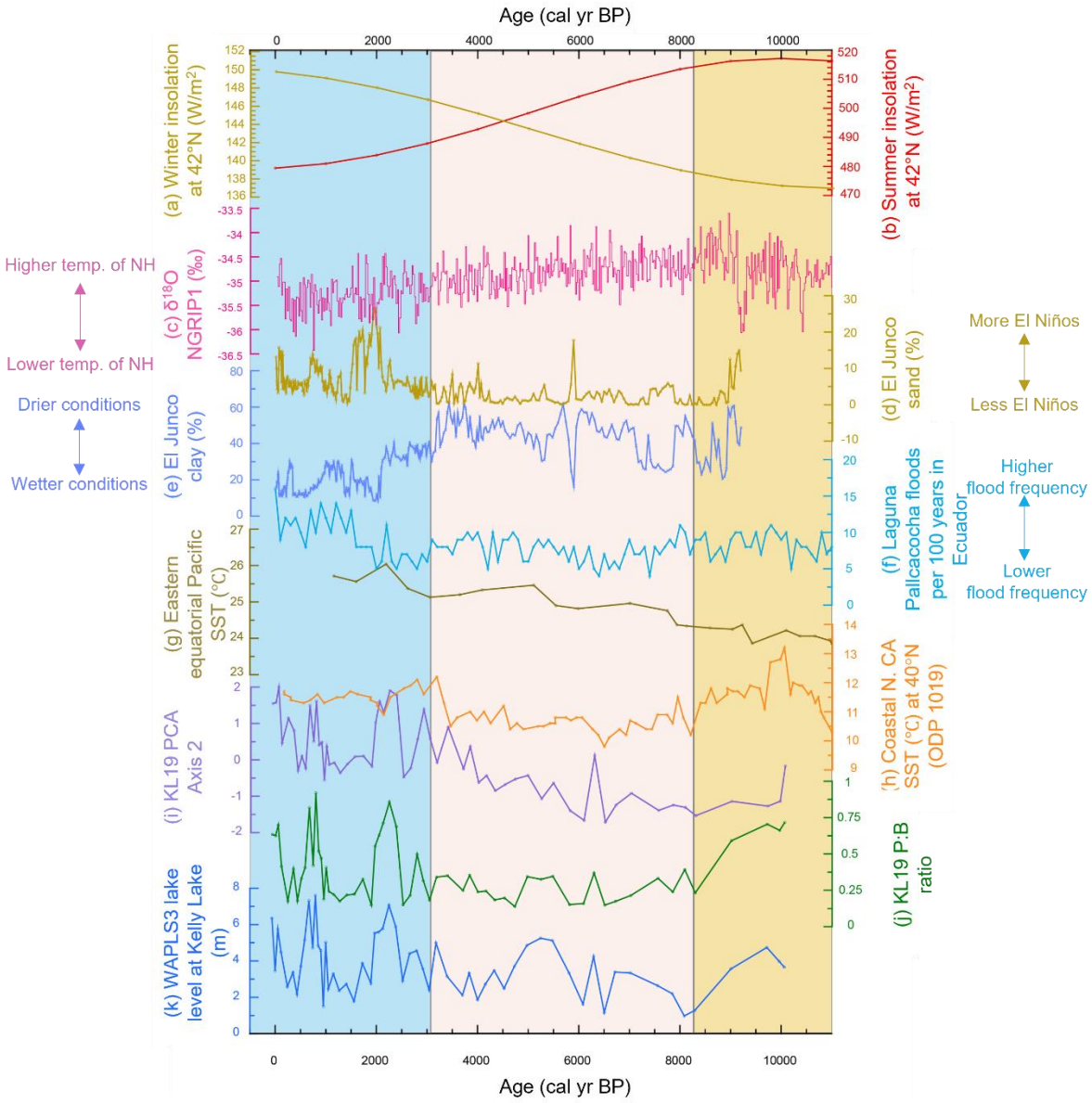

Figure 3-17 *Kelly Lake hydroclimatic variability in comparison to global drivers of climate change over the Holocene. It is divided into three zones based on CONISS zonation. Each zone is colored with different color bands; the early Holocene is colored yellow because it was the time period that the climate was becoming dry. The mid-Holocene is colored pink because it is Holocene Thermal Maximum (HTM), and late Holocene is colored blue because it was the period when the lake experienced high variability in lake level changes. The data used in this figure: (a) & (b) show summer and winter insolation (W/m^2) at 42°N (Laskar et al. 2004), (c) shows the NGRIP1 $\delta^{18}O$ changes (‰) (Grootes and Stuiver 1997b), (d) & (e) shows the % sand and % clay changes in El Junco Lake from Galápagos (Conroy et al. 2008), (f) indicates the reconstructed frequency every 100 years from Laguna Pallacocha, Ecuador (Mark et al. 2022),*

(g) represents the reconstructed eastern equatorial Pacific SSTs (℃) (Dubois et al. 2011), (h) shows the ODP 1019 SSTs (℃) (Barron et al. 2003), and (i), (j), & (k) indicates PCA Axis 2, P:B ratio, and the reconstructed lake level changes at Kelly Lake from this study.

3.7 Conclusion

This study provides a Holocene-length paleohydroclimate record from coastal Northern California. The study provides evidence of the applicability of the WA-PLS and MAT transfer functions that were established from Kelly Lake, a small size and mid-water depth single lake, to reconstruct paleohydroclimatic changes from the same lake. Although there was a limitation regarding differences between the fossil and modern diatom taxa, the reconstructions of paleohydroclimatic variability in the Northern Pacific Coast Ranges were conducted well. The reconstructions are supported in general by other diatom and sedimentary indices from the lake.

Accordingly, this study extended potential wider geographic and environmental scope of the use of the single lake methodology that have been used in boreal lakes in Canada or glacial lakes in Europe, which requires more than 50 natural lakes in general. Therefore, the development and validation of the transfer functions from the mid-water depth and small-sized lake provided an important empirical example of the methodological rationale and the potential of single-lake approach.

The hydroclimate of the Klamath Mountains in the Northern Pacific Coast Ranges underwent distinctive variations during the Holocene divided in to early, mid, and late Holocene. The lake level of Kelly Lake was high at around 10,000 cal yr BP influenced by high northeastern Pacific SSTs (ODP 1019), but the lake experienced abrupt dryness during the early Holocene at around 8,100 cal yr BP, called 8.2 ka event that was found globally. The temperatures in the Northern Hemisphere ($\delta^{18}O$ NGRIP) remained fairly high with fairly high

summer insolation. With this regard, the lake level at Kelly Lake during the mid-Holocene declined over time influenced by the northeastern Pacific SSTs and the equatorial Pacific SSTs. This was also consistent with low ENSO activity found in Laguna Pallcacocha in Ecuador (Mark et al. 2022). During the late Holocene, the lake level of Kelly Lake highly fluctuated while indicating shallow water depth during the MCA and the maximum lake water depth during the LIA. The eastern equatorial Pacific SST warming and increased ENSO during the late Holocene (Mark et al. 2022) are associated with Kelly Lake water depth becoming deeper and exhibiting higher variability by suggesting changes in the Pacific Ocean were important drivers of the hydroclimatic variability in the Northern CA Coast Ranges.

In conclusion, the SSTs off the coast CA (upwelling) and NGRIP (solar forcing) were considered as significant drivers in Northern CA's climate dynamics between ocean and atmosphere (Leidelmeijer et al. 2021). Kelly Lake diatom record was also the first quantitative lake level record in the context of precipitation dipole in California. The paleohydroclimatic variability reconstruction from Kelly Lake in the Klamath Mountains, Northern Pacific Coast Ranges, suggested 1) the applicability and usefulness of the diatom transfer functions developed from a single lake and contributed to the regional hydroclimate reconstruction, 2) the apparent hydroclimatic changes in Kelly Lake from the diatom record, and 3) findings of the influence of orbital and oceanic forcing on the Northern CA Coast Ranges.

Chapter 4 A 110 ka Late Quaternary Diatom Record of Salinity and Lake Water Depth History from Baldwin Lake, Subalpine Southern California

4.1 Abstract

Paleohydrologic indicators, such as salinity and water depth, at Baldwin Lake in the San Bernardino Mountains during the late Quaternary were reconstructed to better understand long-term hydroclimatic variability in Southern California by adding diatom data to the previous studies in the site. Baldwin Lake contains one of the longest limnological records in Southern California, and such long records of natural hydroclimatic variations are significant for understanding future hydroclimatic sensitivity. According to the diatom record of the lake, Baldwin Lake experienced a strong shift in the lake's dynamics at around 70,000 cal yr BP. The shift included a decrease in variability, which from 110,000 to 70,000 cal yr BP had been strongly associated with orbitally forced seasonal changes in radiation. In addition, the salinity of the lake decreased, but the lake also shallowed. From 110,000 to 70,000 cal yr BP, Baldwin Lake had the highest species diversity, of diatoms, high productivity, along with the high values in lake level and salinity, but also experienced high amplitude shifts in these variables. Also, there were two intervals during this period of no-diatoms, and these coincide with times when the summer insolation was the lowest. After the insolation variability became dampened at around 70,000 cal yr BP, most diatom-related signals began to decline sharply in variability amplitude. This decline in productivity and diatom diversity and declines in the amplitude of variability coincides with decreased values of summer insolation and decreased variability in seasonal insolation, reflecting orbital changes. These diatom records were coeval with the previous Baldwin Lake studies. Baldwin Lake diatoms following 70,000 cal yr BP until the last glacial maximum at around 20,000 cal yr BP also suggest several abrupt warming events which appear

to coincide with Dansgaard-Oeschger events, after 60,000 cal yr BP. This study shows good links between the Baldwin Lake diatom records and solar irradiance variability and other global drivers, such as the sea surface temperatures at the equatorial Pacific and the Pacific off the northern California coast. In conclusion, the diatom records suggest sensitivity of regional hydro climate in Southern California to radiative and oceanic drivers over the past 110,000 years.

4.2 Introduction

As Southern California (CA) has a high population density, it is vulnerable to abrupt hydroclimatic changes such as prolonged drought and associated environmental impacts such as fires (MacDonald 2007). Both natural climatic variations and anthropogenic climate change impact the region and will do so in the future. Long records of natural hydroclimatic variations and the sensitivity of the region to external climatic forcing factors are important lines of evidence in understanding and anticipating future hydroclimatic variations in Southern California (Glover 2016; MacDonald et al. 2016; Kirby et al. 2018; Shuman et al. 2018; Holmes et al. 2023).

There have been a number of previous paleolimnologically-based studies to reconstruct hydroclimatic variability in Southern CA (e.g. Baldwin Lake – Kirby et al. (2006), Blazevic et al. (2009), Glover (2016); Glover et al. (2017, 2020); Lower Bear Lake (Big Bear Lake) – Kirby et al. (2012), Starratt et al. (2021); Lake Elsinore – Kirby et al. (2007, 2010, 2018), Martinez (2020); Zaca Lake – Dingemans et al. (2014), Feakins et al. (2014), Kirby et al. (2014), Lund and Platzman (2016), Platzman and Lund (2019); Silver Lake – Kirby et al. (2015), at various time scales. Normally, the Holocene, also known as Marine Isotope Stage (MIS) 1, is the period studied because it is the geologic epoch that we live in. In addition, many lake sediment records

only extend into the Holocene. Understanding hydrologic variability not only during the Holocene, but also back beyond the Holocene is important to understand the full range of natural variability and the sensitivity of the regional climate to external factors.

Baldwin Lake was chosen as a study site for this study because the lake contains one of the longest limnological records in Southern CA (Glover 2016). Kirby et al. (2006) examined several geochemical proxies, such as magnetic susceptibility, % total organic matter, and % total carbonate, and revealed a 65,000-year record representing winter storm variability and North America monsoon variability driven by multi-millennial scale orbital changes and ocean-atmospheric dynamics. Glover (2016) and Glover et al. (2017, 2020) also cored Baldwin Lake but at a different location from the coring point of Kirby et al. (2006) and retrieved a much longer record. Glover et al. (2017) revealed via sedimentational and geochemical analyses that orbital radiative forcing and abrupt North Atlantic driven temperature swings affected the regional climates in Southern CA from MIS 5 (121,000 – 71,000 cal yr BP) to MIS 2 (27,000 – 14,000 cal yr BP). Glover et al. (2020) focused on vegetation and wildfire during the same period by adding more proxies (e.g., pollen, charcoal, molar C:N data). The main findings of the study were 1) Baldwin Lake's productivity has changed in the past being mainly influenced by local summer insolation, and 2) the pollen, charcoal concentration, basin deposition, and summer insolation were not linearly correlated. They also revealed that Baldwin Lake region was characterized by weakened basin erosion, sagebrush expansion, and fires during MIS 4 (71,000 – 65,000 cal yr BP), while it had more weathering, increases in *Juniperus* and *Pinus*, and less fires. Glover et al. (2020) concluded that the vegetation and terrestrial changes around Baldwin Lake was not directly related to the global CO_2 variations and Pacific sea surface temperatures (SSTs).

Previous studies showed that the long record of hydroclimate from Baldwin Lake was useful in understanding natural variability of climate and environments in Southern California and the factors that drove such variability. Therefore, this study will further advance the use of the Baldwin Lake sediments to examine hydroclimate-related factors, such as salinity and water depth, using diatom analysis and supplement the existing multi-millennial hydroclimatic records. Diatom assemblage composition responds to lake environmental and climatic changes sensitively (e.g., salinity, water depth) (Rühland et al. 2015; Zou et al. 2021). Especially in a closed basin, like Baldwin Lake, salinity and water depth changes are amenable to examination because other factors that control salinity and water depth are limited, and precipitation and evaporation account for most of the lake level and salinity changes (Kirby et al. 2006; Fritz et al. 2010; Wolin and Stone 2010). Therefore, diatom microfossils will be an essential proxy to further resolve hydrologic changes in the lake.

This study will contribute to understanding the hydroclimatic variability of Southern CA over a long-timescale through diatom inferred-water depth and salinity, and discuss the regional climate changes with the following research questions:

1. How has the diatom-inferred hydroclimate in Southern California changed over the late Quaternary (MIS 5 – 2) – specifically how did the lake level and salinity change?
2. How does the diatom-based hydroclimatic record at Baldwin Lake compare with previous records from the same site that extend back to MIS 2 and beyond?
3. What were the influences of orbital or oceanic forcings in driving such hydroclimatic fluctuations around Baldwin Lake?

4.3 Study site

Baldwin Lake (34.28°N, 116.8°W) is an intermittent lake in Big Bear Valley in the San Bernardino Mountains (SBM) (~160 km east of the Pacific coastline), which is a part of the Transverse Ranges in Southern CA (Glover et al. 2017) (Figure 4-1). The altitude of the lakebed is 2,040.7 m with a 4.53 km^2 surface area (French and Busby 1974). The surface area of the watershed is 79 km^2 (Glover et al. 2017). Baldwin Lake was separated from Big Bear Lake (Lower Bear Lake) basin during the early MIS 5 (~ 120,000 cal yr BP) by sediment flowing into the basin from Sugarloaf Mountain (Glover 2016). It is known that there is no surface flow between Baldwin Lake and Big Bear Lake today (French and Busby 1974).

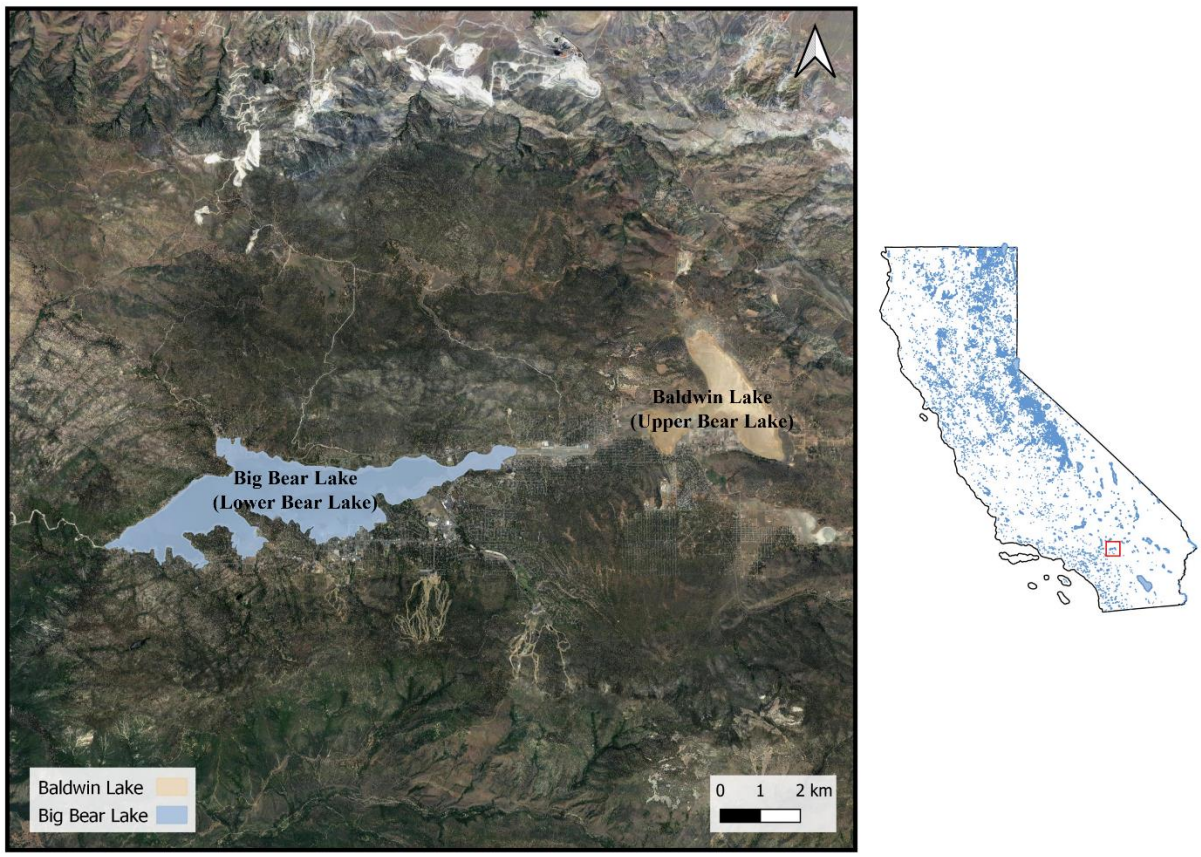

Figure 4-1 *A map of Baldwin Lake (Upper Bear Lake) and Big Bear Lake (Lower Bear Lake) in Big Bear Valley, San Bernardino Mountains, Southern California.*

The sediment of Baldwin Lake consists silt, clayey silt, and scattered sand grains with deposited evaporites irregularly and quartzites from Gold Mountain (Miller 2004) (Figure 4-2A). The surrounding area mainly contains the following sediments: 1) the lakebed sediments but with wind-driven finer fluvial grains deposited (very young), 2) unconsolidated to moderately consolidated undifferentiated surficial deposits (very young), and 3) quartzites with micaceous rocks (late Proterozoic) (Miller 2004). Also, alluvial-fan deposits from the late Pleistocene to late Holocene are also observed (Miller 2004). Figure 4-2B provides the overall geologic framework and geographic landscape. More details about the map and related information can be found in Miller (2004).

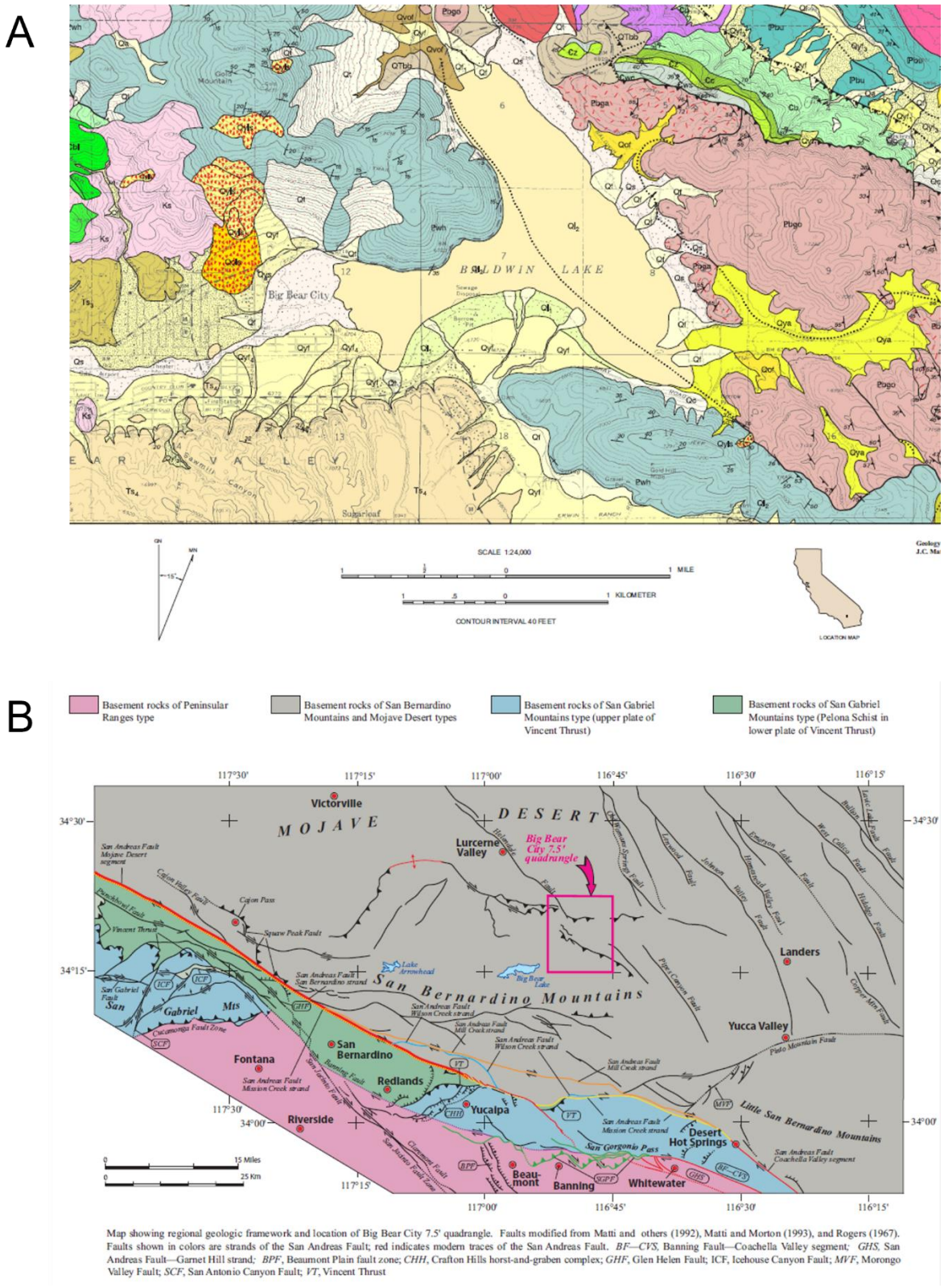

Map showing regional geologic framework and location of Big Bear City 7.5' quadrangle. Faults modified from Matti and others (1992), Matti and Morton (1993), and Rogers (1967). Faults shown in colors are strands of the San Andreas Fault; red indicates modern traces of the San Andreas Fault. *BF—CVS*, Banning Fault—Coachella Valley segment; *GHS*, San Andreas Fault—Garnet Hill strand; *BPF*, Beaumont Plain fault zone; *CHH*, Crafton Hills horst-and-graben complex; *GHF*, Glen Helen Fault; ICF, Icehouse Canyon Fault; *MVF*, Morongo Valley Fault; *SCF*, San Antonio Canyon Fault; *VT*, Vincent Thrust

Figure 4-2 *Geologic maps around Baldwin Lake and San Bernardino Mountains (Miller 2004).*

The contemporary climate of the Baldwin Lake region is Mediterranean with a wet cool winter and warm dry summer. The amount of annual precipitation is under the influences of changes in the position of the eastern Pacific subtropical high and the polar front (Kirby et al. 2006). According to previous studies, Baldwin Lake is a study site as a touchstone that shows the regional precipitation oscillation and atmospheric conditions at a large scale (Kirby et al. 2006). As Baldwin Lake is ephemeral, it can remain dry for several years, but also can hold water for several years after a mesic period (French and Busby 1974).

The climate data for the study area is provided in Figure 4-3. According to the climate data from 1960 to 2016 that were measured at Big Bear Lake (Station #: 040741), the annual average maximum temperature was 16.83 °C and the annual average minimum temperature was -0.06 °C (Western Regional Climate Center 2016b). The annual total precipitation water equivalent was 55.47 cm, the average total snowfall was 159.00 cm (Western Regional Climate Center 2016b). The hottest month was July (27.11 °C), the coldest month was January (-6.5 °C), the highest precipitation and snowfall months were January (11.40 cm) and February (38.61 cm), and the least precipitation and snowfall months were June (0.36 cm) and June to September (0 cm) (Western Regional Climate Center 2016b).

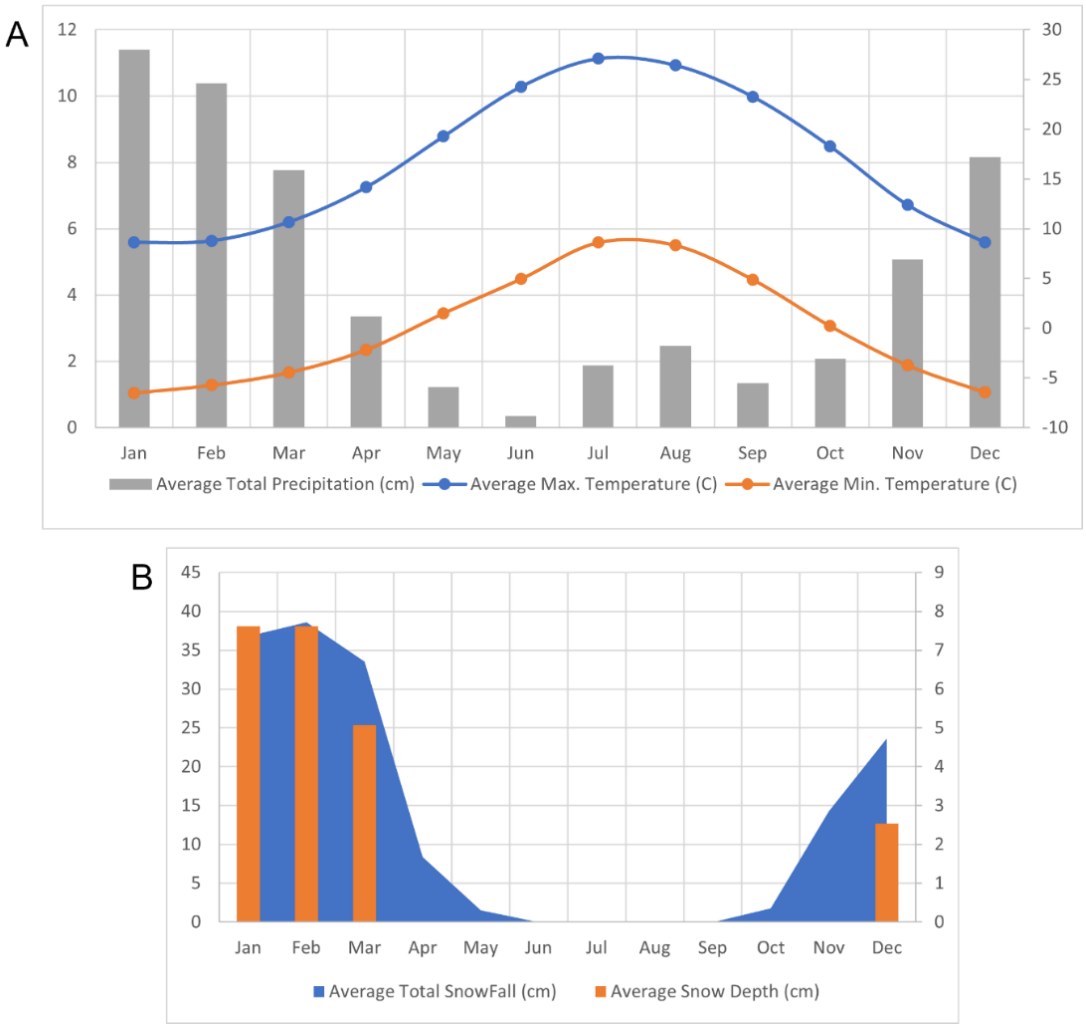

Figure 4-3 *A) Average total precipitation (cm) and Average maximum and minimum temperatures in Big Bear Valley, B) Average total snowfall (cm) and average snow depth (cm) in Big Bear Valley (Western Regional Climate Center 2016b).*

4.4 Methods

The core (BDL12), which was used in this study, was obtained at the depocenter of the lake basin using a CMF-95 truck-mounted hollow stem auger drill in August 2012 (Glover 2016). The recovered total core length was approximately 27 m from two adjacent cores (~ 76cm apart). After BDL12 was analyzed by Dr. Katherine Glover, the cores have been stored at 7 °C in the cold room at UCLA. In 2018, I checked and re-packed the BDL12 cores with plastic wrap

and aluminum foil to see if there were missing or disturbed parts. Most cores were in good shape, but there were missing samples and depths. In particular, the bottom of the core was mostly clastic sediments in a dry condition even though it was wrapped, and it seemed disturbed. More details of BDL12 core descriptions were explained well in the Supplementary Table 1 of Glover et al. (2017).

4.4.1 Chronology

The current study used the same Bayesian age-depth chronology that Glover et al. (2020) produced in Bacon 2.2 (Blaauw and Christen 2011 as mentioned in Glover et al. 2020). For BDL12 age-depth model, radiocarbon dates (^{14}C) using AMS radiocarbon dating, luminescence dates using Infrared Stimulated Luminescence (IRSL) single grain analysis, and five tie points were conducted (Glover 2016; Glover et al. 2017). Subsequently, the original BDL12 age-depth model has been updated in Glover et al. (2020). The age-depth model was run using Bacon 2.2 (Blaauw and Christen 2011). The details can be found in Glover (2016) and Glover et al. (2020)'s supporting information.

The core section from 180 to 2,299 cm of BDL12 was analyzed to focus on Marine Isotope Stages (MIS) 5 – 2 and transitions during the late Quaternary. The MISs are based on oxygen isotopes from deep sea core sediments and indicate the alternation of glacial and interglacial periods. Glover (2016) identified the ages from MIS 5 to MIS 2 in the SBM region as: 127,000 – 71,000 cal yr BP for MIS 5, 71,000 – 57,000 for MIS 4, 57,000 – 29,000 cal yr BP for MIS 3, and 29,000 – 14,000 cal yr BP. Conducting the analyses at the same depth as Dr. Glover's work was a key for a comparison study, so I followed the same depths and intervals that Dr. Glover analyzed for pollen analysis if there were sediment samples remaining. Most were

available except for several depths that were missing or did not have enough sediment. Table 4-1 shows the depths that were analyzed in this study and those not analyzed in this study.

Table 4-1 *Sampling depths from Glover (2016) and this study.*

Study	Depths (cm)
Both in Glover (2016) (pollen) and this study (diatom)	180, 190, 200, 210, 220, 230, 240, 250, 260, 270, 300, 310, 320, 340, 360, 380, 400, 420, 441, 461, 480, 501, 521, 541, 582, 600, 622, 642, 660, 680, 700, 730, 750, 798, 808, 818, 828, 837, 857, 877, 897, 917, 944, 1060, 1080, 1100, 1120, 1140, 1160, 1200, 1220, 1240, 1300, 1395, 1415, 1440, 1460, 1480, 1512, 1532, 1552, 1572, 1621, 1641, 1727, 1747, 1767, 1800, 1820, 1840, 1850, 1896, 1916, 1956, 2017, 2077, 2140, 2160, 2202, 2222, 2242, 2279, 2299 → A total of 83 samples
No samples were left but done in Glover (2016) (pollen)	285, 602, 1320, 1336, 1375, 1997, 2037 → A total of 7 samples

4.4.2 Diatom analysis

Diatom analysis was conducted for BDL12 sediment samples in the flowing manner. Approximate of ~ 0.1 g sample was put in a 100 mL beaker. The samples were treated with 3 ml of H_2O_2 and 6 ml of distilled water and heated for 1 – 2 hours to remove organic materials. After the chemical reaction was done, the top portion of the solution was thrown out, and a microspatula of sodium hexametaphosphate was added to the remained solution to disperse and deflocculate diatoms from sediment grains and let react for ~ 15 minutes. While doing that, pH

was constantly measured to make sure that the solution maintained acidic state because diatom valves are weak in base (Ryves et al. 2001; Han 2015). The solution was filled with distilled water and let deposit diatom valves for 8 hours. The top solution was decanted and filled with distilled water again and left it for one night. Next day, the solution was decanted and precipitated diatom valves were left in the beaker. Using micropipette, 200 and 300 μL of the sample was put on the microscope slides and dried at low temperatures on the hot plate. After the solution dried out, a drop of Pleurox mountmedia was applied to fix the sample on the microscope slides.

Approximately 400 diatom valves were counted at species level from the prepared microscope slides using light microscope (Nikon Labophot-2) at 1000x magnification oil lens. Diatom identification was referred to Krammer and Lange-Bertalot (1986, 1988, 1991a, 1991b) with books and online diatom sources (Kulikovskiy et al. 2016; Lange-Bertalot et al. 2017; Spaulding et al. 2019; Potapova et al. 2020; Jüttner et al. 2022).

Diatom diagram was drawn in R version 4.1.3 (RStudio Team 2020) using the rioja package (Juggins 2020). Also, a depth-constrained cluster analysis (CONISS) with Bray-Curtis distance method was applied to zonate the diatom assemblages in RStudio using the vegan package (Oksanen et al. 2020).

Diatom concentration could not be calculated because there was no water content data available for the BDL12 cores.

4.4.3 Diatom ratios related to lake level and salinity

Two diatom-related ratios were calculated to measure the lake water depth and salinity changes in Baldwin Lake. The BDL12 diatom major species, which appeared > 5% in at least

one sample, were selected to calculate the ratios because there were more than 190 taxa from the downcore sediments, and there were some ambiguous species to be determined as planktonic/benthic and brackish/freshwater.

To investigate lake water depth changes, planktonic to benthic (P:B) ratio was calculated. Normally, tychoplanktons whose lifeform could be planktonic and benthic depending on the life stage were included for P:B ratio calculation. However, one of the tychoplanktonic, *S. pinnata*, counted dominantly for most of the whole core; therefore, the P:B ratio was calculated while excluding tychoplanktons to minimize errors and to see the variations of benthos and planktons.

The brackish to freshwater (Br:Fr) ratio was also calculated to reconstruct salinity changes in Baldwin Lake. There were distinctive brackish species from the downcore sediment, such as genus *Anomoeoneis*, genus *Halamphora*, *Fallacia pygmaea*, etc. The apparent two brackish species, such as *Anomoeoneis* spp. and *Halamphora* spp., were included as brackish species. *Epithemia* spp. and *E. adnata* were also included as brackish taxa because the genus inhabits both in brackish and freshwater (Kashima et al. 1997; Zalat and El-Sheekh 1999; Wojtal 2009) and seemed to appear as brackish mostly in this study site. *Amphora copulata* was also included as brackish because *A. copulata* thrives in hypersaline environments (Govindan et al. 2021). The abundance of *A. copulata* from Baldwin Lake went along with other brackish species mostly; therefore, the species was also included in the brackish ratio. Overall, the four genera of *Amphora*, *Anomoeoneis*, *Halamphora* and *Epithemia* that were common at Kelly Lake and were calculated as brackish species for the Br:Fr ratio. Freshwater species were calculated with the rest of major species except for the brackish taxa.

The equations for P:B and Br:Fr ratios are provided as below:

$$P{:}B\ ratio = \Sigma planktonic\ taxa/\Sigma(planktonic + benthic\ taxa) \times 100 \quad \ldots \text{Equation 4-1}$$

$$Br{:}Fr\ ratio = \Sigma brackish\ taxa/\Sigma(brackish + freshwater\ taxa) \times 100 \quad \ldots \text{Equation 4-2}$$

4.4.4 Species diversity indices

There were many different diatom species and various taxa in Baldwin Lake sediment samples in comparison to the species from the Northern California lake discussed earlier in this dissertation. To estimate the diatom species richness, diversity, and evenness of the data, the Shannon-Wiener diversity index (*H'*), Pielou's evenness (*J'*), and Species richness (*S*) were calculated separately (Shannon 1948; Pielou 1966; Weckström and Korhola 2001). The *H'* index indicates how many different species appeared in a sample, which is relative abundance. *J'* index represents how uniform the species are in a sample. *S* index shows how many diverse species are in a sample.

4.4.5 Principal Component Analysis (PCA)

PCA was performed on the major species to estimate how distinctive assemblage groups are in the samples and to see ordinations between samples. PCA was conducted using CANOCO 5.15 (ter Braak and Šmilauer 2012).

4.5 Results

4.5.1 Chronology (radiocarbon and luminescence dates)

A total of 7 AMS radiocarbon dates and 4 infrared-stimulated luminescence dates were run, and 5 tie-points were selected for BDL12 age-depth model (Glover 2016; Glover et al. 2020). The details of dating can be found in Glover (2016) and Glover et al. (2020). The youngest and oldest ages from BDL12 from the untuned age model were 4,746 cal yr BP at 1 cm and 122,070 cal yr BP at 2,700 cm.

Tuned Age Model in Glover et al. (2017)	Untuned Age Model in Glover et al. (2020)
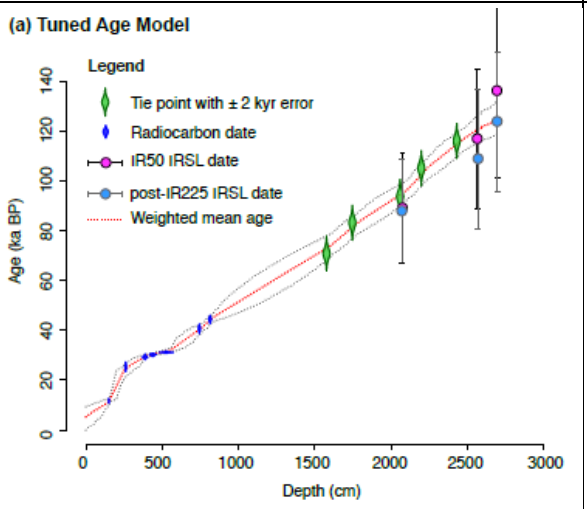	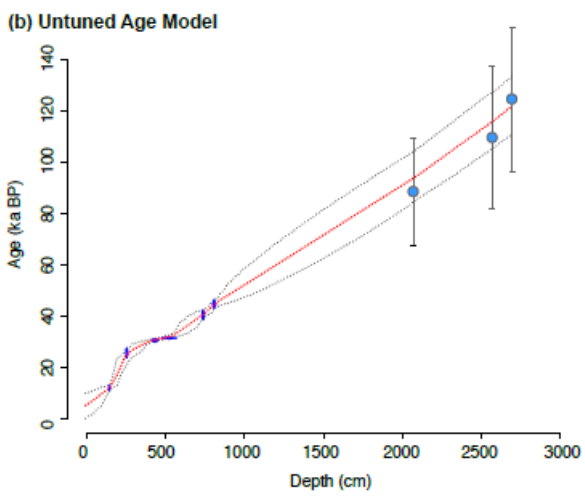

Figure 4-4 *BDL12 chronology done by Glover et al. (2017) and Glover et al. (2020) (Image source: Glover et al. (2020)'s Supplementary Figure 1).*

4.5.2 Diatom diagram with zonation

Approximately 190 taxa appeared from the site. Among them, 33 taxa were selected as major species, which appeared at more than 5% in at least one sample. A diatom diagram was drawn to see the changes in major diatom abundances (Figure 4-5). The gray-shading indicates 5 times the exaggeration from the original values for better visualization of the figure. The CONISS-based zonation identified three zones, Zone 1, 2, and 3. Zone 1 is from 180 – 1100 cm (15066 – 55251 cal yr BP), Zone 2 is 1100 – 1512 cm (55251 – 70608 cal yr BP), and Zone 3 is 1512 – 2299 cm (70608 – 108428 cal yr BP).

The 33 dominant species are *Amphora copulata* (Kützing) Schoeman & R.E.M.Archibald, *Anomoeoneis* spp., *Cocconeis placentula* Ehrenberg, *Cymbella* spp., *Cymbella affinis* Kützing, *Cymbellonitzschia diluviana* Hustedt, *Encyonema minutum* (Hilse) D.G.Mann, *Epithemia* spp., *Epithemia adnata* (Kützing) Brébisson, *Gomphonema* spp., *Gomphonema pumilum* (Grunow) E.Reichardt & Lange-Bertalot, *Halamphora* spp., *Melosira* spp., *Navicula*

spp., *Navicula* sp.1, *Navicula radiosa* Kützing, *Nitzschia* spp., *Nitzschia amphibia* Grunow, *Nitzschia semirobusta* Lange-Bertalot, *Pinnularia* spp., *Planothidium joursacense* (Héribaud) Lange-Bertalot, *Punctastriata mimetica* E.A.Morales, *Staurosirella martyi* (Héribaud) Morales & Manoylov, *Pseudostaurosira brevistriata* (Grunow) D.M.Williams & Round, *Staurosira binodis* (Ehrenberg) Lange-Bertalot, *Staurosira construens* Ehrenberg, *Staurosira venter* (Ehrenberg) Cleve & J.D.Möller, *Staurosirella pinnata* (Ehrenberg) D.M.Williams & Round, *Cyclostephanos dubius* (Hustedt) Round, *Fragilaria* spp., *Fragilariforma mesolepta* (Rabenhorst) Kharitonov, *Stephanodiscus minutulus* (Kützing) Cleve & Möller, and *Fragilaria/Synedra/Ulnaria* spp.

The dominant species for each zone with each maximum and minimum abundance are described in Table 4-2.

Table 4-2 *Dominant diatom taxa from BDL12 in each zone.*

	Major species (maximum and minimum in %) of BDL12
Zone 1 180 – 1100 cm 15.1 – 55.3 ka	*C. placentula* (0.2-56.3), *E. minutum* (0-9.7), *Melosira* spp. (0-5.2), *P. mimetica* (0-29.6), *P. brevistriata* (0-11.8), *S. construens* (0-41.3), *S. venter* (0-10.1), *S. martyi* (0-10.4), *S. pinnata* (11.3-78.2)
Zone 2 1100 – 1512 cm 55.3 – 70.6 ka	*C. placentula* (19.8-81.2), *P. joursacense* (0-7.5), *P. mimetica* (0-15.1), *P. brevistriata* (0-7.5), *S. construens* (0-8.4), *S. pinnata* (0-40.8), *C. dubius* (0-8.8), *S. minutulus* (0-13.3)
Zone 3 1512 – 2299 cm 70.6 – 108.4 ka	*A. copulata* (0-12.1), *Anomoeoneis* spp. (0-7.8), *C. placentula* (2.6-33.1), *Cymbella* spp. (0.3-14.9), *C. affinis* (0-12.6), *C. diluviana* (0-5.8), *Epithemia* spp. (0.8-6.9), *E. adnanta* (0-7.2), *Gomphonema* spp. (0-12.8), *G. pumilum* (0-9.5), *Halamphora* spp. (0-9.7), *Melosira* spp. (0-10.8), *Navicula* spp. (0-8.5), *Navicula* sp.1 (0-12.9), *N. radiosa* (0-7.7), *Nitzschia* spp. (0-8.1), *N. amphibia* (0-6.0), *N. semirobusta* (0-5.2), *Pinnularia* spp. (0-5.2), *P. mimetica* (0-8.3), *S. binodis* (0-11.6), *S. pinnata* (0-18.6), *C. dubius* (0-18.1), *Fragilaria* spp. (0-9.8), *F. mesolepta* (0-15.0), *S. minutulus* (0-7.6), *Fragilaria/Synedra/Ulnaria* spp. (0-5.6)

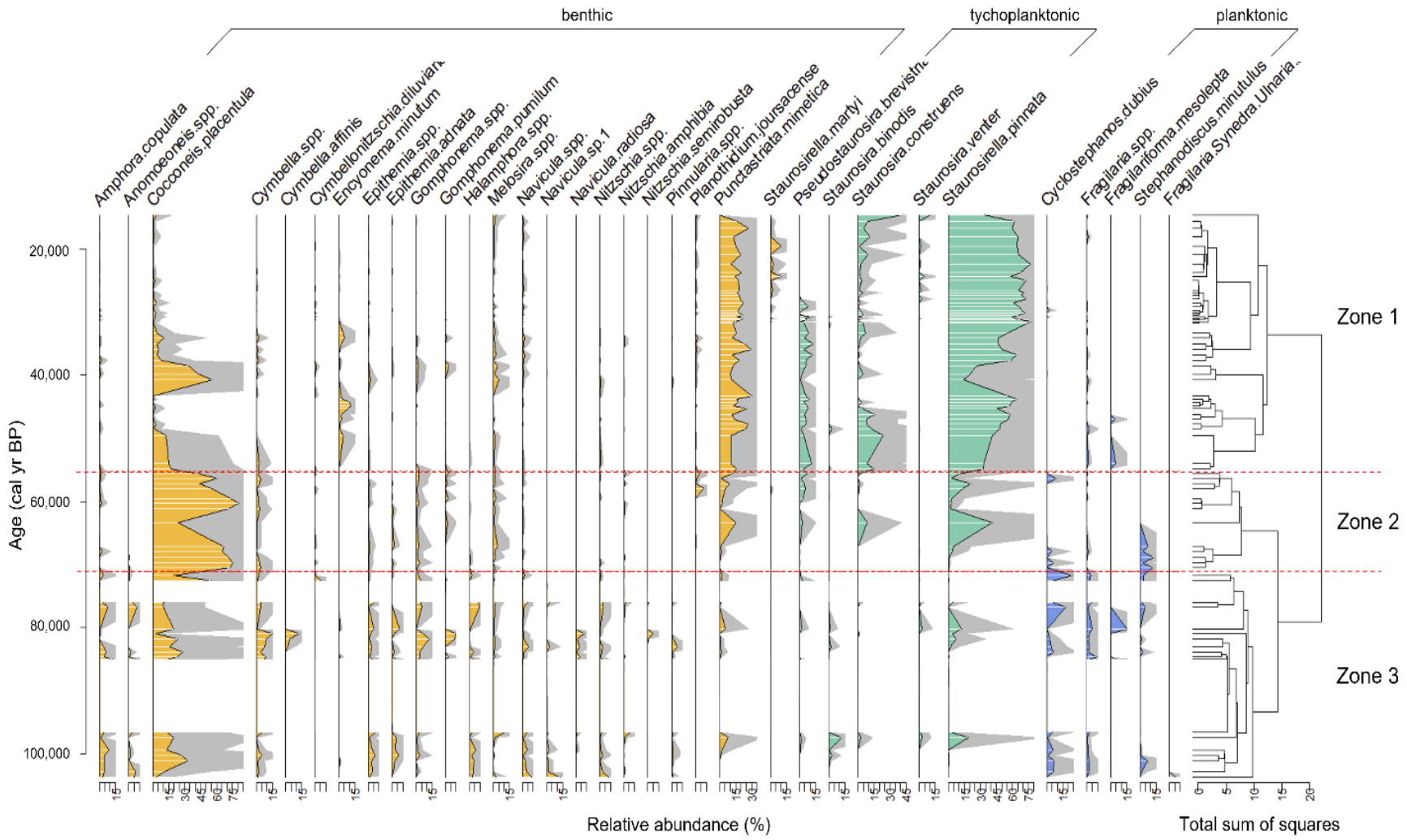

Figure 4-5 *The BDL12 diatom diagram with CONISS zonation.*

There were distinctive diatom species in the Baldwin Lake sediments that were not observed in Kelly Lake, Northern California (Chapter 2 and 3), such as the genus *Anomoeoneis*, genus *Halamphora*, etc. Out of 83 samples, there were seven samples with almost no diatoms - 1552, 1572, 1896, 1916, 1956, 2017, and 2077 cm. These depths contained very few *Fallacia pygmaea* and plenty of silicic/glass materials that were glittery. Also, there were depths with a paucity of diatoms at 1120, 1621, 1641, 2202, and 2299 cm. These depths were counted but barely provided 400 valves and sometimes less.

4.5.3 P:B ratio, and Br:Fr ratio

P:B ratio and Br:Fr ratio were calculated and drawn (Figures 4-6 and 4-7) only including major species. Each ratio was calculated after classifying major diatom taxa based on their autecology.

P:B ratio as an indicator of the water depth of Baldwin Lake is provided below (Figure 4-6B). Only planktonic and only benthic taxa were considered to calculate P:B ratio because one of tychoplanktonic taxa, *S. pinnata*, accounted for the majority of the data throughout the samples. The P:B ratio including *S. pinnata* as planktonic showed very different reconstruction from Figure 4-6B, which is almost opposite. After considering Baldwin Lake history, the current P:B ratio was selected which seemed to show the best scenario for Baldwin Lake. The variations of planktonic and benthic species are described in Figure 4-6A as well.

The planktonic and P:B ratio showed similar patterns and reached maximum at 70,600 cal yr BP (Figure 4-6). The number of planktonic species appearance diminished, and P:B ratio had less variation from 62,000 cal yr BP.

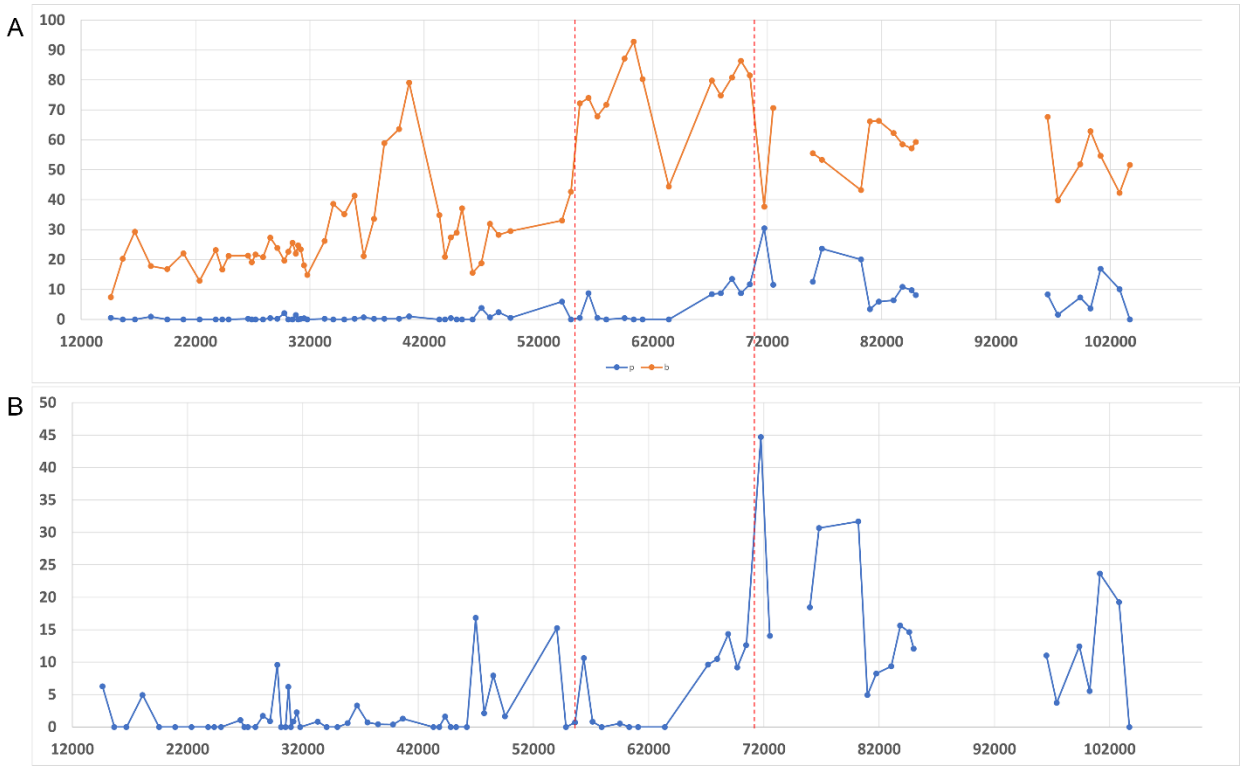

Figure 4-6 *A) Planktonic (blue) and benthic (orange) diatom taxa changes in Baldwin Lake during the late Quaternary, B) P:B ratio from BDL12 over the late Quaternary.*

Br:Fr ratio indicates the salinity changes in Baldwin Lake (Figure 4-7). Brackish species such as *Amphora copulata*, *Anomoeoneis* spp., *Halamphora* spp., *Epithemia* spp., *Epithemia adnata* were included as aforementioned (Robertsson 1995; Kashima et al. 1997; Zalat and El-Sheekh 1999; Levkov 2009; Wojtal 2009; Olivares-Rubio et al. 2017; Ikehata et al. 2022).

As shown in Figure 4-7, Baldwin Lake seemed to maintain high salinity in Zone 2 and 3, which is until around 75,000 cal yr BP. From ca. 72,000 cal yr BP, the salinity fluctuated a little bit until ca. 53,000 cal yr BP and it became static afterward.

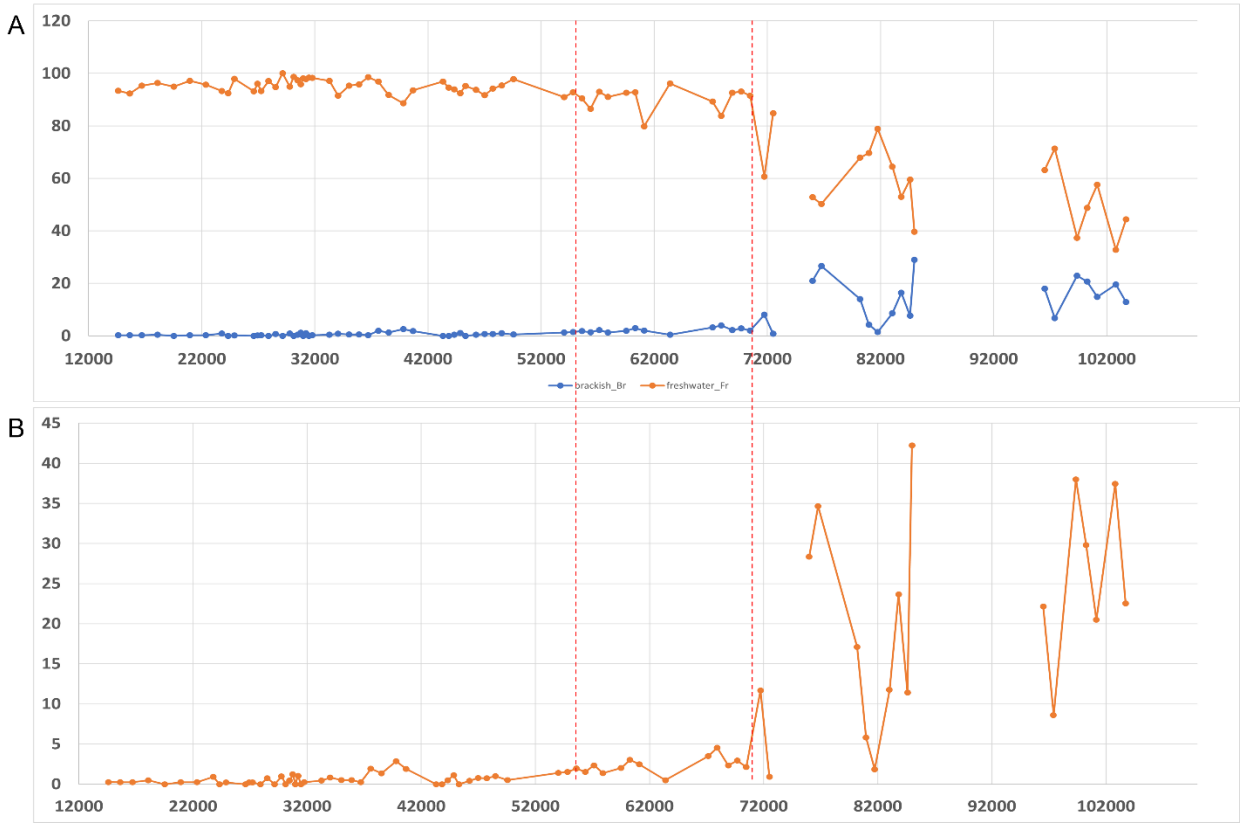

Figure 4-7 *A) Brackish (orange) and freshwater (blue) diatom taxa changes in Baldwin Lake during the late Quaternary, B) The BDL12 Br:Fr ratio changes over the late Quaternary.*

Figure 4-8 compares both P:B and Br:Fr ratios at the same time easily. Both ratios were high until around 75,000 cal yr BP, but Br:Fr ratio reduced abruptly afterward, while P:B ratio started to decline after 70,000 cal yr BP. Br:Fr ratio reached a maximum at ~ 86,200 cal yr BP, and P:B ratio reached its maximum at ~ 70,600 cal yr BP. Both ratios showed high fluctuations until they reached maximum values, and they became steady afterward.

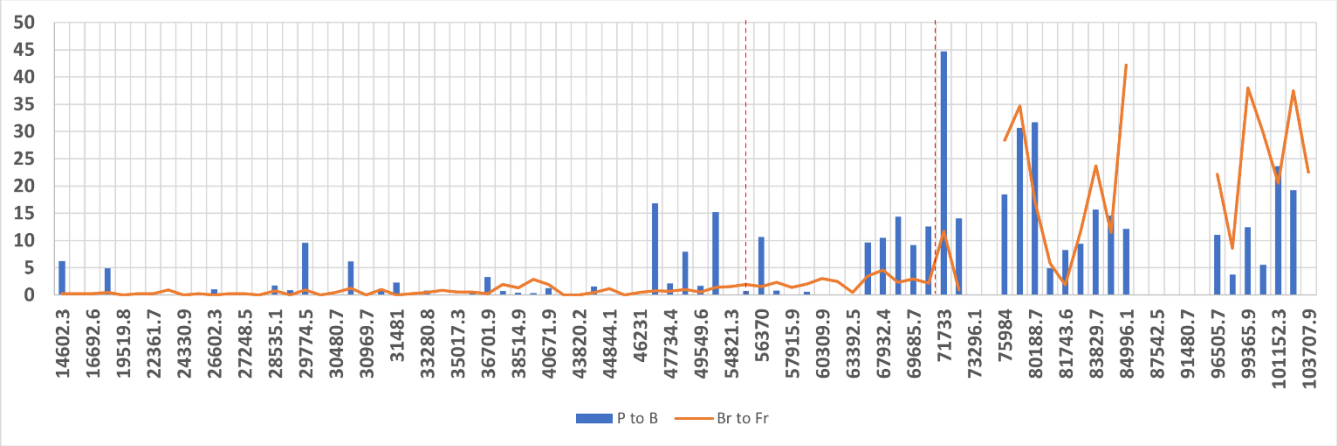

Figure 4-8 *P:B ratio and Br:Fr ratio from BDL12 from MIS 5 to MIS 2.*

4.5.4 Species diversity indices

Species richness (*S*), diversity (*H'*), and evenness (*J'*) were measured based on the whole diatom data. All the species indices appeared very similar. In Zone 3, H', J', and S marked their maximum. As they entered Zone 2, these indices decreased abruptly and maintained low values. Even though they rose as they went into Zone 1, they fluctuated over time.

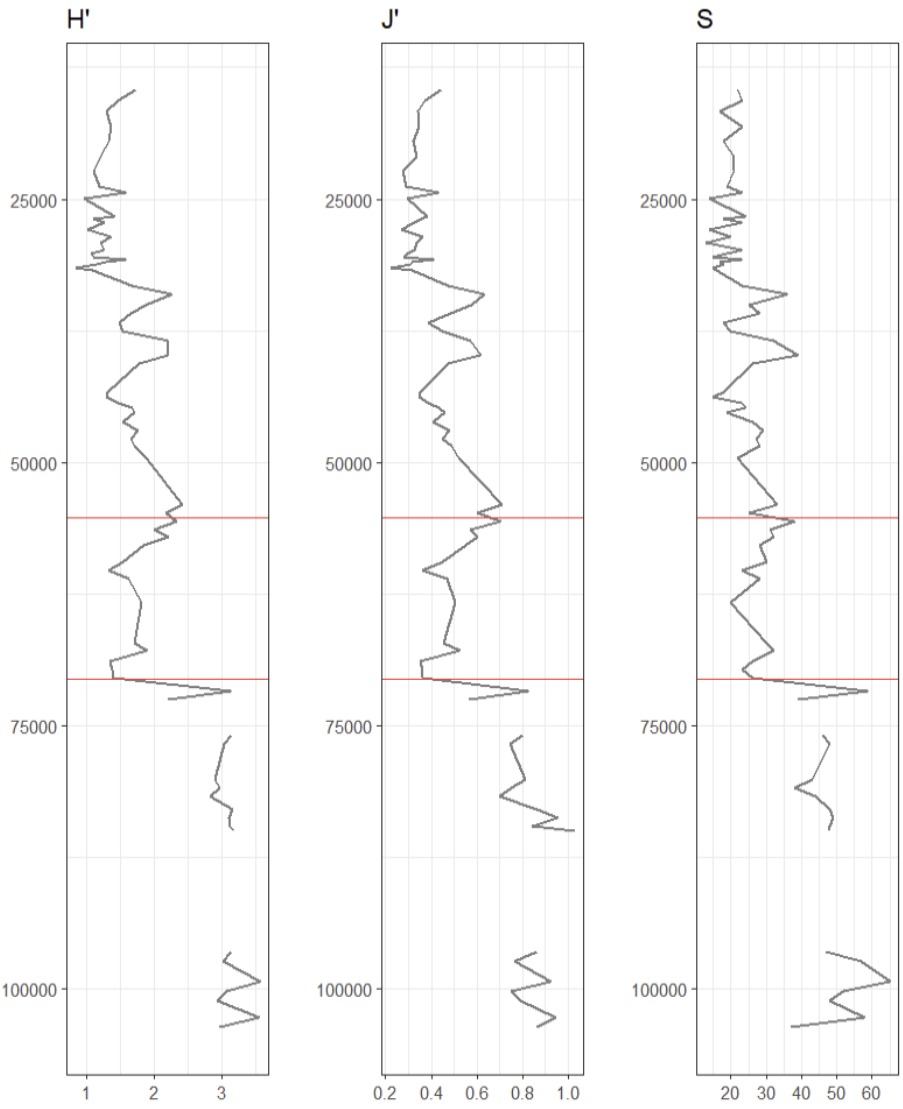

Figure 4-9 *Species diversity indices from BDL12 over the late Quaternary.*

4.5.5 PCA

PCA was run with major diatom species. The cumulative explained variation is 52.7% with four principal components. The eigenvalue percents were 24.51% for Axis 1, 12.55% for Axis 2, 8.70% for Axis 3, and 6.95% for Axis 4 (Table 4-3). The biplots of the PCA results are provided in Figure 4-10.

Table 4-3 *PCA eigenvalues and explained variation from BDL12 diatom.*

	Axis 1	Axis 2	Axis 3	Axis 4
Eigenvalues	0.2451	0.1255	0.087	0.0695
Explained variation (cumulative)	24.51	37.06	45.75	52.7

Based on the species scores and distribution in the biplots, each axis was environmentally interpreted (Figure 4-10). Higher Axis 1 values were considered to reflect higher salinity. The species scores were 0.73 for *A. copulata*, 0.66 for *Anomoeoneis* spp., and 0.69 for *Halamphora* spp. Based on the high scores on salinity-favored species, Axis 1 seemed to reflect salinity. Lower Axis 2 values were interpreted as higher water depth. The species scores of *C. dubius* and *S. minutulus* were -0.16 and -0.06. The values were not highly negative, but other benthic species' values were highly positive. For example, *N. radiosa* and *C. affinis* were 0.81 and 0.69. Axis 3 did not indicate a kind of environmental factor, but it was interpreted as the overall change. In general, higher Axis 3 values corresponded with Zone 1 diatom assemblages, while lower Axis 3 values represented Zone 2 and 3 diatom assemblages. For instance, the species scores of the diatoms that were abundant in Zone 1, such as *S. pinnata, P. mimetica*, and *Navicula* spp. were 0.38, 0.33, and 0.46. In contrast, the species scores of the fluent diatoms in Zone 2 and 3, such as *C. placentula, S. minutulus, C. dubius*, and *E. adnata*, were -0.61, -0.49, -0.29, and -0.28. High Axis 4 values appeared to correspond to low nutrient status or low nitrogen, and low Axis 4 values were interpreted as reflecting high nutrient conditions. *Epithemia adnata* and *Epithemia* spp. showed high species scores on Axis 4, such as 0.65 and 0.38, and the taxa are capable to fix nitrogen by themselves from the atmosphere because of cyanobacteria in the cells (Lowe 2010; Spaulding et al. 2021). Thus, I interpreted that a high Axis 4 value would indicate low nutrients or nitrogen or favorable environments for low-nutrient-tolerant species. On the contrary, the species scores of *C. dubius* and *S. minutulus* were

low (-0.15 and -0.34), and the species are often used as indicators of eutrophication (Anderson 1990; Reavie et al. 2000). Therefore, I interpreted that negative Axis 4 values would suggest high nutrient status.

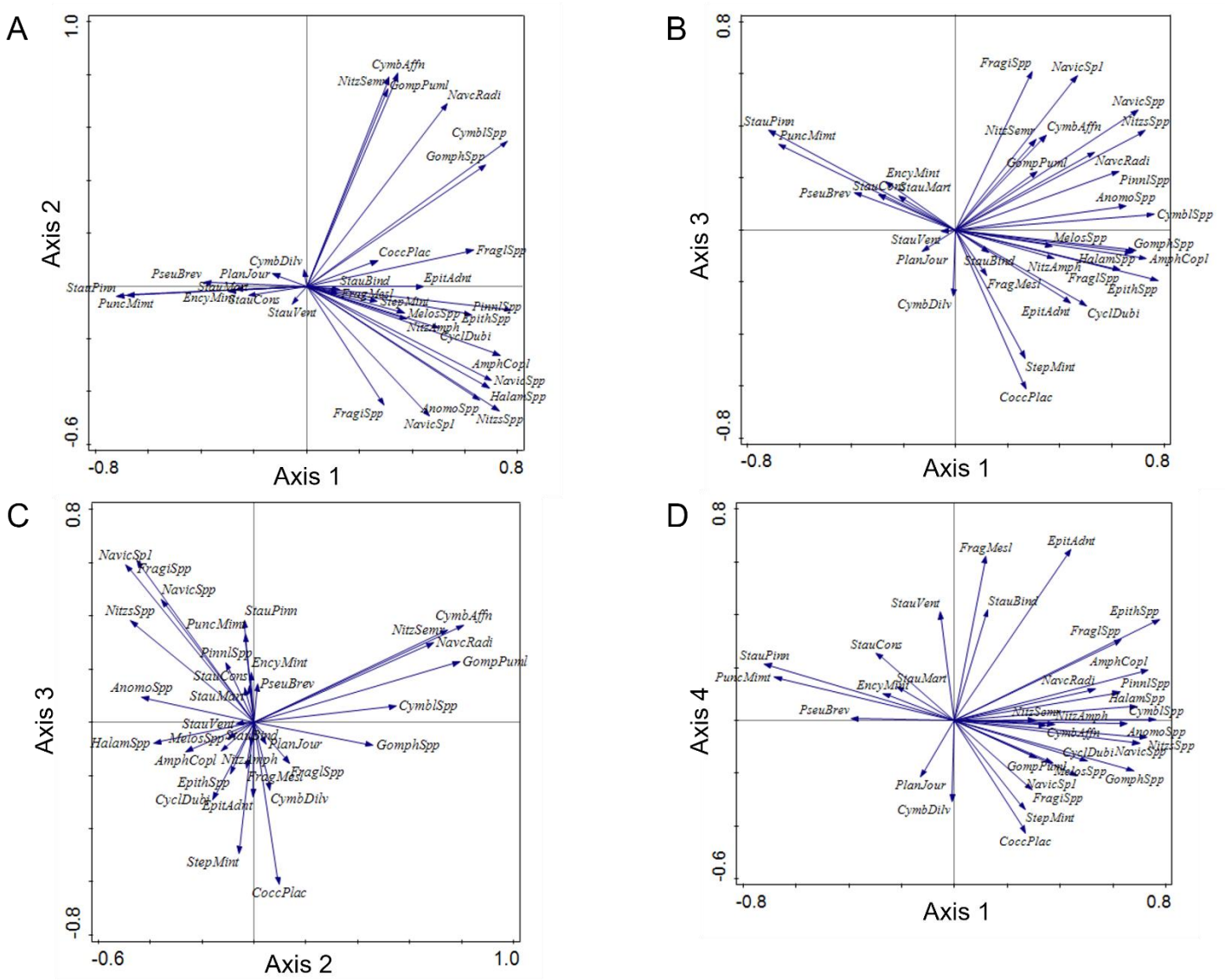

Figure 4-10 *BDL12 PCA biplots. A) Axis 1 and 2, B) Axis 1 and 3, C) Axis 2 and 3, D) Axis 1 and 4.*

Each axis sample score was drawn in Figure 4-11 with zonation. All the axes' trends were similar over time. In the discussion, Axis 1 will be mainly focused on in the later discussion because the explained variations for Axes 2, 3, and 4 were too small to consider.

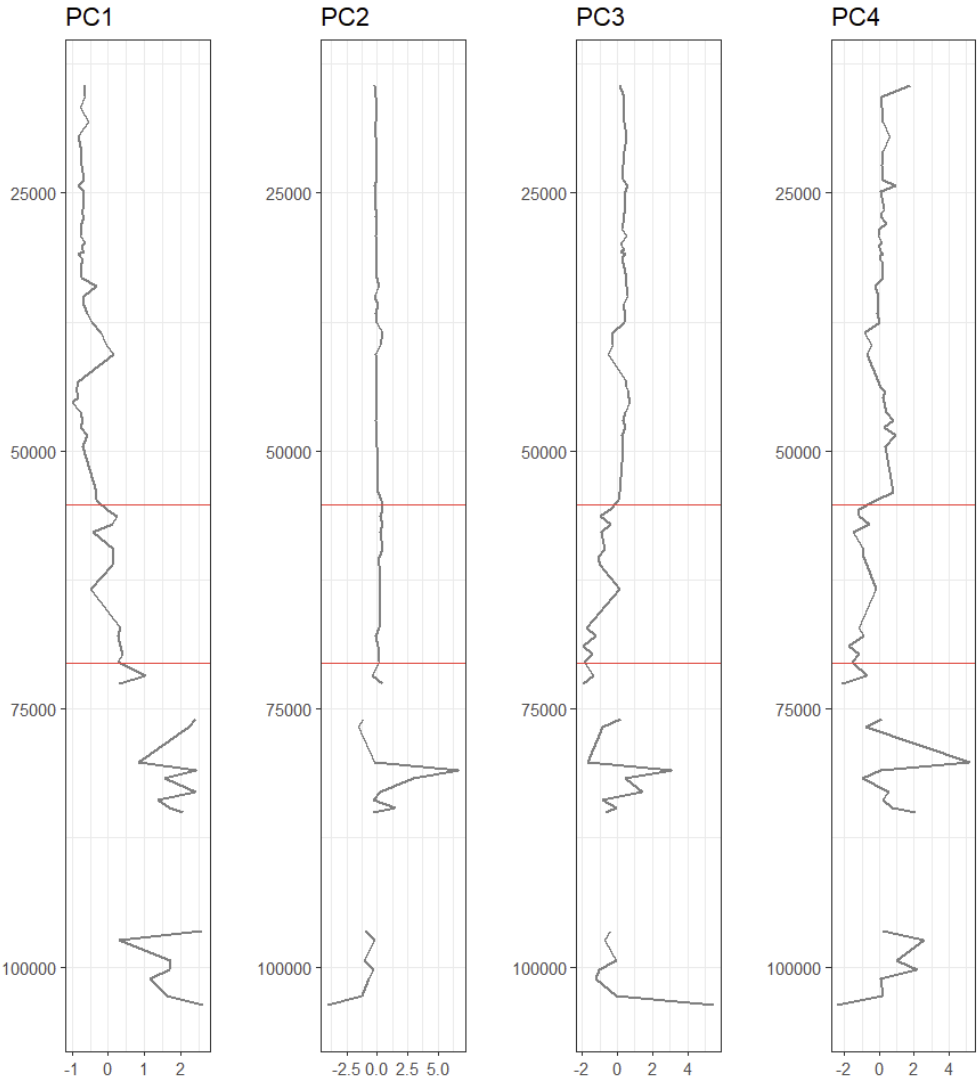

Figure 4-11 *Each PCA axis' eigenvalue changes over the late Quaternary from BDL12 diatoms.*

4.6 Discussion

Based on the results from this study, the Baldwin Lake diatoms provide evidence of changing lake conditions and hydroclimatic variability through salinity and lake-level changes as the lake became intermittent. This discussion is organized to answer the three big research questions raised in the Introduction of this chapter. First, the diatom-inferred reconstruction of hydroclimatic variability at Baldwin Lake over the late Quaternary (MIS 5 – 2) from this study is discussed. Second, the hydroclimatic record from this study is compared to the previous studies from Baldwin Lake. Lastly, the potential influences of external, orbital, or oceanic drivers are discussed that would impact the regional hydroclimatic variability around Baldwin Lake, SBM.

4.6.1 Diatom-inferred hydroclimatic variability and paleoenvironmental changes around Baldwin Lake over the late Quaternary (MIS 5 – 2)

BDL12 diatom assemblages from the late Quaternary are graphed in Figure 4-5. The major species' typical habitat conditions and autecology are provided in Table 4-4. Several species which appear at more than 3% in at least one sample are included in the table to provide additional habitat information. Salinity, water depth, pH, nutrient status, water temperature, conductivity/saprobity, and other environmental information can be deduced. *C. placentula* and *S. pinnata* appeared in all three zones dominantly; therefore, they were considered as generalists because these species are cosmopolitan and have a broad ecological tolerances (Jahn et al. 2009; Fluin et al. 2010; Marohasy and Abbot 2015). Interestingly, they appeared alternatively dominantly at the boundaries of Zone 1 and 2.

Based on the chronology and CONISS zonation, Zone 3 is considered as MIS 5, Zone 2 as MIS 4, and Zone 1 as MIS 2 – 3. MIS 5 has substages from MIS 5a to MIS 5e as described in

detail in Table 2 in Glover et al. (2017). Zone 3 from this study includes all the substages of MIS 5 from Glover et al. (2017).

Table 4-4 *The reconstructed environmental changes of Baldwin Lake from BDL12 dominant diatom taxa.*

	Dominent species	Salinity	Water depth	pH	Nutrient status	Water temperature	Conductivity & Saprobity	Note
Zone 1 (MIS 2 – 3)	***5%:*** *C.placentula, E. minutum, Melosira* spp., *P. mimetica, P. brevistriata, S. construens, S. venter, S. pinnata* ***3%****: F. mesolepta, P. joursacense*	Freshwater	Benthic, Benthic or planktonic Shallow	Weakly acidic Alkaline (pH = 8.2) High pH	Meso-eutrophic		Low conductivity (179 mS/cm)	*P. mimetica:* Moderate P and total N needed is an opportunistic species and has a wide ecological tolerance
Zone 2 (MIS 4)	***5%****: C. placentula, P. joursacense, P. mimetica, P. brevistriata, S. construens, S. pinnata, C. dubius, S. minutulus* ***3%****: Melosira* spp., *Cymbella* spp., *Gomphonema* spp., *A. copulata*	Freshwater, Brackish/halophile	Benthic Deep but shallower than Zone 3	High alkaline pH = 7.3	Eutrophic Meso-eutrophic	19.2 °C	Good water quality High conductivity (430 µS/cm) DO: 6.4 mg/L Low conductivity (179 µS/cm)	*P. joursacense*: optimum of total P is 47.5 µg/L
Zone 3 (MIS 5)	***5%****: C. placentula, A. copulata, Anomoeoneis* spp., *Cymbella* spp., *C. affinis, C. diluviana, Epithemia* spp., *E. adnate, Gomphonema* spp., *G. pumilum, Halamphora* spp., *Melosira* spp., *Navicula* spp., *Navicula* sp.1, *N. radiosa, Nitzschia* spp., *N. amphibia, N. semirobusta, Pinnularia* spp., *P. mimetica, S. binodis, S. pinnata, C. dubius, Fragilaria* spp., *S. minutuls, F/S/U spp.*	Brackish, Freshwater	Planktonic, Benthic or planktonic, benthic Deep	Alkaline (pH = ~ 8.7)	Eutrophic High nutrient concentration	24 °C 19.2 °C	High conductivity (2788 µS/cm) DO: 13 mg/L Elevated levels of dissolved and suspended solids	*Epithemia* spp.: can inhabit low N/P environment High *H', J', S N. radiosa*: benthic, in turbid waters, human disturbances

The salinity in Baldwin Lake seemed to decrease from MIS 5 to MIS 2. During MIS 5 (Zone 3), there were distinctive appearances in several diatom species that did not show up in other periods, such as the genera *Anomoeoneis* and *Halamphora*. These species are known to be brackish (Patrick and Reimer 1966; Levkov 2009; Olivares-Rubio et al. 2017). Besides, *Amphora copulata* and the genus *Epithemia* are known as freshwater species, but they can also inhabit high-salinity environments (Kashima et al. 1997; van Wirdum et al. 2019; Govindan et al. 2021). Therefore, Baldwin Lake during MIS 5 seemed to be a somewhat saline lake, but deeper than later periods. As it entered MIS 4 to 2, salinity-favorable or salinity-tolerant species diminished. Overall, the salinity in Baldwin Lake decreased over time.

Water depth at Baldwin Lake also showed a similar pattern with the salinity changes; it was deep during MIS 5, deep but shallower than before during MIS 4, and became shallow during MIS 2 and MIS 3. This was inferred by the numbers of planktonic taxa and their abundances. During MIS 5, *C. dubius, S. minutulus, Fragilaria* spp., and *Cyclotella meneghiniana* appeared, and three of them were dominant. As it entered MIS 4, *C. dubius* and *S. minutulus* were still dominant, but the types and abundance of total planktons decreased. Accordingly, the lake water depth was inferred to be shallower relatively than the previous. As it entered MIS 3, there were no planktons as the dominant species, and benthos and tychoplanktons flourished. These assemblages maintained steady fairly until MIS 2.

When salinity and water depth at Baldwin Lake decreased, the level of nutrients in the lake also declined from MIS 5 to MIS 2. *N. radiosa* during MIS 5 and *S. minutulus* during MIS 4 and MIS 5 are found in high nutrient environments (Reavie et al. 2000; Potapova 2011). *P. mimetica*, which is a major species during MIS 2 to 4 is often found in meso- to eutrophic environments (Temoltzin Loranca 2018). *E. minutum*, a dominant species in Zone 1, favors oligo- to mesotrophic nutrient concentrations (Lange-Bertalot et al. 2017). Consequently, the nutrient concentration of Baldwin Lake reduced over the late Quaternary.

Changes in pH, water temperature, and conductivity at Baldwin Lake were not shown clearly. Water temperature seemed to follow the atmospheric temperature, but there was not enough information to infer. pH seemed to decline slightly over time because most dominant species were found as alkaliphilic, while the subspecies of *E. minutum*, *E. minutum* var. *pseudogracilis*, are acidophilous (Bishop 2017). Trends in conductivity did not show well, but it seemed to decline over time as well. *N. radiosa* and *N. semirobusta* during MIS 5 are often found in high conductance waters (Potapova 2011; Underwood 2013). Also, *Anomoeoneis*

sphaerophora appear when dissolved and suspended solids increased (Bahls and Luna 2018). However, there was not enough evidence to reconstruct changes in water temperature, pH, and conductivity.

Furthermore, more paleoenvironmental changes can be inferred based on individual taxa's characteristics. *C. placentula* was in low abundance when the salinity was high during MIS 5 but became dominant during MIS 4. This may be because *C. placentula* favors low temperature, while it is less likely to be observed the taxa in brackish environments (Patrick and Reimer 1966; Jahn et al. 2009). *P. mimetica* is an opportunistic species when there is a moderate P concentrations and abundant N concentrations (Morales 2005), and *Epithemia spp*. can flourish when there is a low N concentrations in water (Spaulding et al. 2021). Although P and N cycling is closely related to water depth (Wang et al. 2023), the N concentrations at Baldwin Lake during MIS 5 were low but increased gradually according to the two distinctive taxa. Also, *P. brevistriata* is known as opportunistic species that increase quickly when there is a noticeable environmental change (Dalton et al. 2018; Bergman et al. 2020). *P. brevistriata* appeared abundantly during MIS 4 and MIS 3 (Zone 2 → Zone 1), and this can be related to the unfavorable environmental conditions to diatoms and cold temperatures of MIS 4 and the abrupt transition from MIS 4 to MIS 3, where there were big changes in diatom assemblages in Baldwin Lake (e.g., *C. placentula* and *S. pinnata*).

4.6.2 Reconstruction of Baldwin Lake paleohydrology in comparison to previous studies

The diatom-based reconstruction corroborated that the salinity and water depth of Baldwin Lake decreased gradually from MIS 5 to MIS 2. One distinctive change as shown in the diatom diagram (Figure 4-5), is there was an abrupt change in diatom composition at ca. 70,000 cal yr BP. This suggested that something important was going on in the lake. Therefore, the

subsections of *Section 4.6.2* will describe the more comprehensive environmental changes from MIS 5 – MIS 2 and focus on Dansgaard-Oeschger (D-O) events after MIS 3 at Baldwin Lake. D-O events are known as global warming events during the late Pleistocene (~ 11,5000 – 11,000 cal yr BP) that are inferred from oxygen, nitrogen, and argon isotopes from Greenland ice core records (Dansgaard et al. 1993; Saha 2015).

4.6.2.1 Hydroclimatic variability in Baldwin Lake over the late Quaternary (MIS 5 – MIS 2)

There were two ranges of no diatoms from the BDL12 diatom data – between 73,000 and 76,000 cal yr BP and 86,000 and 97,000 cal yr BP, and they are called no-diatom-depths in this study. The periods apparently had an unfavorable environment for diatoms. For diatom growth, nitrogen (N), phosphorus (P), silicon (Si) are the limiting nutrient factors (Løvstad and Bjørndalen 1990; Nelson and Tréguer 1992). In particular, as diatom frustules are made of silica, Si is one of the key elements for diatoms (Kröger 2007). The no-diatom-depths are consistent with the time periods when biogenic silica (BSi) and organic content reached minimum values as well as when bulk inorganic values reached maximum (yellow highlighted parts in Figure 4-12). It is when summer insolation was low (~ 465 W/m^2), and winter insolation was high (~ 220 W/m^2). The factors suggest that Baldwin Lake at the no-diatom-depths was nonproductive. This perhaps represents very low summer insolation.

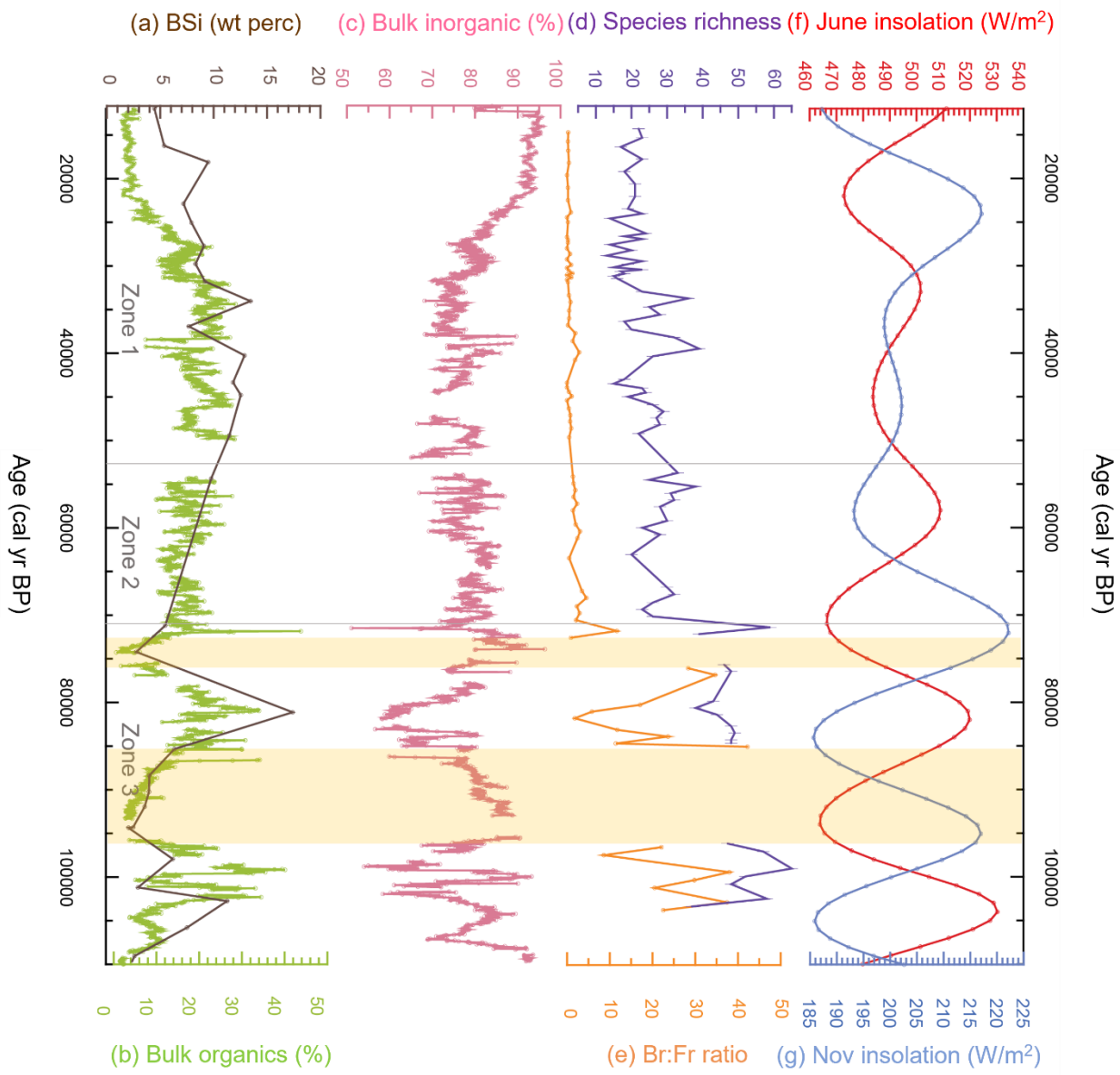

Figure 4-12 *No-diatom-depths from BDL12 from MIS 5 to MIS 2. The no-diatom-depths are highlighted yellow in the figure to indicate the correspondence between geochemical, insolation, and diatom data. BDL12 diatom data was compared to Glover et al. (2017) and 34°N Summer and Winter insolation data (Laskar et al. (2004)). (a) Biogenic silica (wt perc), (b) Bulk organic content (%), (c) Bulk inorganic content (%), (d) Species richness, (e) Br:Fr ratio, (f) 34°N June insolation (W/m^2), and (g) 34°N November insolation. The data sources are Glover et al. (2017) for (a), (b), (c), this study for (d), (e), and Laskar et al. (2004) for (f), (g).*

Also, there was a big shift at around 70,000 cal yr BP where there were big changes in diatom assemblages (Figure 4-13). Let us call it Phase 1, which is almost the same period as MIS

5 (or Zone 3), and Phase 2 after the time period starting ~ 70,000 cal yr BP, which includes MIS 4, 3, and 2 (or Zone 2 and 1). The division of Phases 1 and 2 does not perfectly match the division of Zones 2 and 3, and it would be because the division of Phases are based on diatom signals, and there would be ecological inertia.

During Phase 1, the P:B ratio was high, and several planktonic diatom taxa appeared. At that time, the lake also had large amounts of carbonate and BSi and high Mn:Ti ratios, and this can be related to high salinity at this time. High salinity means high ionic concentration and the composition of total dissolved solids in a lake, and it also indicates high weathering with increase in base cation (Fritz et al. 2010; Cho et al. 2022). Moreover, the high salinity is supported by high abundance in the brackish genus *Anomoeoneis* and a high Br:Fr ratio (Figure 4-13I & K). Although the pH changes in Baldwin Lake did not show a drastic change, the lake had fairly high pH during Phase 1. This high pH can be also related to high primary production and high decomposition (Cho et al. 2022). Accordingly, Baldwin Lake was deep and saline during Phase 1.

The abrupt shift from Phase 1 to 2 seems closely related to the shift in insolation from high variability with periods of very high summer insolation to dampened variability (Figure 4-13). When it entered Phase 2, there was a sudden shift in the lake conditions mineralogically, geochemically, and biologically. Most diatom-related indicators and geochemical indicators were in high variability during Phase 1 and showed seasonal differences, but they showed low variability during Phase 2. Glover et al. (2020) elucidated that Baldwin Lake underwent the most rapid changes in lake conditions during Phase 1 due to the highest amplitude in summer insolation, while the lake during Phase 2 experienced minimal erosions, especially during MIS 4 – 3 and became unproductive eventually in MIS 2.

As indicated with tie-points, Mn:Ti, carbonates, BSi, organics productivity, P:B ratio, Br:Fr ratio, and PC 1 appeared to be positively correlated with summer insolation (Figure 4-13) during Phase 1. When June insolation was high, the indicators appeared high, and they decreased when June insolation was low. Although it showed an offset, the genus *Anomoeoneis* appeared high with some ecological inertia. During Phase 1, Baldwin Lake's water depth was deep because it was a newly formed lake (Glover 2016). At that time, the high variability in insolation led to high summer temperature, and high temperature caused high evaporation, so the lake was likely to be loaded with soluble substances. This led to high salinity in the water of the lake, and these salinity fluctuations can be supported by the changes in the brackish diatom genus *Anomoeoneis*.

After the lake entered Phase 2, most of the values became somewhat stable even though there were little peaks or humps when the dampened summer insolation was high. This was caused by smaller seasonal differences in insolation (Glover et al. 2020). Diatoms need sunlight for photosynthesis; therefore, the weakened insolation gave a high impact on the abundance (Round et al. 1990; Sarthou et al. 2005). Lower summer insolation may have also decreased lake water temperatures and impacted diatom productivity. The species richness diminished as well during Phase 2 (Figure 4-12). On the contrary, *S. pinnata* became abundant, a the taxa which can adapt to low-light environments (Laird et al. 2010). The low-insolation-tolerant diatom taxa replaced the previously dominant species after Phase 2.

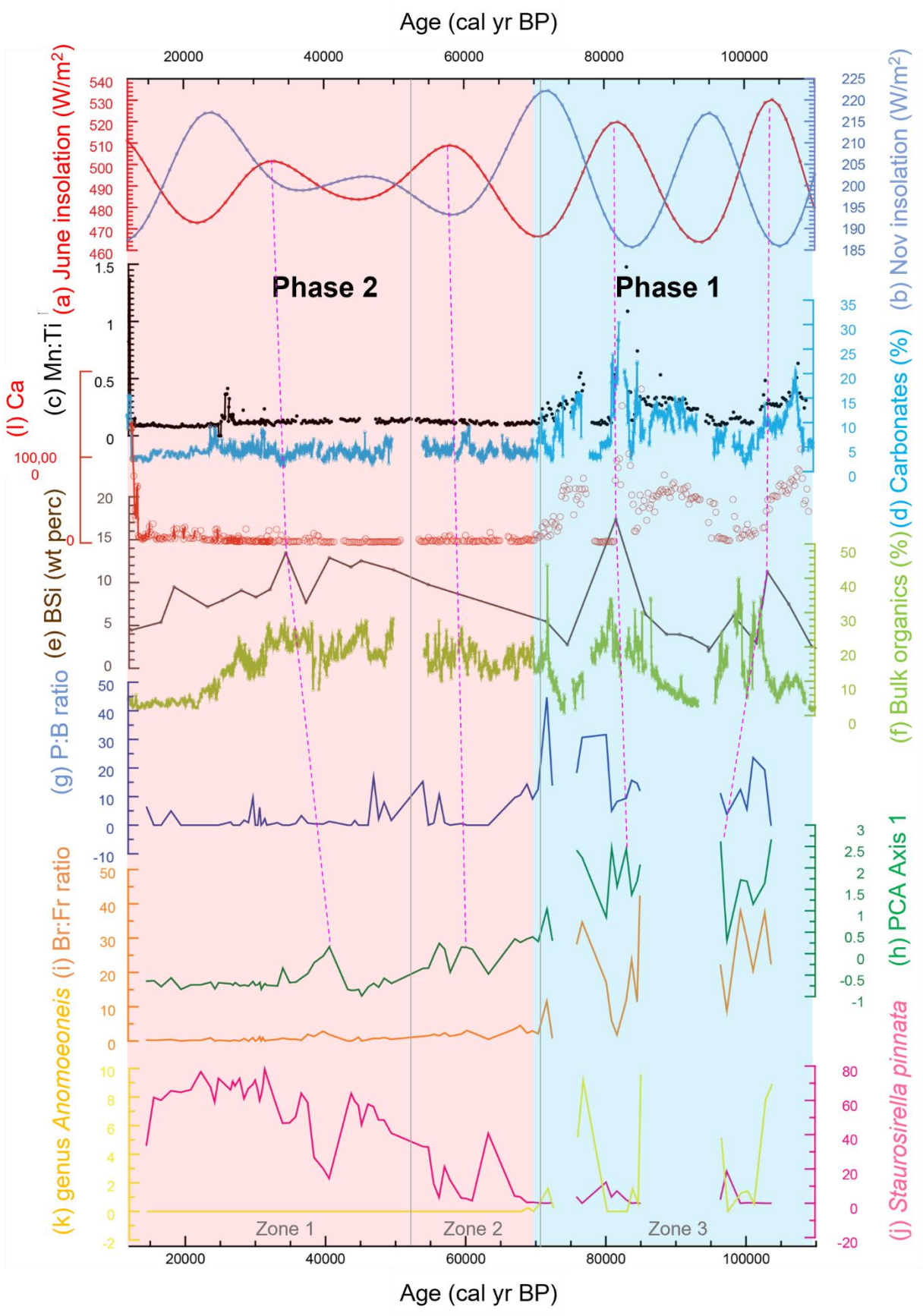
Age (cal yr BP)
20000
40000
60000
80000
100000
(a) June insolation (W/m²)
(b) Nov insolation (W/m²)
Phase 2
Phase 1
(l) Ca
(c) Mn:Ti
(d) Carbonates (%)
(e) BSi (wt perc)
(f) Bulk organics (%)
(g) P:B ratio
(h) PCA Axis 1
(i) Br:Fr ratio
(j) Staurosirella pinnata
(k) genus Anomoeoneis
Zone 1
Zone 2
Zone 3
Age (cal yr BP)

Figure 4-13 *A large shift in insolation and the paleolimnological variables is apparent at approximately 70,000 cal yr BP. Phase 1 (pre ~70,000 cal yr BP) in blue and Phase 2 (post ~ 70,000 cal yr BP) in red. The pink dotted lines connect the geochemical and diatom reaction in the lake when the summer insolation was high. (a) June Insolation (W/m^2), (b) November Insolation (W/m^2), (c) Mn:Ti ratio, (d) Carbonates (%), (e) Biogenic silica (wt perc), (f) Bulk organic content (%), (g) P:B ratio, (h) PCA Axis 1, (i) Br:Fr ratio, (j) Staurosirella pinnata, (k) genus Anomoeoneis, and (l) trace element Ca. The data sources are from Laskar et al. (2004) for (a), (b), Glover et al. (2017) for (c), (d), (e), (f), (l), and this study (g), (h), (i), (j), (k).*

This study starts from 108,000 cal yr BP, and the P:B ratio was very low at that time. The period was right after a prolonged drought at ~ 110,000 cal yr BP proposed by Glover et al. (2020) with declined pine and increased sage and sagebrush. The planktonic taxa, such as *C. dubius*, *S. minutulus*, *Fragilaria* spp. began to rise after the xeric period. The Baldwin diatoms, therefore, implied that there was a dry period, consistent with Glover et al. (2020). In the pollen record from Glover et al. (2020), another drought was detected approximately at 70,000 cal yr BP with low tree abundance and low pollen concentration. This period is close to the boundary between Phase 1 and 2 (Figure 4-13) where the abundances of planktonic taxa and P:B ratio dropped sharply. At this time, a benthic species, *C. placentula,* became abundant abruptly (Figure 4-5), and this was because it is an early colonizer that is a kind of species that dominantly inhabits the new environment (Radloff et al. 2010). The fact that the early colonizer, *C. placentula*, came in and became dominant conveyed that there was an abrupt environmental change at 70,000 cal yr BP.

4.6.2.2 D-O events at Baldwin Lake after 60 ka

D-O events normally brought abrupt warming (~ 10°C) followed by rapid cooling (Ahn and Brook 2007; Saha 2015). These patterns were also detected in the earlier records from Baldwin Lake (Kirby et al. 2006; Glover 2016). Glover et al. (2017) observed D-O interstadials and indicated them in numberings on the bulk organic stratigraphy from Baldwin Lake. This is plotted in Figure 4-14 to investigate the presence of signals of D-O events in diatom-related

values such as PC 1, species richness, Br:Fr ratio, P:B ratio, and *S. pinnata* from 60,000 to 12,000 cal yr BP. Information on orbital variations is also presented and considered.

Diatom-related indicators showed fluctuations as they entered 60,000 cal yr BP when the solar insolation was dampened for about 30,000 years from ca. 60,000 to 30,000 cal yr BP (Figure 4-14). That would cause a very mild climate in the region. This is almost coeval with the period of Phase 2 that was discussed earlier. Most diatom signals seemed to be relatively flat during this period compared to amplitude prior and before. However, when the variations only over this period are considered, there are important and apparent fluctuations in diatom indices. Accordingly, diatom records appear to have detected some D-O interstadials (tie-points in Figure 4-14). In the figure, the red dotted lines show the connections between the observed D-O events in Glover et al. (2017) and the diatom-related indicators in this study. The blue long dashed dotted lines were added to show some possible climatic signals that might be related to D-O interstadials, which was not mentioned in Glover et al. (2017).

Due to the increased temperatures driven by D-O interstadials, Baldwin Lake became productive during the warmer D-O periods. It was not as productive as it was during the high summer insolation MIS 5 based on the geochemical and diatom indicators, but during the D-O events, the lake appears to have had more organic materials available in the lake, became deeper, had more dissolved solids in water (salinity), and more varied species diversity. Particularly, species richness and Br:Fr ratio pointed out clearly the D-O interstadials 3, 4, 5, 6, 8a, 6, 10, 14, and 15 followings the numbers from Glover et al. (2017). However, the diatom records are in lower temporal resolution compared to the bulk organic contents from Glover et al. (2017), so there are some latencies or missing signals.

The BDL12 diatom records also provide evidence of extra environmental signals that the bulk organic content data does not capture (pink highlighted column in Figure 4-14). At the pink highlighted period, summer and winter insolation began to be dampened. The low-light-adapted species, *S. pinnata*, began to become predominant about at this period (Figure 4-14H), and it is consistent with the period when summer and winter insolation began to experience lower seasonal variability. Species richness showed a fairly steep decline following a peak at the beginning of the period (Figure 4-14E). The salinity indicators, Br:Fr ratio and PC 1, were in a declining trend as well, especially right after hitting a huge peak in the beginning of the period (Figure 4-14D & F). P:B ratio also decreased abruptly after its peak (Figure 4-14G). All the sudden changes in the indicators would imply lowstand conditions at Baldwin Lake with decreasing salinity. Correspondingly, Baldwin Lake experienced abrupt environmental changes in that water depth became shallow, and salinity decreased at that time. It is likely suggested less evaporation rather than more precipitation because of declining species richness, salinity, and dampened the seasonal differences in solar radiation.

Kirby et al. (2006) and Glover et al. (2017, 2020) showed that lake productivity in terms of organic contents seemed to track insolation changes at this high-altitude lake, but also there were clear changes in lake conditions around 60,000 and 70,000 years ago. This high variability from the diatom-based indicators seems to match the high variability in insolation, and the variability was very dampened after that and lasted until the Last Glacial Maximum (LGM) began. The diatom composition changes during the period basically support the biogenic silica record and organic content in the lake, and the diatoms elucidated what the lake conditions were. Therefore, the regional climate of San Bernardino Mountains where Baldwin Lake is located experienced sudden and consequential changes at ca. 60,000 and 70,000 cal yr BP. The climate

changes impacted the regional climates and lacustrine environments and brought about abrupt and distinctive changes in the diatom composition of the lake.

In conclusion, some of the peaks in some of the diatom measures (e.g., species richness) seemed to correspond to the positive D-O events, but the relationship between them is not perfect. Also, variability in the diatoms was higher during the period of D-O variability than it was after that; most diatom indicators, such as species richness, Br:Fr ratio, P:B ratio, and PCA Axis 1, were flattened after ~ 24,000 cal yr BP, which was when seasonal differences in insolation began to increase. This is also correlated to the fact that Baldwin Lake was transitioned to intermittent lake during MIS 1 (~ 14,000 cal yr BP) with low sedimentation and desiccation (Glover et al. 2017). During that period of low insolation variability between the summer and winter insolation, the D-O interstadials were observed clearly, and there was variability in the lake during that time period. Once it went back to high seasonal variability after D-O interstadials 3, the lake did not seem to have the same ups and downs and to be as quite variable reflecting higher frequency short-term perturbations like the D-O events.

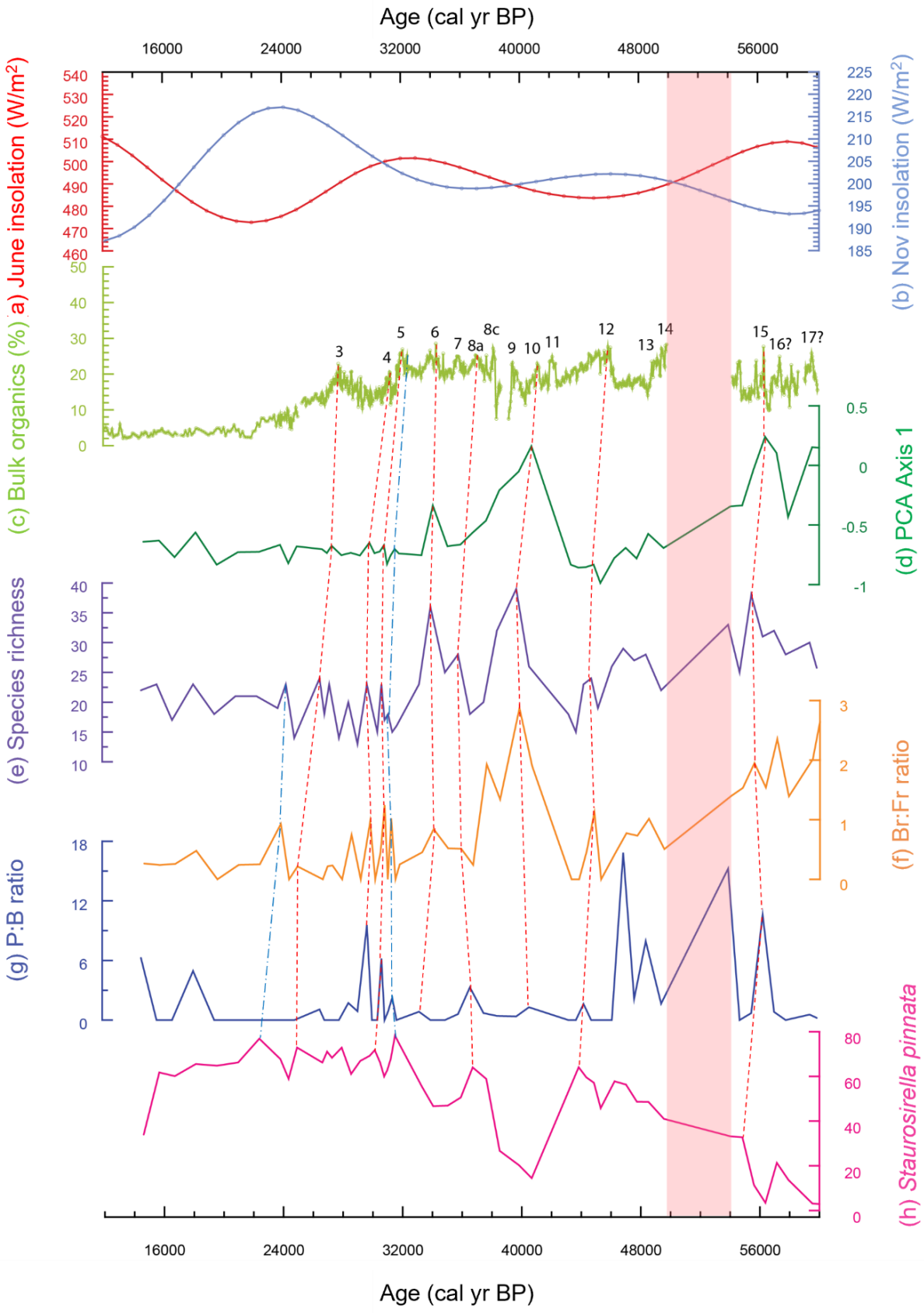
Age (cal yr BP)
16000
24000
32000
40000
48000
56000
a) June insolation (W/m²)
(b) Nov insolation (W/m²)
(c) Bulk organics (%)
3
4
5
6
7
8a
8c
9
10
11
12
13
14
15
16?
17?
(d) PCA Axis 1
(e) Species richness
(f) Br:Fr ratio
(g) P:B ratio
(h) Staurosirella pinnata
Age (cal yr BP)

Figure 4-14 *D-O events from diatom records in Baldwin Lake from 60,000 to 12,000 cal yr BP. The pink highlighted column indicates the period when summer and winter insolations began to be dampened. The red dotted lines show the correspondence between the observed D-O event in Glover et al. (2017) and this study. The blue long dashed dotted lines display some additional D-O related interstadials that could be observed from BDL12 diatom data. (a) June Insolation (W/m^2), (b) November Insolation (W/m^2), (c) Bulk organic content (%), (d) PCA Axis 1, (e) Species richness, (f) Br:Fr ratio, (g) P:B ratio, (h) Staurosirella pinnata. The data sources are from Laskar et al. (2004) for (a), (b), Glover et al. (2017) for (c), this study for (d), (e), (f), (g), (h).*

4.6.3 External, orbital, or oceanic forcings that drove such hydroclimatic fluctuations in Baldwin Lake, San Bernardino Mountains

Baldwin Lake experienced an abrupt shift as it entered MIS 3 and several D-O events as explained previously. This shift can be seen with various proxies at a global scale to explore external, orbital, or oceanic forcings that drove such hydroclimatic fluctuations in Baldwin Lake, SBM. Baldwin Lake's P:B ratio, Br:Fr ratio, PCA Axis 1, species richness, and bulk organics were plotted in Figure 4-15, and 34°N summer and winter insolation, CO_2 concentration changes that were measured in Antarctica, GISP2 $\delta^{18}O$, eastern equatorial Pacific SSTs, and ODP1012 (at 32°N) SSTs were also provided as global-scale proxies for comparison (Figure 4-15).

During MIS 5 (Zone 1), the seasonal differences in solar insolation were large, and Baldwin Lake had high productivity and higher biodiversity when summer insolation was high, and vice versa. In particular, the BDL12 diatom preservation was awful when solar irradiance was the lowest and the lake had the lowest productivity (Figure 4-15A & J), and the no-diatom-depths with poor diatom preservation contained literally no diatoms in sediments (the missing ranges in Figure 4-15G, H, I, & K). The reason why there were no diatoms in the samples was probably a very cold climate due to the low summer insolation, so that the lake environment was not very productive for diatoms as the bulk organics were also low (Figure 4-15J).

One possible explanation for the deep but saline lake conditions is that the SBM region had high precipitation when it had high summer insolation, and it caused deeper water depth of the lake. In addition, Baldwin Lake basin was new regime and newly formed (Glover 2016); therefore, the lake might have had an active regime with a lot more suspended solids and mineral debris in solution coming into the lake from the surrounding valleys and mountains by winds and/or runoff at that time period of high summer insolation. Moreover, it is clear that the SBM region was under the influence of coastal SSTs (Figure 4-15F) because diatom-related indicators were coeval with the changes of the Northeastern Pacific SSTs; the no-diatom-depths match the time period when the Northeastern Pacific SSTs declined (Herbert et al. 2001), and species richness, PCA Axis 1, Br:Fr and P:B ratios roughly coincide with the rise in the Northeastern Pacific SSTs at around 100,000 and 80,000 cal yr BP. In general, Baldwin Lake may have been deeper, but it may have had a high evaporation regime during MIS 5. However, it is quite difficult to assert so because there were no diatoms preserved during the period of low summer insolation.

As the variability of insolation went down as it started transitioning into MIS 4, 3, and 2, PCA Axis 1, Br:Fr and P:B ratio, and bulk organics declined gradually and showed low variability (Figure 4-15) with some highest values that were associated with D-O events (Figure 4-14). The declining trends were because of the lessened seasonal variability in insolation, particularly during MIS 2 (Figure 4-15). Moreover, Br:Fr ratio went along with species richness between 60,000 and 12,000 cal yr BP (Figure 4-14E & F). Normally, species richness declines with cooler temperatures (Sorvari et al. 2002; McCain 2007). Consequently, Baldwin Lake sediments definitely captured the insolation variability.

Baldwin Lake diatoms can also be related to other global proxies (Figure 4-15). During MIS 5, the high CO_2 concentration from Antarctica and high SSTs from eastern equatorial Pacific Ocean were contemporaneous with the high trends in diatom-related indicators. CO_2 concentration in the atmosphere is closely related to climatic changes between glacial and interglacial periods (Ahn and Hur 2014). Also, Northeastern Pacific SSTs at 32°N (ODP1012) also suggested the temperatures off the coast of California were higher during MIS 5, and the warmer conditions would have been more conducive to higher precipitation in California (Ji et al. 2019; Ilbay-Yupa et al. 2021; Barlow et al. 2021). In the meantime, GISP2 $\delta^{18}O$ had low variability during MIS 5, and it began to increase gradually during MIS 4 and had high variability as it entered MIS 3. The SSTs around the equator gradually decreased over time, while the SSTs off the coast of California maintained high values with fluctuations during MIS 5 and low values until the mid of MIS 2, and they rose again afterward. As the highly fluctuations in seasonal insolation became dampened, the oceans at the equator and near California became cooler. The lowered insolation variability caused less seasonal difference, and this is reflected in changes in the diatom composition at Baldwin Lake, which is supported by the lowered species diversity index (species richness). This was caused by the decrease in organic production in the lake and low light conditions, which were essential for diatom growth (Round et al. 1990; Sarthou et al. 2005; Thangaraj et al. 2020). Also, the lowered SSTs from the CA coast would cause less precipitation, which caused less runoff into the lake (Ji et al. 2019; Ilbay-Yupa et al. 2021; Barlow et al. 2021).

In conclusion, Baldwin Lake and the SBM region were influenced by solar irradiance largely, and the Baldwin Lake sediments contained a good record to detect the changes in it. The SSTs at equator and California coast also affect the diatom records at the lake.

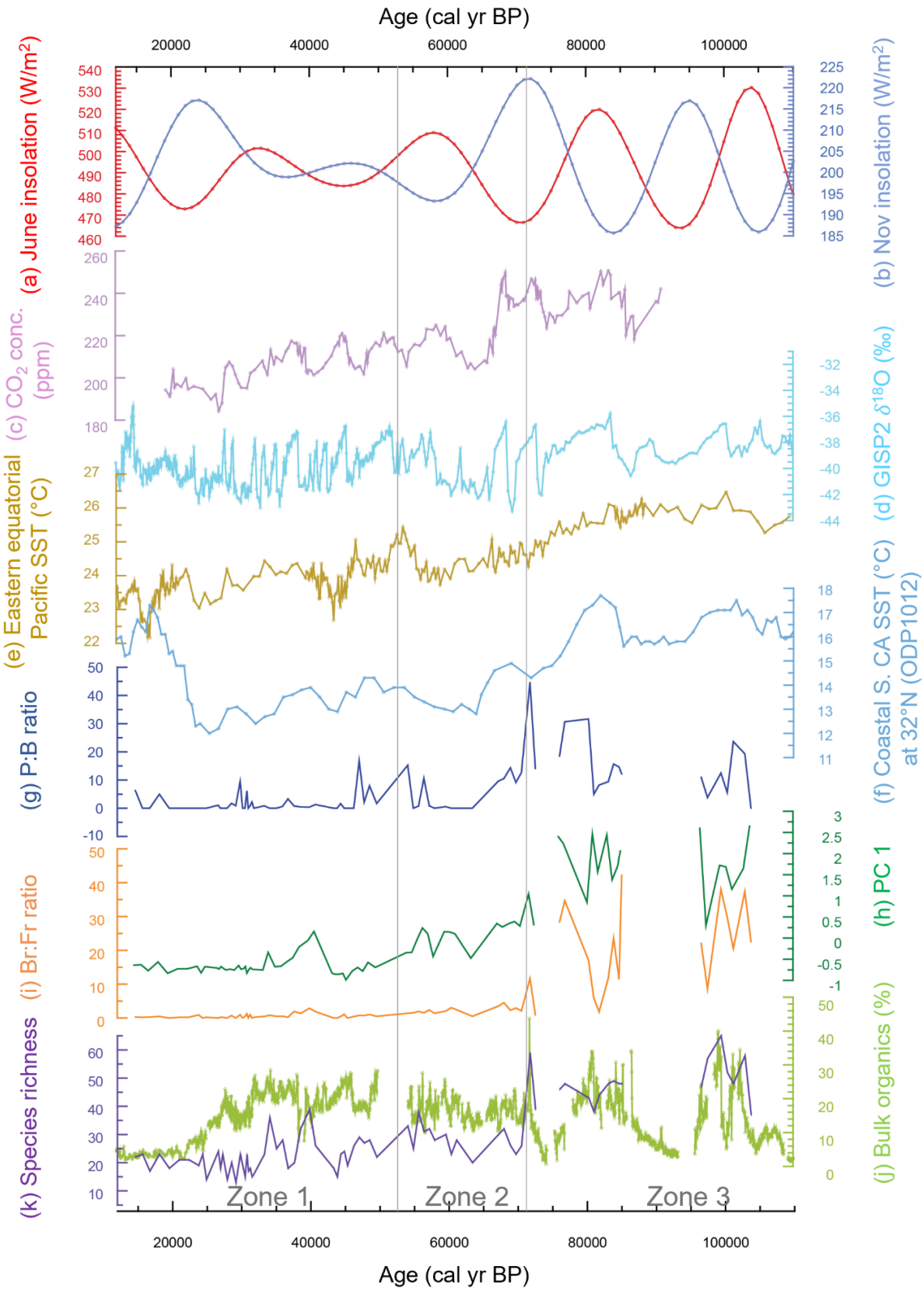
Age (cal yr BP)
20000
40000
60000
80000
100000
(a) June insolation (W/m²)
(b) Nov insolation (W/m²)
(c) CO2 conc. (ppm)
(d) GISP2 δ18O (‰)
(e) Eastern equatorial Pacific SST (°C)
(f) Coastal S. CA SST (°C) at 32°N (ODP1012)
(g) P:B ratio
(h) PC 1
(i) Br:Fr ratio
(j) Bulk organics (%)
(k) Species richness
Zone 1
Zone 2
Zone 3

Figure 4-15 *BDL12 diatom records (this study) and bulk organics (Glover et al. 2017) compared to global drivers. The data used in this figure: (a) & (b) show summer and winter insolation (W/m^2) at 34°N (Laskar et al. 2004), (c) Atmospheric CO_2 concentration in Antarctica (ppm) (Ahn and Brook 2007), (d) GISP2 $\delta^{18}O$ changes (‰) (Grootes and Stuiver 1997a), (e) eastern equatorial Pacific SSTs (°C) (Dubois et al. 2011), (f) ODP1012 SSTs (°C) (Herbert et al. 2001), (g) & (h) & (i) & (k) are P:B ratio, PCA Axis 1, Br:Fr ratio, and species richness from this study, respectively, (j) Bulk organics (%) (Glover et al. 2017).*

4.7 Conclusion

The current Baldwin Lake in SBM, an ephemeral lake, has little water all year round except in years when it has enough rain. In contrast to the stability in current years, the lake's dynamic in the past shifted strong, especially at around 70,000 cal yr BP when it transitioned from the MIS 5 to MIS 4. It was a time period when solar insolation was changed from in high variability to the dampened variability. The strong relationship between radiation variability and the regional climate changes in SBM was recorded in Baldwin Lake sediment.

During MIS 5 (or Phase 1 in this study), diatom assemblage in Baldwin Lake reached the maximum species diversity, evenness, and richness, and a lot of brackish species appeared. The lake water depth was also deep to inhabitable environments for many planktonic species. This was closely associated with high amplitudes of summer radiation and high variability of insolation during MIS 5. There were two big gaps in depths with no diatoms at ~ 76,000 to 73,000 cal yr BP and ~ 97,000 to 86,000 cal yr BP. The no-diatom-depths were coeval with the periods when the minimum in summer insolation. The signals were also detected in bulk organic/inorganic contents and BSi (Glover 2016; Glover et al. 2017).

After around 70000 cal yr BP (MIS 4 – MIS 2), the insolation variability became dampened, and it caused a lot of environmental and ecological changes in Baldwin Lake. The diatom-related signals, such as P:B ratio, Br:Fr ratio, and PC 1, had lowered variability. These

were consistent with the high to low variability in changes in BSi, bulk organic content, bulk inorganic content, Mn:Ti , Ca, and carbonates during the same period (Glover et al. 2017, 2020). It was apparent that geochemical changes within the lake were largely influential to the diatom composition. Pollen records from Glover et al. (2020) also showed that the surrounding vegetation of Baldwin Lake also had a big shift at ~ 70,000 cal yr BP with abundant non-arboreal (shrubs and upland herbs) pollens and abrupt decline in *Pinus* and low amount of other arboreal pollens. One of diatom species from BDL12, *Staurosirella pinnata*, responded this big shift oppositely to others, and this was because the species adapted to low light conditions during the period with the dampened insolation variability and became dominant in the lake (Laird et al. 2010).

Several D-O interstadials were also found in BDL12 diatom record between 60000 and 12000 cal yr BP, which were compared to D-O events observed by Glover et al. (2017). According to (Glover et al. 2017), there were fourteen D-O warmings (3, 4, 5, 6, 8a, 8c, 9, 10, 11, 12, 13, 14, 15) that were detected with two potential periods (16, 17) in Bulk organic content. The BDL12 diatom-related indicators, such as species richness, PC 1, Br:Fr ratio, P:B ratio were matched to the warmings, and it turned out that seven warmings (3, 4, 5, 6, 8a, 10, 15) were in a good match or correlated. These abrupt warming events brought abrupt lake conditions as well, and it changed Baldwin Lake's diatom composition rapidly.

The regional climate in SBM was apparently well linked to solar insolation variability and global drivers, such as eastern equatorial SSTs and Northeastern Pacific SSTs off the coast California, atmospheric CO_2 concentration, and the $\delta^{18}O$ NGRIP of hemispheric temperature was also in alignment with the BDL12 records. During MIS 5, Baldwin Lake had high variability in lake level and salinity, and the lake was relatively deeper and more brackish. As it entered MIS 4

and 3, the indicators from the lake began to have lower variability, and it became very low or close to flat during MIS 2. The changes in the variability were synchronous with the seasonal variability in insolation at 34°N. Baldwin Lake is considered as located in the interior of CA, but the BDL12 diatom record provided the influences of oceanic drivers apparently on the regional climate changes in the SBM region and Southern CA as well as orbital forcing as Glover (2016) and Kirby et al. (2006) postulated.

Baldwin Lake contained the longest record in Southern CA. The lake was thoroughly researched by previous studies (Kirby et al. 2006; Blazevic et al. 2009; Glover 2016; Glover et al. 2017, 2020). This study added diatom proxy to understand better hydroclimatic related factors in the lake, such as salinity and water depth. The BDL12 diatoms showed a good record in explaining that the lake experienced an abrupt big change in salinity (high → low) and lake level (deep → shallow) at around 70,000 cal yr BP. The orbital forcings were more powerful to the regional climate than expected, and it suggests that abrupt climatic and environmental shifts could be anticipatable in the future.

Chapter 5 Conclusions

This dissertation studies hydroclimatic variations during the late Quaternary both in Northern and Southern California based upon evidence from modern and fossil diatoms found in lake sediments. The research revealed that California hydroclimate has varied appreciably at different timescales, impacted by not only orbital/radiative forcings but also oceanic forcings. Kelly Lake represented the Holocene hydroclimatic changes in the Klamath Mountains, Northern California Coast Ranges, and Baldwin Lake in the San Bernardino Mountains, subalpine Southern California showed the hydrologic variations from MIS 5 to MIS 2.

The first research question of this dissertation was to examine the applicability of diatom-inferred lake level transfer function using multiple sediment samples from a single lake with small size and medium water depth (Kelly Lake, ~ 4 ha, maximum water depth of 5.7 m) in coastal Northern California where there are not many natural lakes. The diatom-inferred transfer function methods have been mostly conducted using single sediment samples from multiple lakes (> 50) in Canada and Europe (Reed 1998; Rosén et al. 2000; Battarbee et al. 2001; Rühland et al. 2003; Laird et al. 2010, 2011; Gushulak et al. 2017). The relationship between diatom assemblages and lake water depth in Kelly Lake was assessed by a depth-constrained cluster analysis, a one-way analysis of similarity, principal component analysis, and canonical correspondence analysis. Two transfer functions to estimate lake-water-depth based on diatoms were developed using the Modern Analogue Technique (MAT) and Weighted Averaging Partial Least Squares (WA-PLS). The transfer functions provided good performances with high R^2 and low RMSEP values. Both models showed no tendency in residuals and proved that they were applicable for the quantitative reconstruction of Kelly Lake water depth changes during the Holocene.

This study validated the general veracity and potential wider geographic and environmental scope of the use of the single lake methodology for constructing lake-depth transfer functions. Many parts of the world lack the glacial history of Canada or Europe and the multitude of lakes available for traditional training-set development. Kelly Lake also provides a shallower maximum depth, smaller size, somewhat more temperate climate regime and likely different bedrock geology/pedology than other single-lake sites published thus far. The results highlighted the potential of wider application of paleolimnological research techniques to reconstruct past environments in a wider range of lakes, geographies and environments. Thus, Chapter 2 study showed that the single-lake approach could be applied to smaller and shallower lakes than had been the norm for those used in this approach in the past. A lake like Kelly Lake is typical of the lakes often used in paleolimnological studies. The results provided an important empirical example of the methodological rationale and potential wider range of lakes for using a single-lake approach. As such, it is possible that the single-lake approach will become as, or more, widely used than the multi-lake approach, thus opening the door for more geographically comprehensive studies, in regions where lakes are rare.

The second research question focused on the ability to reconstruct the quantitative lake level history in Kelly Lake using the MAT and WA-PLS transfer functions and to examine whether the lake water depth models could perform well in reconstruction. Although both transfer functions represented similar trends in lake level variation of Kelly Lake during the Holocene, the WA-PLS transfer function performed better than the MAT reconstruction; the reconstructed deepest water depth from the MAT model was low in comparison with the current lake water depth. It was because the MAT reconstruction estimates the past lake levels by measuring the dissimilarity between the modern and fossil samples. The dissimilarity was fairly big because the

deepest water depth from the surface sediment samples was 5.2 m, while the actual deepest Kelly Lake water depth was 5.7 m. Therefore, the MAT reconstruction provided shallower estimates than it was actually likely to be. Therefore, the WA-PLS lake level reconstruction received the greatest consideration in the reconstruction of Kelly Lake water depth history.

Kelly Lake experienced three distinctive hydroclimatic periods during the Holocene, namely early, mid-, and late Holocene. The lake also seemed to undergo abrupt cold and dry climate event (i.e., 8.2 ka event) during the early Holocene, with the lowest lake level of ~ 0.98 m. The lake water depth recovered slowly to the previous lake level experienced prior to the 8.2 ka event. The lake level began to fluctuate with high variability from ~ 4,500 cal yr BP, and the lake level began to rise during the late Holocene. The lake level changes and transitions from the early to late Holocene were associated with increasingly strong oceanic variability such as El Niño-Southern Oscillation signals and the global drivers of sea surface temperatures in the Eastern Equatorial Pacific and off the coast of California.

The last research question of this dissertation was to study how the hydroclimate of Baldwin Lake in subalpine Southern California changed over the late Quaternary (MIS 5 to MIS 2) while mainly focusing on salinity and lake water depth, which are essential indicators of hydrologic variations (Gasse et al. 1997; Smol and Cumming 2000; Fritz et al. 2010; Wolin and Stone 2010; Gushulak et al. 2017). The diatom-based reconstructed salinity and lake water depth changes suggested that the lake was highly influenced by the insolation variability. When the radiative forcing transitioned from high variability to low variability at around 70,000 cal yr BP, the diatom flora reflected this. At the transition Baldwin Lake experienced abrupt changes ecologically and geochemically. The results supported what the previous studies demonstrated in

terms of the sensitivity of Baldwin Lake to large-scale climatic forcing, particularly orbital changes in insolation (Kirby et al. 2006; Glover 2016; Glover et al. 2017, 2020).

The natural long-term hydroclimatic variability in California, and the drivers of that variability, is significant to understand in the current situation when abrupt droughts, deluges, and fires are becoming increasing challenges to the state. This dissertation examined past hydroclimatic variability at different time scales to understand this better in the long-term context of the Holocene and the late Pleistocene. Since the 21st century has begun, hydroclimatic abnormalities and abrupt weather extremes are becoming an increasing peril, and it is becoming a more and more serious problem to solve, especially in this populous state. Hopefully this dissertation contributes to understanding the context for future projections of how California's hydroclimate will change in light of anthropogenic global warming and natural variations. Perhaps the most important message being the sensitivity that California climate has shown to external radiative and oceanic drivers in the past.

Chapter 6 Appendix

6.1 Chapter 2 Supplemental Tables and Figures

Figure 6-S1 Observed depths and Secchi depths transects from Kelly Lake. The surface samples were collected from three transects (A, B, C): Samples # 1 - 9 were taken from Transect A; Samples # 10 - 26 were taken from Transect B; Samples # 33 - 40 were taken from Transect C. Sample # 27 and 28 were taken at the margin area of the lake, and Sample # 29 and 30 were taken in a very shallow coastal area northwest of the lake, and Sample # 31 and 32 were taken on the moss outside of the northwest of the lake where the inlet was.

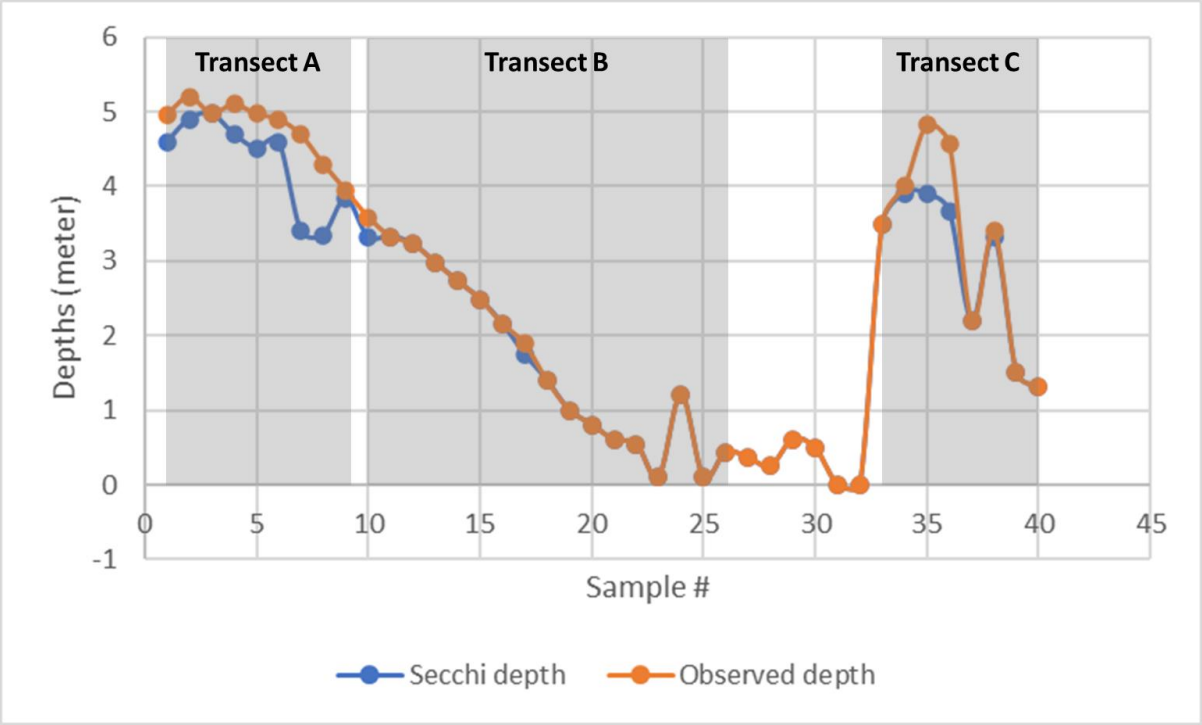

Figure 6-S2 Unconstrained cluster analysis. Sample depth and zonation from Fig. 4 is indicated (yellow = shallow zone), (green = mid-depth zone), and (blue = deep=water zone).

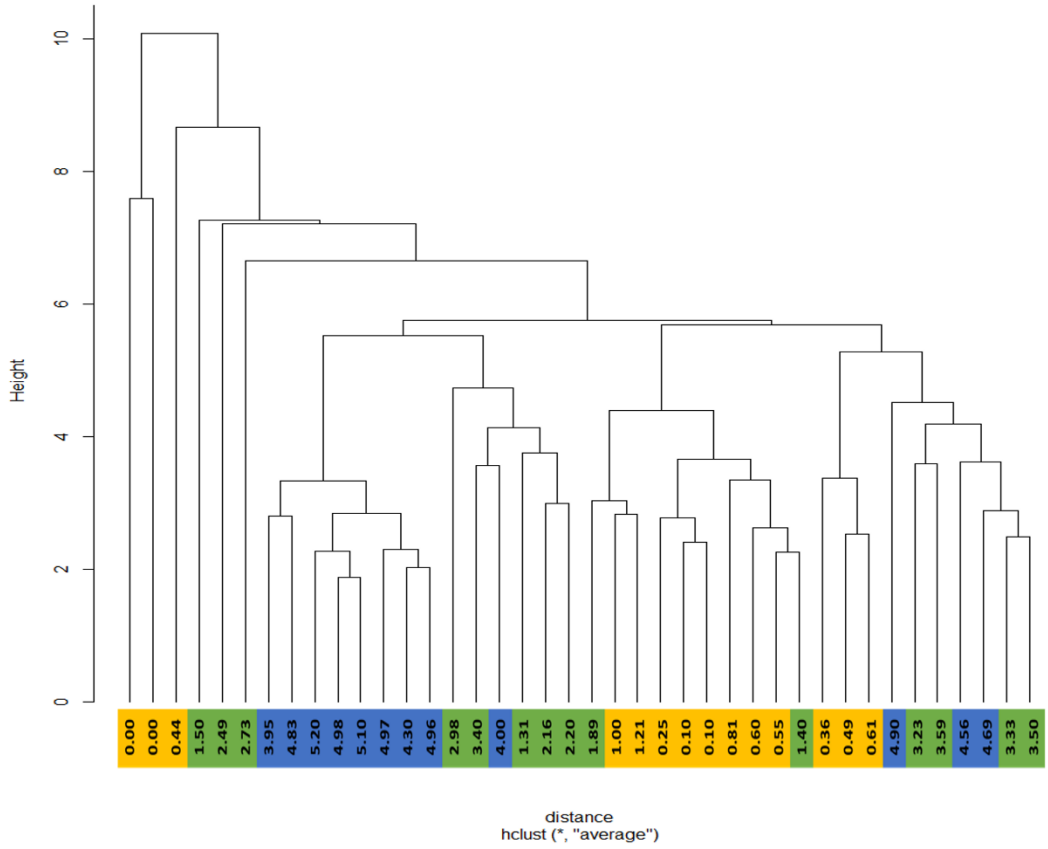

Figure 6-S3 Monte Carlo permutation test (999 permutations) ($p<0.01$).

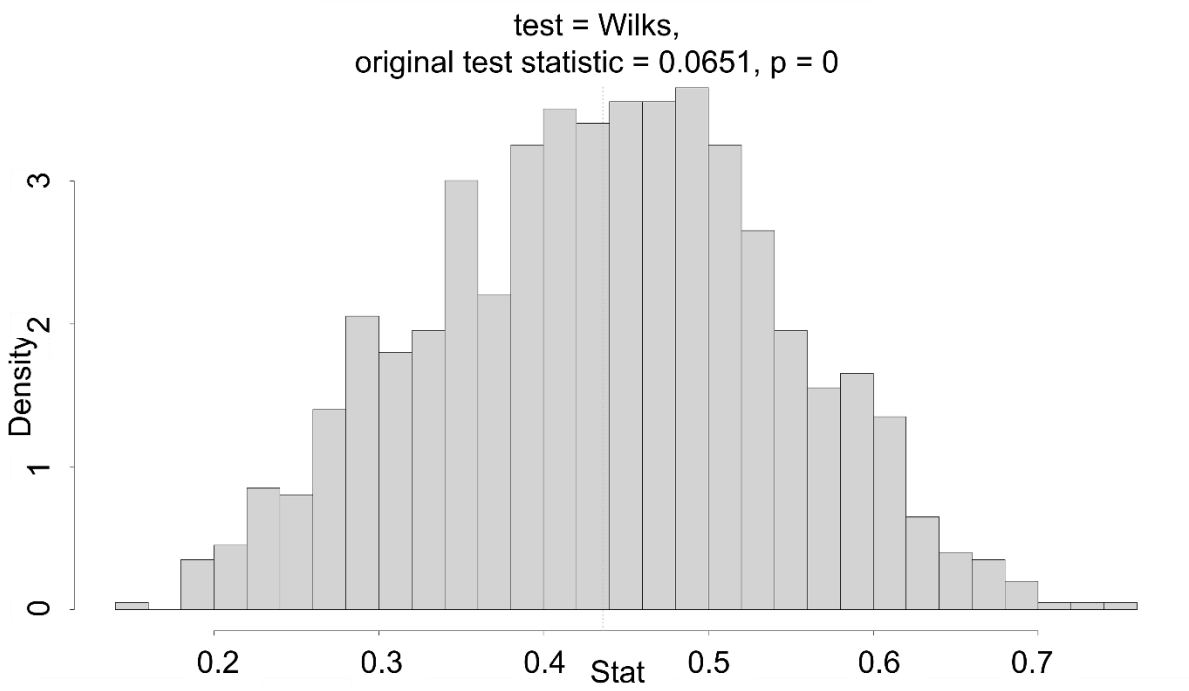

Table 6-S1 Sample ID, depth, Secchi depth, and diatom counts.

Sample ID	Observed depth	Secchi depth	Diatom counts
KLSS2019-31	0	0	445
KLSS2019-32	0	0	438
KLSS2019-23	0.1	0.1	440
KLSS2019-25	0.1	0.1	432
KLSS2019-28	0.25	0.25	459
KLSS2019-27	0.36	0.36	447
KLSS2019-26	0.44	0.44	455
KLSS2019-30	0.49	0.49	446
KLSS2019-22	0.55	0.55	447
KLSS2019-21	0.6	0.6	441
KLSS2019-29	0.61	0.61	436

KLSS2019-20	0.81	0.81	420
KLSS2019-19	1	1	430
KLSS2019-24	1.21	1.21	419
KLSS2019-40	1.31	1.31	442
KLSS2019-18	1.4	1.4	451
KLSS2019-39	1.5	1.5	446
KLSS2019-17	1.89	1.75	438
KLSS2019-16	2.16	2.16	420
KLSS2019-37	2.2	2.2	450
KLSS2019-15	2.49	2.49	493
KLSS2019-14	2.73	2.73	427
KLSS2019-13	2.98	2.98	436
KLSS2019-12	3.23	3.23	451

KLSS2019-11	3.33	3.33	435
KLSS2019-38	3.4	3.32	440
KLSS2019-33	3.5	3.5	463
KLSS2019-10	3.59	3.32	432
KLSS2019-9	3.95	3.83	488
KLSS2019-34	4	3.91	428
KLSS2019-8	4.3	3.35	414
KLSS2019-36	4.56	3.66	518
KLSS2019-7	4.69	3.4	431
KLSS2019-35	4.83	3.9	478
KLSS2019-6	4.9	4.6	428
KLSS2019-1	4.96	4.59	469
KLSS2019-5	4.97	4.51	438

KLSS2019-3	4.98	4.97	436
KLSS2019-4	5.1	4.7	496
KLSS2019-2	5.2	4.9	463

Table 6-S2 137Cs and 210Pb data for core KLGC19-2.

Sample Interval (cm)	*137Cs Activitiy (dpm/g)*	*Total 210Pb Activity (dpm/g)*
0-5	2.62±0.15	38.72±1.83
5-10	7.04±0.15	24.58±1.13
10-15	4.12±0.23	11.24±1.40
15-22	0.86±0.11	8.55±1.01
22-28	0.34±0.08	5.22±0.82
28-35	0.11±0.04	0.23±0.09

Table 6-S3 Sampling points with coordinates and water depths (observed and Secchi-disc).

Sample #	Secchi Depth (m)	Actual Depth (m)	Coord.	Note
KLSS 2019-1	**4.59**	**4.96**	**41°54.790' N, 123°30.998' W**	
KLSS 2019-2	**4.90**	**5.20**	**41°54.789' N, 123°30.994' W**	
KLSS 2019-3	**4.97**	**4.98**	**41°54.792' N, 123°30.989' W**	
KLSS 2019-4	**4.70**	**5.10**	**41°54.790' N, 123°30.989' W**	
KLSS 2019-5	**4.51**	**4.97**	**41°54.791' N, 123°30.986' W**	
KLSS 2019-6	**4.60**	**4.90**	**41°54.789' N, 123°30.982' W**	
KLSS 2019-7	**3.40**	**4.69**	**41°54.786' N, 123°30.972' W**	
KLSS 2019-8	**3.35**	**4.30**	**41°54.786' N, 123°30.968' W**	
KLSS 2019-9	**3.83**	**3.95**	**41°54.785' N, 123°30.962' W**	
KLSS 2019-10	**3.32**	**3.59**	**41°54.785' N, 123°30.965' W**	
KLSS 2019-11	**3.33 (3.08)**	**3.33**	**41°54.788' N, 123°30.959' W**	**Many submerged aquatic plants**
KLSS 2019-12	**3.23 (3.12)**	**3.23**	**41°54.788' N, 123°30.962' W**	**Many submerged aquatic plants**
KLSS 2019-13	**2.98**	**2.98**	**41°54.786' N, 123°30.957' W**	

KLSS 2019-14	**2.73**	**2.73**	**41°54.789’ N, 123°30.960’ W**	
KLSS 2019-15	**2.49**	**2.49**	**41°54.782’ N, 123°30.957’ W**	
KLSS 2019-16	**2.16**	**2.16**	**41°54.788’ N, 123°30.948’ W**	
KLSS 2019-17	**1.75**	**1.89**	**41°54.787’ N, 123°30.946’ W**	**Due to turbulence, the Secchi depth and the observed depth were different**
KLSS 2019-18	**1.40**	**1.40**	**41°54.785’ N, 123°30.943’ W**	
KLSS 2019-19	**1.00**	**1.00**	**41°54.786’ N, 123°30.943’ W**	**A lot of aquatic plants**
KLSS 2019-20	**0.81**	**0.81**	**41°54.782’ N, 123°30.940’ W**	
KLSS 2019-21	**0.60**	**0.60**	**41°54.781’ N, 123°30.939’ W**	
KLSS 2019-22	**0.55**	**0.55**	**41°54.790’ N, 123°30.930’ W**	
KLSS 2019-23	**0.10**	**0.10**	**41°54.790’ N, 123°30.930’ W**	
KLSS 2019-24	**1.21**	**1.21**	**41°54.787’ N, 123°30.940’ W**	
KLSS 2019-25	**0.10**	**0.10**	**41°54.823’ N, 123°30.929’ W**	
KLSS 2019-26	**0.44**	**0.44**	**41°54.825’ N, 123°30.932’ W**	

KLSS 2019-27	**0.36**	**0.36**	**41°54.85031’ N, 123°30.60239’ W**	
KLSS 2019-28	**0.25**	**0.25**	**41°54.814’ N, 123°30.958’ W**	
KLSS 2019-29	**0.61**	**0.61**	**41°54.848’ N, 123°31.134’ W**	**At mud polygons**
KLSS 2019-30	**0.49**	**0.49**	**41°54.847’ N, 123°31.144’ W**	
KLSS 2019-31	**0.00**	**0.00**	**41°54.836’ N, 123°31.159’ W**	**Moss area springs, cold water**
KLSS 2019-32	**0.00**	**0.00**	**41°54.836’ N, 123°31.159’ W**	**Moss area with springs**
KLSS 2019-33	**3.50**	**3.50**	**41°54.969’ N, 123°31.995’ W**	
KLSS 2019-34	**3.91**	**4.00**	**41°54.775’ N, 123°31.003’ W**	
KLSS 2019-35	**3.90**	**4.83**	**41°54.785’ N, 123°31.004’ W**	
KLSS 2019-36	**3.66**	**4.56**	**41°54.783’ N, 123°31.003’ W**	
KLSS 2019-37	**2.20**	**2.20**	**41°54.760’ N, 123°31.005’ W**	
KLSS 2019-38	**3.32**	**3.40**	**41°54.764’ N, 123°31.019’ W**	
KLSS 2019-39	**1.50**	**1.50**	**41°54.762’ N, 123°30.997’ W**	
KLSS 2019-40	**1.31**	**1.31**	**41°54.763’ N, 123°30.986’ W**	

Chapter 7 References

Aguiar W, Meissner KJ, Montenegro A, et al (2021) Magnitude of the 8.2 ka event freshwater forcing based on stable isotope modelling and comparison to future Greenland melting. Sci Rep 11:5473. https://doi.org/10.1038/s41598-021-84709-5

Ahn J, Brook EJ (2007) Atmospheric CO2 and climate from 65 to 30 ka B.P. Geophysical Research Letters 34:. https://doi.org/10.1029/2007GL029551

Ahn J, Hur SD (2014) Atmospheric CO_2 records from ice cores. Journal of the Geological Society of Korea 50:277–292

Allen RJ, Luptowitz R (2017) El Niño-like teleconnection increases California precipitation in response to warming. Nat Commun 8:16055. https://doi.org/10.1038/ncomms16055

Anderson NJ (1990) The biostratigraphy and taxonomy of small Stephanodiscus and Cyclostephanos species (Bacillariophyceae) in a eutrophic lake, and their ecological implications. British Phycological Journal 25:217–235. https://doi.org/10.1080/00071619000650211

Bahls L, Luna T (2018) Diatoms from Wrangell-St. Elias National Park, Alaska, USA. PhytoKeys 113:33–57. https://doi.org/10.3897/phytokeys.113.29456

Bahls LL, Weber EE, Jarvie JO (1985) Ecology and distribution of major diatom ecotypes in the southern Fort Union coal region of Montana. US Geol Surv, Prof Pap;(United States) 1289:

Bailey-Watts AE (1986) The Ecology of Planktonic Diatoms, Especially Fragilaria Crotonensis, Associated with Artificial Mixing of a Small Scottish Loch in Summer. Diatom Research 1:153–168. https://doi.org/10.1080/0269249X.1986.9704966

Barlow M, Hoell A, Agel L (2021) An Evaluation of CMIP6 Historical Simulations of the Cold Season Teleconnection between Tropical Indo-Pacific Sea Surface Temperatures and Precipitation in Southwest Asia, the Coastal Middle East, and Northern Pakistan and India. Journal of Climate 34:6905–6926. https://doi.org/10.1175/JCLI-D-19-1026.1

Barron JA, Heusser L, Herbert T, Lyle M (2003) High-resolution climatic evolution of coastal northern California during the past 16,000 years. Paleoceanography 18:. https://doi.org/10.1029/2002PA000768

Bartozek ECR, Zorzal-Almeida S, Bicudo DC (2018) Surface sediment and phytoplankton diatoms across a trophic gradient in tropical reservoirs: new records for Brazil and São Paulo State. Hoehnea 45:69–92. https://doi.org/10.1590/2236-8906-51/2017

Battarbee RW (2000) Palaeolimnological approaches to climate change, with special regard to the biological record. Quaternary Science Reviews 19:107–124. https://doi.org/10.1016/S0277-3791(99)00057-8

Battarbee RW, Juggins S, Gasse F, et al (2001) European Diatom Database (EDDI). An information system for palaeoenvironmental reconstruction

Bergman J, Plikk A, Heimdahl J, et al (2020) When the River Began—The Formation of River Motala Ström and Human Presence in the Early Holocene, Sweden. Quaternary 3:25. https://doi.org/10.3390/quat3030025

Birks HJB (2010) Numerical methods for the analysis of diatom assemblage data. In: Stoermer EF, Smol JP (eds) The Diatoms: Applications for the Environmental and Earth Sciences, 2nd edn. Cambridge University Press, Cambridge, pp 23–54

Bishop I (2017) Encyonema minutum var. pseudogracilis. Diatoms.org

Blaauw M, Christen JA (2011) Flexible paleoclimate age-depth models using an autoregressive gamma process

Blazevic MA, Kirby ME, Woods AD, et al (2009) A sedimentary facies model for glacial-age sediments in Baldwin Lake, Southern California. Sedimentary Geology 219:151–168. https://doi.org/10.1016/j.sedgeo.2009.05.003

Bloom AM, Moser KA, Porinchu DF, MacDonald GM (2003) Diatom-inference models for surface-water temperature and salinity developed from a 57-lake calibration set from the Sierra Nevada, California, USA. Journal of Paleolimnology 29:235–255. https://doi.org/10.1023/A:1023297407233

Blumentritt DJ, Lascu I (2014) Comparing magnetic susceptibility techniques from recent lake sediments

Bonnell TR, Vilette C (2021) Constructing and analysing time-aggregated networks: The role of bootstrapping, permutation and simulation. Methods in Ecology and Evolution 12:114–126. https://doi.org/10.1111/2041-210X.13351

Bradbury PJ, Colman SM, Dean WE (2004a) Limnological and Climatic Environments at Upper Klamath Lake, Oregon during the past 45 000 years. Journal of Paleolimnology 31:167–188. https://doi.org/10.1023/B:JOPL.0000019232.74649.02

Bradbury PJ, Colman SM, Dean WE (2004b) Limnological and Climatic Environments at Upper Klamath Lake, Oregon during the past 45 000 years. Journal of Paleolimnology 31:167–188. https://doi.org/10.1023/B:JOPL.0000019232.74649.02

Briles CE (2017) Controls on Mountain Plant Diversity in Northern California: A 14,000-Year Overview. Annals of the American Association of Geographers 107:238–249. https://doi.org/10.1080/24694452.2016.1232617

Briles CE, Whitlock C, Bartlein PJ, Higuera P (2008) Regional and local controls on postglacial vegetation and fire in the Siskiyou Mountains, northern California, USA. Palaeogeography, Palaeoclimatology, Palaeoecology 265:159–169. https://doi.org/10.1016/j.palaeo.2008.05.007

Briles CE, Whitlock C, Skinner CN, Mohr J (2011) Holocene forest development and maintenance on different substrates in the Klamath Mountains, northern California, USA. Ecology 92:590–601. https://doi.org/10.1890/09-1772.1

California S of (2022) Governor Newsom Signs Budget Putting Money Back in Californians' Pockets and Investing in State's Future. In: California Governor. https://www.gov.ca.gov/2022/06/30/governor-newsom-signs-budget-putting-money-back-in-californians-pockets-and-investing-in-states-future/. Accessed 24 Feb 2023

Chen X, Dong ZY, Meng K, et al (2012) Electricity Price Forecasting With Extreme Learning Machine and Bootstrapping. IEEE Transactions on Power Systems 27:2055–2062. https://doi.org/10.1109/TPWRS.2012.2190627

Cho A, Lim J, Kim Y, Ahn US (2022) Variability of East Asian winter monsoon during Middle–Late Holocene: A study based on a crater lake on Jeju Island, South Korea. Palaeogeography, Palaeoclimatology, Palaeoecology 603:111193. https://doi.org/10.1016/j.palaeo.2022.111193

Colombaroli D, Gavin DG (2010) Highly episodic fire and erosion regime over the past 2,000 y in the Siskiyou Mountains, Oregon. Proceedings of the National Academy of Sciences 107:18909–18914. https://doi.org/10.1073/pnas.1007692107

Conroy JL, Overpeck JT, Cole JE, et al (2008) Holocene changes in eastern tropical Pacific climate inferred from a Galápagos lake sediment record. Quaternary Science Reviews 27:1166–1180. https://doi.org/10.1016/j.quascirev.2008.02.015

Crawford JN, Mensing SA, Lake FK, Zimmerman SR (2015) Late Holocene fire and vegetation reconstruction from the western Klamath Mountains, California, USA: A multi-disciplinary approach for examining potential human land-use impacts. The Holocene 25:1341–1357

Cremer H, Koolmees H (2010) Common diatoms (Centrales and Fragilariaceae, Bacillariophyta) of modern and fossil freshwater environments in the Netherlands. Nova Hedwigia 343–381. https://doi.org/10.1127/0029-5035/2010/0090-0343

Cunningham L, Raymond B, Snape I, Riddle MJ (2005) Benthic diatom communities as indicators of anthropogenic metal contamination at Casey Station, Antarctica. J Paleolimnol 33:499–513. https://doi.org/10.1007/s10933-005-0814-0

Dalton AS, Patterson RT, Roe HM, et al (2018) Late Holocene climatic variability in Subarctic Canada: Insights from a high-resolution lake record from the central Northwest Territories. PLOS ONE 13:e0199872. https://doi.org/10.1371/journal.pone.0199872

Dansgaard W, Johnsen SJ, Clausen HB, et al (1993) Evidence for general instability of past climate from a 250-kyr ice-core record. Nature 364:218–220. https://doi.org/10.1038/364218a0

Davies SJ, Metcalfe SE, Caballero ME, Juggins S (2002) Developing diatom-based transfer functions for Central Mexican lakes. Hydrobiologia 467:199–213. https://doi.org/10.1023/A:1014971016298

Dean WE (1974) Determination of carbonate and organic matter in calcareous sediments and sedimentary rocks by loss on ignition; comparison with other methods. Journal of Sedimentary Research 44:242–248. https://doi.org/10.1306/74D729D2-2B21-11D7-8648000102C1865D

Dean WE, Bradbury JP, Anderson RY, Barnosky CW (1984) The Variability of Holocene Climate Change: Evidence from Varved Lake Sediments. Science 226:1191–1194. https://doi.org/10.1126/science.226.4679.1191

Dettinger MD, Cayan DR, Diaz HF, Meko DM (1998) North–South Precipitation Patterns in Western North America on Interannual-to-Decadal Timescales. Journal of Climate 11:3095–3111. https://doi.org/10.1175/1520-0442(1998)011<3095:NSPPIW>2.0.CO;2

Dingemans T, Mensing SA, Feakins SJ, et al (2014) 3000 years of environmental change at Zaca Lake, California, USA. Frontiers in Ecology and Evolution 2:

Dong C, MacDonald G, Okin GS, Gillespie TW (2019) Quantifying Drought Sensitivity of Mediterranean Climate Vegetation to Recent Warming: A Case Study in Southern California. Remote Sensing 11:2902. https://doi.org/10.3390/rs11242902

Dubois N, Kienast M, Kienast S, et al (2011) Millennial-scale variations in hydrography and biogeochemistry in the Eastern Equatorial Pacific over the last 100 kyr. Quaternary Science Reviews 30:210–223. https://doi.org/10.1016/j.quascirev.2010.10.012

Elmslie BG, Gushulak CA, Boreux MP, et al (2020) Complex responses of phototrophic communities to climate warming during the Holocene of northeastern Ontario, Canada. The Holocene 30:272–288. https://doi.org/10.1177/0959683619883014

Faith JT, Lyman RL (2019) Paleozoology and Paleoenvironments: Fundamentals, Assumptions, Techniques, 1st edn. Cambridge University Press

Fauvel M, Zullo A, Ferraty F (2014) Nonlinear parsimonious feature selection for the classification of hyperspectral images. In: 2014 6th Workshop on Hyperspectral Image and Signal Processing: Evolution in Remote Sensing (WHISPERS). pp 1–4

Feakins SJ, Kirby ME, Cheetham MI, et al (2014) Fluctuation in leaf wax D/H ratio from a southern California lake records significant variability in isotopes in precipitation during the late Holocene. Organic Geochemistry 66:48–59. https://doi.org/10.1016/j.orggeochem.2013.10.015

Finkelstein SA, Bunbury J, Gajewski K, et al (2014) Evaluating diatom-derived Holocene pH reconstructions for Arctic lakes using an expanded 171-lake training set. Journal of Quaternary Science 29:249–260. https://doi.org/10.1002/jqs.2697

Fluin J, Tibby J, Gell P (2010) The palaeolimnological record from lake Cullulleraine, lower Murray River (south-east Australia): implications for understanding riverine histories. J Paleolimnol 43:309–322. https://doi.org/10.1007/s10933-009-9333-8

French JJ, Busby MW (1974) Flood-hazard study, 100-year stage for Baldwin Lake, San Bernardino County, California

Fritz SC (1990) Twentieth-century salinity and water-level fluctuations in Devils Lake, North Dakota: Test of a diatom-based transfer function. Limnology and Oceanography 35:1771–1781. https://doi.org/10.4319/lo.1990.35.8.1771

Fritz SC, Cumming BF, Gasse F, Laird KR (2010) Diatoms as indicators of hydrologic and climatic change in saline lakes. The diatoms: applications for the environmental and earth sciences 186–208

Fritz SC, Ito E, Yu Z, et al (2000) Hydrologic Variation in the Northern Great Plains During the Last Two Millennia. Quat res 53:175–184. https://doi.org/10.1006/qres.1999.2115

Fritz SC, Juggins S, Battarbee RW, Engstrom DR (1991) Reconstruction of past changes in salinity and climate using a diatom-based transfer function. Nature 352:706–708. https://doi.org/10.1038/352706a0

Gasse F, Barker P, Gell PA, et al (1997) Diatom-inferred salinity in palaeolakes: An indirect tracer of climate change. Quaternary Science Reviews 16:547–563. https://doi.org/10.1016/S0277-3791(96)00081-9

Gasse F, Juggins S, Khelifa LB (1995) Diatom-based transfer functions for inferring past hydrochemical characteristics of African lakes. Palaeogeography, Palaeoclimatology, Palaeoecology 117:31–54. https://doi.org/10.1016/0031-0182(94)00122-O

Glover KC (2016) Southern California climate and vegetation over the past 125,000 years from lake sequences in the San Bernardino Mountains. University of California, Los Angeles

Glover KC, Chaney A, Kirby ME, et al (2020) Southern California Vegetation, Wildfire, and Erosion Had Nonlinear Responses to Climatic Forcing During Marine Isotope Stages 5–2 (120–15 ka). Paleoceanography and Paleoclimatology 35:e2019PA003628. https://doi.org/10.1029/2019PA003628

Glover KC, George J, Heusser L, MacDonald GM (2021) West Coast vegetation shifts as a response to climate change over the past 130,000 years: geographic patterns and process from pollen data. Physical Geography 42:542–560. https://doi.org/10.1080/02723646.2021.1990506

Glover KC, MacDonald GM, Kirby ME, et al (2017) Evidence for orbital and North Atlantic climate forcing in alpine Southern California between 125 and 10 ka from multi-proxy analyses of Baldwin Lake. Quaternary Science Reviews 167:47–62. https://doi.org/10.1016/j.quascirev.2017.04.028

Gomes DF, Albuquerque ALS, Torgan LC, et al (2014) Assessment of a diatom-based transfer function for the reconstruction of lake-level changes in Boqueirão Lake, Brazilian Nordeste. Palaeogeography, Palaeoclimatology, Palaeoecology 415:105–116. https://doi.org/10.1016/j.palaeo.2014.07.009

Govindan N, Maniam GP, Ab. Rahim MH, et al (2021) Production of Renewable Lipids by the Diatom Amphora copulata. Fermentation 7:37. https://doi.org/10.3390/fermentation7010037

Gregory-Eaves I, Smol JP, Finney BP, Edwards ME (1999) Diatom-based Transfer Functions for Inferring past Climatic and Environmental Changes in Alaska, U.S.A. Arctic, Antarctic, and Alpine Research 31:353–365. https://doi.org/10.1080/15230430.1999.12003320

Grimm EC (1987) CONISS: a FORTRAN 77 program for stratigraphically constrained cluster analysis by the method of incremental sum of squares. Computers & Geosciences 13:13–35. https://doi.org/10.1016/0098-3004(87)90022-7

Grootes PM, Stuiver M (1997a) Oxygen 18/16 variability in Greenland snow and ice with 10−3- to 105-year time resolution. Journal of Geophysical Research: Oceans 102:26455–26470. https://doi.org/10.1029/97JC00880

Grootes PM, Stuiver M (1997b) NOAA/WDS Paleoclimatology - GISP2 Ice Core 110,000 Year Oxygen Isotope Data. In: NOAA National Centers for Environmental Information. https://doi.org/10.25921/jtjy-9030. Accessed 20 Mar 2023

Guo Y, Zhu L, Frenzel P, et al (2016) Holocene lake level fluctuations and environmental changes at Taro Co, southwestern Tibet, based on ostracod-inferred water depth reconstruction. The Holocene 26:29–43. https://doi.org/10.1177/0959683615596829

Gushulak CAC, Cumming BF (2020) Diatom assemblages are controlled by light attenuation in oligotrophic and mesotrophic lakes in northern Ontario (Canada). J Paleolimnol 64:419–433. https://doi.org/10.1007/s10933-020-00146-w

Gushulak CAC, Laird KR, Bennett JR, Cumming BF (2017) Water depth is a strong driver of intra-lake diatom distributions in a small boreal lake. J Paleolimnol 58:231–241. https://doi.org/10.1007/s10933-017-9974-y

Haberyan KA (2018) A >22,000 yr diatom record from the plateau of Zambia. Quaternary Research 89:33–42. https://doi.org/10.1017/qua.2017.31

Hammer O, Harper DAT, Ryan PD (2001) PAST: Paleontological Statistics Software Package for Education and Data Analysis. Palaeontologia Electronica 4:1–9

Han J (2015) A Diatom-Based Reconstruction of the Paleoenvironmental Changes during the Last Deglaciation in Jeju Island, Korea. Thesis, 서울대학교 대학원

Han J, Kirby M, Carlin J, et al (2023) A diatom-inferred water-depth transfer function from a single lake in the northern California Coast Range. J Paleolimnol. https://doi.org/10.1007/s10933-023-00281-0

Hatsuzuka D, Sato T (2022) Impact of SST on Present and Future Extreme Precipitation in Hokkaido Investigated Considering Weather Patterns. Journal of Geophysical Research: Atmospheres 127:e2021JD036120. https://doi.org/10.1029/2021JD036120

Heiri O, Lotter AF, Lemcke G (2001) Loss on ignition as a method for estimating organic and carbonate content in sediments: reproducibility and comparability of results. Journal of Paleolimnology 25:101–110. https://doi.org/10.1023/A:1008119611481

Herbert TD, Schuffert JD, Andreasen D, et al (2001) Collapse of the California Current During Glacial Maxima Linked to Climate Change on Land. Science 293:71–76. https://doi.org/10.1126/science.1059209

Hill MO (1973) Diversity and Evenness: A Unifying Notation and Its Consequences. Ecology 54:427–432. https://doi.org/10.2307/1934352

Hobbs WO, Edlund MB, Umbanhowar CE, et al (2017) Holocene evolution of lakes in the forest-tundra biome of northern Manitoba, Canada. Quaternary Science Reviews 159:116–138. https://doi.org/10.1016/j.quascirev.2017.01.014

Hofmann AM, Geist J, Nowotny L, Raeder U (2020) Depth-distribution of lake benthic diatom assemblages in relation to light availability and substrate: implications for paleolimnological studies. J Paleolimnol 64:315–334. https://doi.org/10.1007/s10933-020-00139-9

Hoidal N (2013) Meridion circulare var. constrictum. In: Diatoms of North America. https://diatoms.org/species/meridion_circulare_var._constrictum. Accessed 9 May 2022

Holmes J, Burn M, Cisneros-Dozal LM, et al (2023) An 1800-year oxygen-isotope record of short- and long-term hydroclimate variability in the northern neotropics from a Jamaican marl lake. Quaternary Science Reviews 301:107930. https://doi.org/10.1016/j.quascirev.2022.107930

Holmes JA (2001) Ostracoda. Tracking Environmental Change Using Lake Sediments: Volume 4: Zoological Indicators 125–151

Homann J, Oster JL, de Wet CB, et al (2022) Linked fire activity and climate whiplash in California during the early Holocene. Nat Commun 13:7175. https://doi.org/10.1038/s41467-022-34950-x

Hudson AM, Emery-Wetherell MM, Lubinski PM, et al (2021) Reconstructing paleohydrology in the northwest Great Basin since the last deglaciation using Paisley Caves fish remains (Oregon, U.S.A.). Quaternary Science Reviews 262:106936. https://doi.org/10.1016/j.quascirev.2021.106936

Huyer A (1983) Coastal upwelling in the California current system. Progress in Oceanography 12:259–284. https://doi.org/10.1016/0079-6611(83)90010-1

Ikehata K, Nakamura N, Kulkarni HV, et al (2022) Isolation and evaluation of brackish diatoms for the photobiological treatment of reverse osmosis concentrate. AQUA - Water Infrastructure, Ecosystems and Society 71:1083–1094. https://doi.org/10.2166/aqua.2022.082

Ilbay-Yupa M, Lavado-Casimiro W, Rau P, et al (2021) Updating regionalization of precipitation in Ecuador. Theor Appl Climatol 143:1513–1528. https://doi.org/10.1007/s00704-020-03476-x

Irwin WP (1994) Geologic Map of the Klamath Mountains, California and Oregon. In: USGS National Geologic Map Database. https://ngmdb.usgs.gov/Prodesc/proddesc_10149.htm. Accessed 2 May 2022

Jackson ST, Williams JW (2004) MODERN ANALOGS IN QUATERNARY PALEOECOLOGY: Here Today, Gone Yesterday, Gone Tomorrow? Annual Review of Earth and Planetary Sciences 32:495–537. https://doi.org/10.1146/annurev.earth.32.101802.120435

Jahn R, Kusber W-H, Romero O (2009) Cocconeis pediculus EHRENBERG and C. placentula EHRENBERG var. placentula (Bacillariophyta): Typification and taxonomy. Fottea 9:275–288. https://doi.org/10.5507/fot.2009.027

Ji C, Zhang Y, Cheng Q, et al (2019) Analyzing the variation of the precipitation of coastal areas of eastern China and its association with sea surface temperature (SST) of other seas. Atmospheric Research 219:114–122. https://doi.org/10.1016/j.atmosres.2018.12.027

Juggins S (2020) rioja: Analysis of Quaternary Science Data. In: R package version 0.9-26. https://cran.r-project.org/web/packages/rioja/index.html. Accessed 9 May 2022

Juggins S (2007) C2: Software for ecological and palaeoecological data analysis and visualisation (user guide version 1.5). Newcastle upon Tyne: Newcastle University 77:680

Jüttner I, Carter C, Chudaev D, et al (2022) Diatom Flora of Britian and Ireland. In: Amgueddfa Cymru - National Museum Wales. https://naturalhistory.museumwales.ac.uk/diatoms/. Accessed 9 May 2022

Karthick B, Kociolek JP, Mahesh MK, Ramachandra TV (2011) The diatom genus Gomphonema Ehrenberg in India: Checklist and description of three new species. Nova Hedwigia 93:211

Kashima K, Matsubara H, Kuzucuoğlu C, Karabiyikoğlu M (1997) Diatom Assemblages from Inland Saline Lakes in the Central Part of Turkey —Their Application for Quantitative Reconstructions of Paleosalinity Changes During the Late Quaternary—. Japan Review 235–249

Katsuki K, Takahashi K, Okada M (2003) Diatom Assemblage and Productivity Changes during the Last 340,000 Years in the Subarctic Pacific. Journal of Oceanography 59:695–707. https://doi.org/10.1023/B:JOCE.0000009598.93075.78

Kemp AC, Telford RJ (2015) Transfer functions. In: Handbook of Sea-Level Research. John Wiley & Sons, Ltd, pp 470–499

Kingsbury MV, Laird KR, Cumming BF (2012) Consistent patterns in diatom assemblages and diversity measures across water-depth gradients from eight Boreal lakes from north-western Ontario (Canada). Freshwater Biology 57:1151–1165. https://doi.org/10.1111/j.1365-2427.2012.02781.x

Kirby ME, Feakins SJ, Hiner CA, et al (2014) Tropical Pacific forcing of Late-Holocene hydrologic variability in the coastal southwest United States. Quaternary Science Reviews 102:27–38. https://doi.org/10.1016/j.quascirev.2014.08.005

Kirby ME, Heusser L, Scholz C, et al (2018) A late Wisconsin (32–10k cal a BP) history of pluvials, droughts and vegetation in the Pacific south-west United States (Lake Elsinore, CA). Journal of Quaternary Science 33:238–254. https://doi.org/10.1002/jqs.3018

Kirby ME, Knell EJ, Anderson WT, et al (2015) Evidence for insolation and Pacific forcing of late glacial through Holocene climate in the Central Mojave Desert (Silver Lake, CA). Quaternary Research 84:174–186. https://doi.org/10.1016/j.yqres.2015.07.003

Kirby ME, Lund SP, Anderson MA, Bird BW (2007) Insolation forcing of Holocene climate change in Southern California: a sediment study from Lake Elsinore. J Paleolimnol 38:395–417. https://doi.org/10.1007/s10933-006-9085-7

Kirby ME, Lund SP, Bird BW (2006) Mid-Wisconsin sediment record from Baldwin Lake reveals hemispheric climate dynamics (Southern CA, USA). Palaeogeography, Palaeoclimatology, Palaeoecology 241:267–283. https://doi.org/10.1016/j.palaeo.2006.03.043

Kirby ME, Lund SP, Patterson WP, et al (2010) A Holocene record of Pacific Decadal Oscillation (PDO)-related hydrologic variability in Southern California (Lake Elsinore, CA). J Paleolimnol 44:819–839. https://doi.org/10.1007/s10933-010-9454-0

Kirby ME, Zimmerman SRH, Patterson WP, Rivera JJ (2012) A 9170-year record of decadal-to-multi-centennial scale pluvial episodes from the coastal Southwest United States: a role for atmospheric rivers? Quaternary Science Reviews 46:57–65. https://doi.org/10.1016/j.quascirev.2012.05.008

Kirby MEC, Patterson WP, Lachniet M, et al (2019) Pacific Southwest United States Holocene Droughts and Pluvials Inferred From Sediment δ18O(calcite) and Grain Size Data (Lake Elsinore, California). Frontiers in Earth Science 7:74. https://doi.org/10.3389/feart.2019.00074

Knight CA, Anderson L, Bunting MJ, et al (2022) Land management explains major trends in forest structure and composition over the last millennium in California's Klamath Mountains. Proceedings of the National Academy of Sciences 119:e2116264119. https://doi.org/10.1073/pnas.2116264119

Knight CA, Baskaran M, Bunting MJ, et al (2021) Linking modern pollen accumulation rates to biomass: Quantitative vegetation reconstruction in the western Klamath Mountains, NW California, USA. The Holocene 31:814–829

Krammer K, Lange-Bertalot H (1986) Bacillariophyceae 1. Teil: Naviculaceae. Süßwasserflora von Mitteleuropa

Krammer K, Lange-Bertalot H (1988) Bacillariophyceae 2: Teil: Bacillariaceae, Epithmiaceae, Surirellaceae. In: Ettl H, Gärtner G, Gerloff J, Heynig H, Mollenhauer D (eds) Süßwasserflora von Mitteleuropa, Band 2/2. Gustav Fischer Verlag, Stuttgart. Süßwasserflora von Mitteleuropa

Krammer K, Lange-Bertalot H (1991a) Bacillariophyceae. 3: Teil: Centrales, Fragilariaceae, Eunotiaceae. In: Ettl H, Gärtner G, Gerloff J, Heynig H, Mollenhauer D (eds) Süßwasserflora von Mitteleuropa, Band 2/3. Gustav Fischer Verlag, Stuttgart. Süßwasserflora von Mitteleuropa

Krammer K, Lange-Bertalot H (1991b) Bacillariophyceae. 4: Teil: Achnanthaceae. In: Ettl H, Gärtner G, Gerloff J, Heynig H, Mollenhauer D (eds) Süßwasserflora von Mitteleuropa, Band 2/4. Gustav Fischer Verlag, Stuttgart. Süßwasserflora von Mitteleuropa

Kröger N (2007) Prescribing diatom morphology: toward genetic engineering of biological nanomaterials. Current Opinion in Chemical Biology 11:662–669. https://doi.org/10.1016/j.cbpa.2007.10.009

Kulikovskiy MS, Glushchenko AM, Genkal SI, Kuznetsova IV (2016) Identification book of diatoms from Russia. Filigran, Yaroslavl

Laird KR, Cumming BF (2009) Diatom-inferred lake level from near-shore cores in a drainage lake from the Experimental Lakes Area, northwestern Ontario, Canada. J Paleolimnol 42:65–80. https://doi.org/10.1007/s10933-008-9248-9

Laird KR, Kingsbury MV, Cumming BF (2010) Diatom habitats, species diversity and water-depth inference models across surface-sediment transects in Worth Lake, northwest Ontario, Canada. J Paleolimnol 44:1009–1024. https://doi.org/10.1007/s10933-010-9470-0

Laird KR, Kingsbury MV, Lewis CFM, Cumming BF (2011) Diatom-inferred depth models in 8 Canadian boreal lakes: inferred changes in the benthic:planktonic depth boundary and implications for assessment of past droughts. Quaternary Science Reviews 30:1201–1217. https://doi.org/10.1016/j.quascirev.2011.02.009

Lange-Bertalot H, Hofmann G, Werum M, et al (2017) Freshwater benthic diatoms of Central Europe: over 800 common species used in ecological assessment. Koeltz Botanical Books Schmitten-Oberreifenberg

Laskar J, Robutel P, Joutel F, et al (2004) A long-term numerical solution for the insolation quantities of the Earth. A&A 428:261–285. https://doi.org/10.1051/0004-6361:20041335

Legates DR (2000) Remote sensing in hydroclimatology: an introduction. Professional Geographer 52:233–234

Leidelmeijer JA, Kirby MEC, MacDonald G, et al (2021) Younger Dryas to early Holocene (12.9 to 8.1 ka) limnological and hydrological change at Barley Lake, California (northern California Coast Range). Quaternary Research 103:193–207. https://doi.org/10.1017/qua.2021.9

Leira M, López-Rodríguez M del C, Carballeira R (2017) Epilithic diatoms (Bacillariophyceae) from running watersin NW Iberian Peninsula (Galicia, Spain). Anales del Jardín Botánico de Madrid 74:e062–e062. https://doi.org/10.3989/ajbm.2421

Levkov Z (2009) Amphora sensu lato. Diatoms.org

Loisel J, MacDonald GM, Thomson MJ (2017) Little Ice Age climatic erraticism as an analogue for future enhanced hydroclimatic variability across the American Southwest. PLOS ONE 12:e0186282. https://doi.org/10.1371/journal.pone.0186282

Løvstad Ø, Bjørndalen K (1990) Nutrients (P, N, Si) and growth conditions for diatoms and Oscillatoria spp. in lakes of south-eastern Norway. Hydrobiologia 196:255–263. https://doi.org/10.1007/BF00006137

Lowe R (2010) Epithemia adnata. Diatoms.org

Lund SP, Platzman E (2016) Paleomagnetic chronostratigraphy of late Holocene Zaca Lake, California. The Holocene 26:814–821

MacDonald GM (2007) Severe and sustained drought in southern California and the West: Present conditions and insights from the past on causes and impacts. Quaternary International 173–174:87–100. https://doi.org/10.1016/j.quaint.2007.03.012

MacDonald GM, Moser KA, Bloom AM, et al (2008) Evidence of temperature depression and hydrological variations in the eastern Sierra Nevada during the Younger Dryas stade. Quaternary Research 70:131–140. https://doi.org/10.1016/j.yqres.2008.04.005

MacDonald GM, Moser KA, Bloom AM, et al (2016) Prolonged California aridity linked to climate warming and Pacific sea surface temperature. Sci Rep 6:33325. https://doi.org/10.1038/srep33325

Mann ME, Gleick PH (2015) Climate change and California drought in the 21st century. Proceedings of the National Academy of Sciences 112:3858–3859. https://doi.org/10.1073/pnas.1503667112

Mark SZ, Abbott MB, Rodbell DT, Moy CM (2022) XRF analysis of Laguna Pallcacocha sediments yields new insights into Holocene El Niño development. Earth and Planetary Science Letters 593:117657. https://doi.org/10.1016/j.epsl.2022.117657

Marohasy J, Abbot J (2015) Review of the salinity optima of the diatom Staurosirella pinnata : implications for water reform in Australia

Martinez LN (2020) Climate, Fire, and Environmental Dynamics at Lake Elsinore, California, from Late Marine Isotope Stage 3 through the Holocene. University of California, Los Angeles

McCain CM (2007) Could temperature and water availability drive elevational species richness patterns? A global case study for bats. Global Ecology and Biogeography 16:1–13. https://doi.org/10.1111/j.1466-8238.2006.00263.x

Melles M, Svendsen JI, Fedorov G, et al (2022) Quaternary environmental and climatic history of the northern high latitudes – recent contributions and perspectives from lake sediment records. Journal of Quaternary Science 37:721–728. https://doi.org/10.1002/jqs.3456

Menzel U (2022) CCP: Significance Tests for Canonical Correlation Analysis (CCA)

Miller FK (2004) Preliminary Geologic Map of the Big Bear City 7.5'Quadrangle, San Bernardino County, California

Mills K, Schillereff D, Saulnier-Talbot É, et al (2017) Deciphering long-term records of natural variability and human impact as recorded in lake sediments: a palaeolimnological puzzle. WIREs Water 4:e1195. https://doi.org/10.1002/wat2.1195

Mohr JA, Whitlock C, Skinner CN (2000) Postglacial vegetation and fire history, eastern Klamath Mountains, California, USA. The Holocene 10:587–601

Moos MT, Laird KR, Cumming BF (2005) Diatom assemblages and water depth in Lake 239 (Experimental Lakes Area, Ontario): implications for paleoclimatic studies. J Paleolimnol 34:217–227. https://doi.org/10.1007/s10933-005-2382-8

Morales E (2010b) Pseudostaurosira parasitica. In: Diatoms of North America. https://diatoms.org/species/pseudostaurosira_parasitica. Accessed 9 May 2022

Morales E (2010a) Pseudostaurosira brevistriata. In: Diatoms of North America. https://diatoms.org/species/pseudostaurosira_brevistriata. Accessed 9 May 2022

Morales E, Rosen B, Spaulding S (2013) Fragilaria crotonensis. In: Diatoms of North America. https://diatoms.org/species/fragilaria_crotonensis. Accessed 9 May 2022

Morales EA (2005) Observations of the morphology of some known and new fragilarioid diatoms (Bacillariophyceae) from rivers in the USA. Phycological Research 53:113–133. https://doi.org/10.1111/j.1440-183.2005.00378.x

Nelson DM, Tréguer P (1992) Role of silicon as a limiting nutrient to Antarctic diatoms: evidence from kinetic studies in the Ross Sea ice-edge zone. Marine Ecology Progress Series 80:255–264

Oksanen J, Blanchet FG, Friendly M, et al (2020) vegan: Community Ecology Package. In: R package version 2.5-7. https://cran.r-project.org/web/packages/vegan/index.html. Accessed 9 May 2022

Olivares-Rubio HF, Cabrera LI, Godínez-Ortega JL, et al (2017) Halamphora oceanica (Catenulaceae, Bacillariophyta), a new species from the epipelagic region of the southwestern Gulf of Mexico. Phytotaxa 317:188–198. https://doi.org/10.11646/phytotaxa.317.3.3

Oster JL, Sharp WD, Covey AK, et al (2017) Climate response to the 8.2 ka event in coastal California. Sci Rep 7:3886. https://doi.org/10.1038/s41598-017-04215-5

Overpeck JT, Webb T, Prentice IC (1985) Quantitative Interpretation of Fossil Pollen Spectra: Dissimilarity Coefficients and the Method of Modern Analogs. Quaternary Research 23:87–108. https://doi.org/10.1016/0033-5894(85)90074-2

Park J (2011) A modern pollen–temperature calibration data set from Korea and quantitative temperature reconstructions for the Holocene. The Holocene 21:1125–1135. https://doi.org/10.1177/0959683611400462

Park J, Han J, Jin Q, et al (2017) The Link between ENSO-like Forcing and Hydroclimate Variability of Coastal East Asia during the Last Millennium. Sci Rep 7:8166. https://doi.org/10.1038/s41598-017-08538-1

Park LE, Cohen AS (2011) Paleoecological response of ostracods to early Late Pleistocene lake-level changes in Lake Malawi, East Africa. Palaeogeography, Palaeoclimatology, Palaeoecology 303:71–80. https://doi.org/10.1016/j.palaeo.2010.02.038

Patrick R, Reimer CW (1966) The diatoms of the United States. Academy of Natural Sciences

Pielou EC (1966) The measurement of diversity in different types of biological collections. Journal of Theoretical Biology 13:131–144. https://doi.org/10.1016/0022-5193(66)90013-0

Platzman ES, Lund SP (2019) High-resolution environmental magnetic study of a Holocene sedimentary record from Zaca Lake, California. The Holocene 29:17–25

Potapova M (2009a) Odontidium mesodon. In: Diatoms of North America. https://diatoms.org/species/odontidium_mesodon. Accessed 9 May 2022

Potapova M (2011) Navicula radiosa. Diatoms.org

Potapova M (2009b) Rossithidium pusillum. Diatoms.org

Potapova MG, Minerovic AD, Veselá J, Smith CR (2020) Diatom New Taxon File at the Academy of Natural Sciences (DNTF-ANS). In: Diatom New Taxon File at the Academy of Natural Sciences (DNTF-ANS). http://symbiont.ansp.org/dntf/. Accessed 9 May 2022

Radloff PL, Contreras C, Whisenant A, Bronson JM (2010) Nutrient effects in Small Brazos basin streams final report. WQTS-2010-02. Water Quality Program, Texas Parks and Wildlife Department …

Ramón Mercau J, Laprida C (2016) An ostracod-based calibration function for electrical conductivity reconstruction in lacustrine environments in Patagonia, Southern South America. Ecological Indicators 69:522–532. https://doi.org/10.1016/j.ecolind.2016.05.026

Reavie ED, Smol JP, Sharpe ID, et al (2000) Paleolimnological analyses of cultural eutrophication patterns in British Columbia lakes. Can J Bot 78:873–888. https://doi.org/10.1139/b00-058

Reed JM (1998) A diatom-conductivity transfer function for Spanish salt lakes. Journal of Paleolimnology 19:399–416. https://doi.org/10.1023/A:1007934627134

Rioual P (2000) Diatom assemblages and water chemistry of lakes in the French Massif Central: a methodology for reconstruction of past limnological and climate fluctuations during the Eemian period. University of London, University College London (United Kingdom)

Robertsson A-M (1995) Palaeoenvironment during Preboreal-Boreal in Närke, south central Sweden. Quaternary International 27:103–109. https://doi.org/10.1016/1040-6182(94)00067-F

Rosén P, Hall R, Korsman T, Renberg I (2000) Diatom transfer-functions for quantifying past air temperature, pH and total organic carbon concentration from lakes in northern Sweden. Journal of Paleolimnology 24:109–123. https://doi.org/10.1023/A:1008128014721

Round FE, Crawford RM, Mann DG (1990) Diatoms: biology and morphology of the genera. Cambridge university press

RStudio Team (2020) RStudio: Integrated Development for R. https://www.rstudio.com/. Accessed 9 May 2022

Rühland K, Priesnitz A, Smol JP (2003) Paleolimnological Evidence from Diatoms for Recent Environmental Changes in 50 Lakes across Canadian Arctic Treeline. Arctic, Antarctic, and Alpine Research 35:110–123

Rühland KM, Paterson AM, Smol JP (2015) Lake diatom responses to warming: reviewing the evidence. J Paleolimnol 54:1–35. https://doi.org/10.1007/s10933-015-9837-3

Rushing C, Bulusu A, Hurwitz HI, et al (2015) A leave-one-out cross-validation SAS macro for the identification of markers associated with survival. Computers in Biology and Medicine 57:123–129. https://doi.org/10.1016/j.compbiomed.2014.11.015

Ryves DB, Juggins S, Fritz SC, Battarbee RW (2001) Experimental diatom dissolution and the quantification of microfossil preservation in sediments. Palaeogeography, Palaeoclimatology, Palaeoecology 172:99–113. https://doi.org/10.1016/S0031-0182(01)00273-5

Saha R (2015) Millennial-scale oscillations between sea ice and convective deep water formation. Paleoceanography 30:1540–1555. https://doi.org/10.1002/2015PA002809

Sarthou G, Timmermans KR, Blain S, Tréguer P (2005) Growth physiology and fate of diatoms in the ocean: a review. Journal of Sea Research 53:25–42. https://doi.org/10.1016/j.seares.2004.01.007

Saulnier-Talbot É (2016) Paleolimnology as a Tool to Achieve Environmental Sustainability in the Anthropocene: An Overview. Geosciences 6:26. https://doi.org/10.3390/geosciences6020026

Shannon CE (1948) A mathematical theory of communication. The Bell System Technical Journal 27:379–423. https://doi.org/10.1002/j.1538-7305.1948.tb01338.x

Shuman B, Donnelly JP (2006) The influence of seasonal precipitation and temperature regimes on lake levels in the northeastern United States during the Holocene. Quaternary Research 65:44–56. https://doi.org/10.1016/j.yqres.2005.09.001

Shuman BN, Routson C, McKay N, et al (2018) Placing the Common Era in a Holocene context: millennial to centennial patterns and trends in the hydroclimate of North America over the past 2000 years. Climate of the Past 14:665–686. https://doi.org/10.5194/cp-14-665-2018

Slate JE, Stevenson RJ (2007) The Diatom Flora of Phosphorus-Enriched and Unenriched Sites in an Everglades Marsh. Diatom Research 22:355–386. https://doi.org/10.1080/0269249X.2007.9705721

Smol JP, Cumming BF (2000) Tracking Long-Term Changes in Climate Using Algal Indicators in Lake Sediments. Journal of Phycology 36:986–1011. https://doi.org/10.1046/j.1529-8817.2000.00049.x

Sorvari S, Korhola A, Thompson R (2002) Lake diatom response to recent Arctic warming in Finnish Lapland. Global Change Biology 8:171–181. https://doi.org/10.1046/j.1365-2486.2002.00463.x

Spaulding SA, Bishop IW, Edlund MB, et al (2019) Diatoms of North America. In: Diatoms of North America. https://diatoms.org/. Accessed 9 May 2022

Spaulding SA, Potapova MG, Bishop IW, et al (2021) *Diatoms.org* : supporting taxonomists, connecting communities. Diatom Research 36:291–304. https://doi.org/10.1080/0269249X.2021.2006790

Starratt SW (2012) Holocene diatom flora and climate history of Medicine Lake, Northern California, USA. Nova Hedwigia, Beiheft 141:485504

Starratt SW, Kirby ME, Glover K (2021) Diatom Record of Holocene Moisture Variability in the San Bernardino Mountains, California, USA. In: Rosen MR, Finkelstein DB, Park Boush L, Pla-Pueyo S (eds) Limnogeology: Progress, Challenges and Opportunities : A Tribute to Elizabeth Gierlowski-Kordesch. Springer International Publishing, Cham, pp 329–365

Stevenson RJ (1984) Epilithic and epipelic diatoms in the Sandusky River, with emphasis on species diversity and water pollution. Hydrobiologia 114:161–175. https://doi.org/10.1007/BF00031868

Strub PT, Allen JS, Huyer A, et al (1987) Seasonal cycles of currents, temperatures, winds, and sea level over the northeast Pacific continental shelf: 35°N to 48°N. Journal of Geophysical Research: Oceans 92:1507–1526. https://doi.org/10.1029/JC092iC02p01507

Swain DL (2015) A tale of two California droughts: Lessons amidst record warmth and dryness in a region of complex physical and human geography. Geophysical Research Letters 42:9999–10,003. https://doi.org/10.1002/2015GL066628

Swain DL, Langenbrunner B, Neelin JD, Hall A (2018) Increasing precipitation volatility in twenty-first-century California. Nature Clim Change 8:427–433. https://doi.org/10.1038/s41558-018-0140-y

Temoltzin Loranca Y (2018) Palaeoenvironments and Palaeoclimates During The Late Holocene in Lake Siscunsi (Colombia), A Multiproxy Perspective. Thesis, Faculty of Graduate Studies and Research, University of Regina

ter Braak CJ, Šmilauer P (2012) Canoco reference manual and user's guide: software for ordination, version 5.0

Thangaraj S, Giordano M, Sun J (2020) Comparative Proteomic Analysis Reveals New Insights Into the Common and Specific Metabolic Regulation of the Diatom Skeletonema dohrnii to the Silicate and Temperature Availability. Frontiers in Plant Science 11:

Thomas ER, Wolff EW, Mulvaney R, et al (2007) The 8.2ka event from Greenland ice cores. Quaternary Science Reviews 26:70–81. https://doi.org/10.1016/j.quascirev.2006.07.017

Underwood D (2013) Nitzschia semirobusta. Diatoms.org

van Wirdum F, Andrén E, Wienholz D, et al (2019) Middle to Late Holocene Variations in Salinity and Primary Productivity in the Central Baltic Sea: A Multiproxy Study From the Landsort Deep. Frontiers in Marine Science 6:

Wang S-YS, Yoon J-H, Becker E, Gillies R (2017) California from drought to deluge. Nature Clim Change 7:465–468. https://doi.org/10.1038/nclimate3330

Wang Y, Jiang X, Li Y-L, et al (2023) Interactive Effects of Nutrients and Salinity on Phytoplankton in Subtropical Plateau Lakes of Contrasting Water Depths. Water 15:69. https://doi.org/10.3390/w15010069

Weckström J, Korhola A (2001) Patterns in the distribution, composition and diversity of diatom assemblages in relation to ecoclimatic factors in Arctic Lapland. Journal of Biogeography 28:31–45. https://doi.org/10.1046/j.1365-2699.2001.00537.x

Wehr JD, Sheath RG, Kociolek JP (2015) Freshwater algae of North America: ecology and classification. Elsevier

Western Regional Climate Center (2016a) HAPPY CAMP RS, CALIFORNIA - Climate Summary. https://wrcc.dri.edu/cgi-bin/cliMAIN.pl?ca3761. Accessed 13 Apr 2023

Western Regional Climate Center (2016b) BIG BEAR LAKE, CALIFORNIA - Climate Summary. https://wrcc.dri.edu/cgi-bin/cliMAIN.pl?ca0741. Accessed 26 Mar 2023

Whitlock C, Marlon J, Briles C, et al (2008) Long-term relations among fire, fuel, and climate in the north-western US based on lake-sediment studies. Int J Wildland Fire 17:72–83. https://doi.org/10.1071/WF07025

Whitlock C, Skinner CN, Bartlein PJ, et al (2004) Comparison of charcoal and tree-ring records of recent fires in the eastern Klamath Mountains, California, USA. Canadian Journal of Forest Research 34:2110–2121

Wigdahl-Perry CR, Saros JE, Schmitz J, et al (2016) Response of temperate lakes to drought: a paleolimnological perspective on the landscape position concept using diatom-based reconstructions. J Paleolimnol 55:339–356. https://doi.org/10.1007/s10933-016-9883-5

Williams AP, Cook BI, Smerdon JE (2022) Rapid intensification of the emerging southwestern North American megadrought in 2020–2021. Nat Clim Chang 12:232–234. https://doi.org/10.1038/s41558-022-01290-z

Wise EK (2010) Spatiotemporal variability of the precipitation dipole transition zone in the western United States. Geophysical Research Letters 37:. https://doi.org/10.1029/2009GL042193

Wojtal AZ (2009) The Diatoms of Kobylanka Stream Near Kraków (Wyżyna Krakowsko-Częstochowska Upland, S Poland). Polish Botanical Journal 54:129–330

Wolin JA, Stone JR (2010) Diatoms as indicators of water level change in freshwater lakes. The diatoms: applications for the environmental and earth sciences 174–185

Woodhouse CA (2004) A paleo perspective on hydroclimatic variability in the western United States. Aquat Sci 66:346–356. https://doi.org/10.1007/s00027-004-0723-8

Woodhouse CA, Meko DM, MacDonald GM, et al (2010) A 1,200-year perspective of 21st century drought in southwestern North America. Proceedings of the National Academy of Sciences 107:21283–21288. https://doi.org/10.1073/pnas.0911197107

Yang J-R, Duthie HC (1995) Regression and Weighted Averaging Models Relating Surficial Sedimentary Diatom Assemblages to Water Depth in Lake Ontario. Journal of Great Lakes Research 21:84–94. https://doi.org/10.1016/S0380-1330(95)71023-1

Yoon Soon-Ock, Hwang B, Hwang S (2017) Reconstruction of Paleo-Temperature During the Holocene Using WA-PLS Analysis of Modern Pollen From the Surface Soil in the Southeastern Part of the Korean Peninsula. JOURNAL OF THE KOREAN GEOMORPHOLOGICAL ASSOCIATION 24:13–25. https://doi.org/10.16968/JKGA.24.4.13

Zalat AA, El-Sheekh MM (1999) Diatom assemblages from two brackish Egyptian lakes. Egyptian Journal of Botany 39:53–76

Zamora-Reyes D, Black B, Trouet V (2021) Enhanced winter, spring, and summer hydroclimate variability across California from 1940 to 2019. International Journal of Climatology n/a: https://doi.org/10.1002/joc.7513

Zhang E, Jones R, Bedford A, et al (2007) A chironomid-based salinity inference model from lakes on the Tibetan Plateau. J Paleolimnol 38:477–491. https://doi.org/10.1007/s10933-006-9080-z

Zorzal-Almeida S, Fernandes V (2013) Effects of intensive fish-farming and domestic wastewater on the periphytic algal community in a tropical coastal lagoon (Juara, Brazil). Acta Scientiarum Biological Sciences 35:335–342. https://doi.org/10.4025/actascibiolsci.v35i3.17094

Zou Y, Wang L, He H, et al (2021) Application of a Diatom Transfer Function to Quantitative Paleoclimatic Reconstruction — A Case Study of Yunlong Lake, Southwest China. Frontiers in Earth Science 9: